THESIS APPROVAL

GRADUATE SCHOOL, KASETSART UNIVERSITY

Master of Engineering (Civil Engineering)

DEGREE

Civil Engineering | Civil Engineering

FIELD | **DEPARTMENT**

TITLE: Seismic Evaluation of Existing Gravity Load Designed Building in Bhutan

NAME: Mr. Lobzang Dorji

THIS THESIS HAS BEEN ACCEPTED BY

THESIS ADVISOR

(Assistant Professor Kitjapat Phuvoravan, Ph.D.)

THESIS CO-ADVISOR

(Assistant Professor Piya Chotickai, Ph.D.)

THESIS CO-ADVISOR

(Mr. Barames Vardhanabhuti, Ph.D.)

DEPARTMENT HEAD

(Associate Professor Korchoke Chantawarangul, Ph.D.)

APPROVED BY THE GRADUATE SCHOOL ON _____

DEAN

(Associate Professor Gunjana Theeragool, D.Agr.)

THESIS

SEISMIC EVALUATION OF EXISTING GRAVITY LOAD DESIGNED BUILDING IN BHUTAN

LOBZANG DORJI

A Thesis Submitted in Partial Fulfillment of
the Requirements for the Degree of
Master of Engineering (Civil Engineering)
Graduate School, Kasetsart University
2010

Lobzang Dorji 2010: Seismic Evaluation of Existing Gravity Load Designed Building in Bhutan. Master of Engineering (Civil Engineering),
Major Field: Civil Engineering, Department of Civil Engineering.
Thesis Advisor: Assistant Professor Kitjapat Phuvoravan, Ph.D. 148 pages.

The gravity load designed buildings are expected to undergo excursion in the nonlinear region under seismic force effect. To examine such behavior of the structures, the conventional linear seismic analysis cannot be adopted which demands nonlinear analysis approach. Most of the existing buildings in Bhutan are designed and constructed before the introduction of seismic design concept and it is required to evaluate the seismic performance of such existing structures. In this study, the seismic evaluation of one of the existing reinforced concrete buildings designed for gravity load has been evaluated by using nonlinear static pushover analysis. The selected gravity load designed building in this case study shows good resistance to seismic load, therefore it does not require structural intervention as the inelastic deformation of structural components are not so important to pose threat to the stability of the building. The study also shows that infill contributes to increase the initial stiffness of the structure while the ultimate lateral capacity and its corresponding roof displacement do not affect much. The effect on lateral capacity of the building due to variation of compressive strength of concrete was observed to be inconsequential. Increase in yield strength of reinforcement produces hefty increase in lateral capacity of the building but the initial stiffness remains all most constant. When shallow foundation of the building was modeled as hinge and flexible base (uncouple component model), the lateral capacity of the building gives underestimate results as compare to assumed fixed base foundation for seismic evaluation.

/ /

Student's signature Thesis Advisor's signature

ACKNOWLEDGEMENT

I would like to express the deepest appreciation to my committee chair, Assistant Professor Dr. Kitjapat Phuvoravan for his supervision, advice, and guidance from the very early stage of this research as well as giving me extraordinary experiences throughout the work. Without his guidance and persistent help this thesis would not have been possible. I gratefully thank you so much. I acknowledge Assistant Professor Dr. Piya Chotickai and Dr. Barames Vardhanabhuti for their constructive comments on this thesis. I am thankful that in the midst of all their activities, they accepted to be members of thesis committee. In addition, I thank Associate Professors Dr.Trakool Aramraks and Dr. Warakorn Mairiang, and to all the staff members in International Programe in Civil engineering for their kind help.

It is a great jubilation to pay tribute to Royal Govt. of Thailand and Bhutan for providing scholarship to pursue higher study. Collective and individual acknowledgments are also owed to my colleagues at Chulaborn Research Institute, Asian Institute of Technology, Jigme Namgyel Polytechnic and Kasetsart University whose present somehow perpetually refreshed, helpful, and memorable.

My father, Cheada and mother Sheachang earns special mention for their inseparable support and aspirations. They are the once who sincerely raised me with their caring and gently love. I am fully beholden to my wife Sonam Choden and two daughters, Kelden Pelmo and Lekzing Namkha Pelmo whose dedication, love and persistent confidence in me, has taken the load off my shoulder. I owe them for being magnanimously let their intelligence, passions, and ambitions collide with mine. Furthermore, to my brothers and sisters with their thoughtful support, thank you.

Finally, I would like to thank everyone who was important to the victorious recognition of thesis, as well as expressing my apology that I could not reveal their names individually.

Lobzang Dorji

April 2010

TABLE OF CONTENTS

Page

LIST OF TABLES

LIST OF FIGURES

LIST OF FIGURES (Continued)

LIST OF FIGURES (Continued)

Appendix Figures

LIST OF FIGURES (Continued)

LIST OF ABBREVIATIONS

ACI	=	American Concrete Institute
ADRS	=	Acceleration-Displacement Response Spectra
AISC	=	American Institute of Steel Construction
ATC	=	American Technology of Concrete
BBS	=	Bhutan Broadcasting Service
BSSC	=	Building Seismic Safety Council
BW	=	Brick Wall
CP	=	Collapse Prevention
CSM	=	Capacity Spectrum Method
DCM	=	Displacement Coefficient Method
F	=	Failure
FEMA	=	Federal Emergency Management Agency
FF	=	Flexural Failure
FY	=	Flexural Yielding
IO	=	Immediate Occupancy
IS	=	Indian Standard
LD	=	Linear Dynamic
LS	=	Linear Static
FEMA	=	Federal Emergency Management Agency
FF	=	Flexural Failure
FY	=	Flexural Yielding
IO	=	Immediate Occupancy
IS	=	Indian Standard
LD	=	Linear Dynamic
LS	=	Linear Static
LS	=	Life Safety
MDOF	=	Multi-degree of Freedom
MoWHS	=	Ministry of Work and Human Settlement

LIST OF ABBREVIATIONS (Continued)

ND	=	Nonlinear Dynamic
NEHRP	=	National Earthquake Hazards Reduction Program
NS	=	Nonlinear Static
NSP	=	Nonlinear Static Pushover
PBS	=	Performance Base Design
RC	=	Reinforced Concrete
SDOF	=	Single Degree of Freedom
SQCA	=	Standard and Quality Control Authority
UBC	=	Uniform Building Code

SEISMIC EVALUATION OF EXISTING GRAVITY LOAD DESIGNED BUILDING IN BHUTAN

INTRODUCTION

In the urban and semi-urban areas of Bhutan, there has been an increase in the stock of reinforced concrete buildings like any other countries all over the world. Many of these buildings were built before the introduction of seismic codes or with the utilization of traditional and inadequate seismic design criteria. The seismic design regulations have not been applied to these buildings as seismic designed concept was introduced very recently (late 1980s) in our country. Therefore, these buildings were particularly designed to carry only vertical loads presuming that the infill contributes sufficiently to the lateral strength of the structures to withstand the lateral loadings.

The parameters like strength and stiffness of the structures are greatly influenced by masonry infill walls revealed from the past literature. Ignoring the composite action is not always safe as the interaction between the walls and surrounding frame under horizontal forces alter dynamics characteristics of the composite structures in the seismic areas. It has been generally recognized that infill walls escalate the response of reinforced concrete frame buildings in low to moderate seismic regions, but yet they demonstrate poor seismic performance under high seismic demand (Das and Murty, 2004).

However, masonry infill walls are used extensively in reinforced concrete frame structures. This masonry infill fulfill architectural and other functional requirements, such as forming a significant portion of building envelop, partitioning, temperature and sound barriers, while also providing adequate compartmentalization against fire hazard. Masonry is a locally available building material that has a long history of successful use in the construction industry. The Figure 1 shows existing gravity load designed buildings in Bhutan.

Figure 1 Typical existing building in Bhutan.

Therefore the evaluation of seismic susceptibility of existing reinforced concrete building structures particularly those designed to resist only gravity load has a pivotal role in the determination and reduction of earthquake effects. The most hazardous cost of earthquakes in the near future are likely to appear from existing gravity load designed buildings in our country as most of the time attention has been largely focused on the seismic design of new buildings.

Thus, seismic evaluation of existing gravity load designed buildings in Bhutan is highly demanded as Bhutan is situated in the very severe earth quake zone as per Indian system of categorization.

Statement of problem

Most of the existing buildings in Bhutan are reinforced concrete buildings with regular plans in which the space created between columns and beams are filled with walls referred to as masonry infill walls or infill panels. These buildings are mostly gravity load designed accordance to Indian Standard.

Bhutan is situated on the Himalayan foothills which fall under highest seismicity zone as per Indian system of categorization. A report published by the researcher, Roger Bilham of University of Colorado in the United States, 2001 has predicted that a major earthquake magnitude of 8.1 to 8.3 on the Richter scale will occur in Bhutan and neighboring seismically active front of Himalaya's very soon.

Despite the high risk of earthquake, the seismic design concept of building in Bhutan was recently introduced. Therefore, should the predicted earthquake occur, the consequence would be devastating leading to loss of lives and economic losses, further more cause would be critical interference in terms of functioning the nation. Therefore it is utmost important to assess the existing gravity load designed buildings for the determination and evaluation of structural safety in the building type structures so much more here after in this field.

In the past Bhutan has been rocked by several moderate to severe earthquakes. In 1988, two major earthquakes had experienced in this country; first earthquake magnitude measuring 4.8 on the Richter scale on 5th July, 1988 and the second measuring 4.9 on the Richter scale followed on 20th December, 1988. In between 1937 and 1988, country has been suffered by more than thirty earthquakes of varying magnitudes.

Records from the Department of Geology and Mines indicate that in 1941 earthquake magnitude measuring 6.75 on the Richter scale was the most severe that had ever occurred in Bhutan until date. On 26th March, 2003, earthquake magnitude measuring 5.5 on the Richter scale rocked the country. The earthquakes magnitude each measuring 5.8 and 5.5 on the Richter scale knocked the country on 14th February, 2006. The cracks of varying degrees across the walls and above openings like windows and doors were reported from most of the affected buildings.

In 21st September 2009, one of the major earthquakes occurred in our country in which the epicenter was fall in between Trashigang and Mongar districts (province) with the earthquake magnititude of 6.3 on the Richter scale. From that earthquake

numbers of lives were claimed and thousands of people left homeless. On top of that there were large damages like cracks over the walls on reinforced concrete buildings and historical monuments as reported in the kuensel (Bhutan news paper) and Bhutan Broadcasting Service (BBS).

The Standard and Quality Control Authority under the Ministry of Works and Human Settlement, recently has begun to take initiatives in this area by conducting awareness campaigns and meetings with stakeholders. The people are now aware about the importance of seismic design of buildings in our region. But still there is a growing concern about the buildings constructed without seismic considerations, especially the buildings constructed before the introduction of seismic design concept in Bhutan.

However, it doesn't mean that all gravity loads designed buildings would collapse and threaten to life safety to the occupancies during earthquake event as they don't account for lateral loads. But it is always good enough to evaluate the seismic performance of gravity load designed buildings by following standard methods proposed by expertise in order to get insight behavior of such type of buildings during earthquake event.

For these reasons, the seismic evaluation methods and standard guidelines for the existing buildings are available currently. Therefore to implement the recommended seismic evaluation procedures to evaluate the seismic performance of existing reinforced concrete buildings, the Non-linear Static Pushover analysis and Capacity Spectrum method were used by following the acceptance criteria given in ATC-40, FEMA and IS code-1893-2000 in this study.

OBJECTIVES

In general, the determination of displacement and lateral capacity demands of building structures, may exhibit inelastic behavior during earthquake, and is quite important. If these demands are not estimated accurately during the evaluation phase of the building structures, a local or progressive collapse becomes unavoidable during severe earthquake.

The main objectives of this study are as follows:

1. To evaluate the seismic performance of existing gravity load designed building.

2. To study the effects on lateral capacity of building due to variation of material strength, infill masonry wall thickness and modeling of shallow foundation.

Scope

The gravity load designed of five-storey reinforced concrete building which is used as residential purposes and situated in high seismicity zone as per Indian earthquake zone map was considered in this study.

The selected residential buildings model was analyzed as the reference buildings. The seismic evaluation was carried on bare frame and fully in filled frames along both global directions by considering only flexural controlled failure of the components (shear failure not accounted) in this study. The parametric studies were performed along Y-direction in the analytical model. Nonlinear static pushover analysis was used for the evaluation of reinforced concrete building in accordance with IS: 1893- 2000, ATC-40, FEMA-273 and FEMA-356 by using SAP2000 Finite Element Programmed soft ware in this study.

Benefits

The present study deals with seismic evaluation of existing gravity load designed building in our country. The results of this study would benefits in the process of compiling the rational information for the seismic demand capacity of existing buildings. The Standard and Quality Control Authority under the Ministry of Work and Human Settlement (MoWHS) is trying to gather information as much as possible in this area since most of the existing buildings are designed and constructed before introduction of seismic design philosophy in our country despite our country situated in high seismic zone as per Indian seismic zoning.

Thesis Organization

This thesis is composed of five main headings and four appendices. The five main headings are Introduction, Literature review, Research Methodology, Result and Discussion, and Conclusions and Recommendations. Introduction includes overall view of the study, problem statement, scope and objective of the study. The review of the previous research on seismic evaluation of buildings by nonlinear pushover analysis base on FEMA and ATC-40 guide lines and its modeling procedures of structural as well as non-structural components are discussed under Literature Review. In Research Methodology, detail information about the analytical models and its method used in the analysis are presented. The evaluation and comparison of the analysis results are offered under Results and Discussions. Finally, Conclusions and Recommendations contain the summary of the analysis results, and the recommendations for future studies base on present study.

The appendices are given in Appendix A-D attached to this thesis. In Appendix A, the calculations of diagonal strut width and spring constants for foundation modeling are presented. Appendix B includes pushover capacity curves and sequence of failure under parametric studies. The step by step procedures for pushover analysis are given in Appendix C. Existing building drawings are attached in Appendix D.

LITERATURE REVIEW

1. General

Advances in earthquake-related technology during the past few decades have led to a realization that seismic risk to life and property can be reduced significantly by evaluating seismic performance of existing seismically deficient buildings such as gravity load designed buildings and its infill configuration. The post-earthquake response of building failures has awakened structural and design engineers to work harder to obtain more considerable information in this field.

Special attention has been recently given to the investigation on the seismic vulnerability of existing reinforced concrete buildings designed for gravity load only as typically found in most seismic-prone countries constructed before the introduction of adequate seismic design code provisions.

In the following section, seismic evaluation methods and standards guide lines, analytical method, nonlinear static pushover analysis, capacity spectrum method; past study on seismic evaluation of gravity load designed buildings, modeling of components and finally modeling of shallow foundation are discussed herein.

2. Seismic evaluation methods and standard guide lines

Many literature reviews can be found on seismic evaluation of existing building and performance based designed of new building base on current published report of FEMA-356, FEMA-273 and ATC-40 guide lines. The main objective of these reports was to develop a comprehensive and first hand practical methodology that could guide engineers and designers in all seismic zones over United States of America in evaluating seismic vulnerability of existing buildings. This also provides uniform guidelines to specify and mitigate seismic prone to existing buildings and its individual structural components. These reported guidelines are practicable to all

types of building constructions and its material used, be it reinforced or unreinforced masonry building. The evaluation procedures start with the classification of building types and construction types. Then identification of evaluation statement that are most appropriate for each building type. In the analysis, calculation of capacities and demands of the building elements are involved in order to check against the allowable Capacity Demand. The capacities are normally calculated based on the building code provision in UBC and AISC. Demands were computed by equivalent lateral force procedures or dynamic lateral force.

Building Seismic Safety Council (BSSC), 1992 reported the National Earthquake Hazards Reduction Program (NEHRP), Handbook for Seismic Evaluation of Existing Buildings, FEMA-178. This handbook reveals similar procedures or guide lines depicted to that of ATC-40 for evaluation of existing buildings.

The published reports ATC-40-1996 currently available provides a good guidelines and procedures on Seismic Evaluation and Retrofit of Concrete Buildings. In this document, it describes beyond linearly elastic capacity of the structure to overcome the limitations occurred by the previous methods by introducing simplified nonlinear static analysis. This document presents several other methods for performing the nonlinear static analysis; however capacity spectrum method (CSM) and displacement coefficient method (DCM) are given more emphasis particularly in this document. Simplified nonlinear analysis procedures using pushover methods require determination of three primary elements: Capacity, Demand and Performance point. Capacity is the representation of the structure's ability to resist seismic demand. Demand represents the earthquakes ground motion. The performance point is the point where capacity and demand curves meet. The performance point represents the global behavior of the structure. In addition, ATC-40 provides detailed guidelines for modeling and acceptance criteria for variety of reinforced concrete element. However, the guidelines for evaluation for un-reinforced masonry walls and precast concrete components are not covered in this report.

The Federal Emergency Management Agency (FEMA), 1997 published NEHRP guidelines for the Seismic Rehabilitation of Buildings, FEMA-273 which was upgraded to FEMA-356 in 2000. This guidelines and procedures reported both traditional linear and nonlinear analysis. This document also presents additional features to overcome the limitation possessed by ATC-40 such as modeling techniques of non-structural components like partition and masonry walls which are no exception in the case of seismic evaluation of existing reinforced concrete buildings. Therefore in this study, both the guide lines were adopted simultaneously for seismic evaluation of existing building.

3. Analytical Method

Due to technological advancement in structural and computer engineering make it possible to determine the inelastic behavior of the building structures. There are several analysis methods, both elastic (linear) and inelastic (nonlinear) for the analysis of the existing buildings. The most common methods are: Linear Static (LS), Linear Dynamic (LD), Nonlinear Static (NS) and Nonlinear Dynamic (ND). Due to its simplicity, linear analysis, LS and LD, are normally used by the practicing structural engineers. However, these methods cannot predict the inelastic response of the building because the building components have infinite strength and constant stiffness during the analysis. For nonlinear analysis, NS and ND, a nonlinear building model attempts to capture the strength and the stiffness degradation of the building components as they are damaged. Therefore, the seismic behavior of the buildings can be predicted by using these analysis methods. However, nonlinear dynamic (ND) analysis method is often lengthy, complex and demanding (Korkmaz et al. 2007). It is not practical for general use and many codes preferred to use of nonlinear static procedures called nonlinear static pushover analysis for the seismic analysis of existing reinforced concrete structures.

In FEMA-356 and ATC-40 also suggested using the nonlinear pushover analysis. In most of the practical cases from the past literature review, simplified method so called nonlinear static analysis has been implemented. In this study

nonlinear static analysis (Nonlinear Static Pushover) was used for the evaluation seismic performance of the selected building.

4. Nonlinear static pushover analysis

Pushover analysis is commonly used to refer as nonlinear static procedures (NSP) applied to evaluate the seismic performance of existing structures, as well as design of new buildings. Pushover analysis is a powerful tool for performance based design (PBD) methodology, which is presented in several recent seismic regulations and guidelines. Pushover analysis is carried out by applying a series of inelastic static analyses on the building using a pre-selected lateral load pattern based on the first vibration mode of the structure or equivalent static lateral load patterns in seismic regulations. The load pattern remains unchanged during the pushover but its magnitude is increased incrementally until the building reaches a specific target displacement (Mohamed Nour 2007). In general, this target displacement is taken to represent the top displacement of the building when it experiences an earthquake ground excitation. The results of pushover analysis are used to estimate the capacity of the building by plotting the variation of the top displacement with the base shear of the building. This curve is known as the pushover or capacity curve of the building, as illustrated in Figure 2.

Pushover analysis has been developed based on the assumptions that the seismic response of the building is dominated by a single mode and that the shape of this mode remains invariant throughout the analysis. This enables to relate the response of the multi-degree of freedom (MDOF) building with the response of an equivalent single degree of freedom (SDOF) system, as illustrated in Figure 3. Despite lack of rigorous theoretical basis, earlier studies have shown that Pushover analysis has yielded adequate estimates of the maximum seismic response of MDOF systems in which the response is mainly controlled by a single mode (Mohamed Nour 2007).

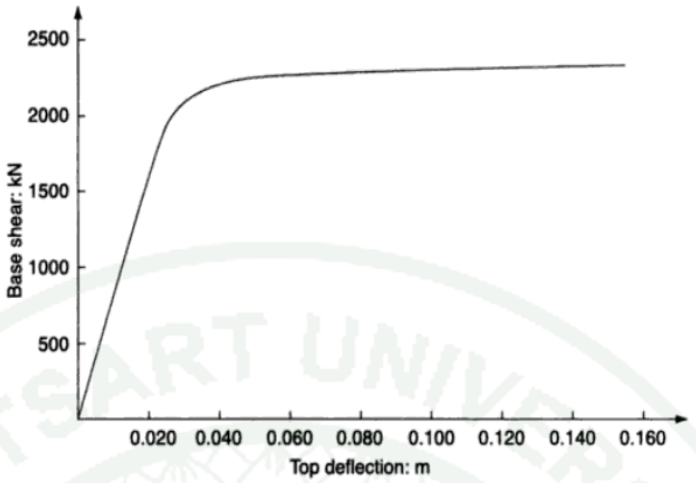

Figure 2 Pushover curve

Source: Edmund and David (2004)

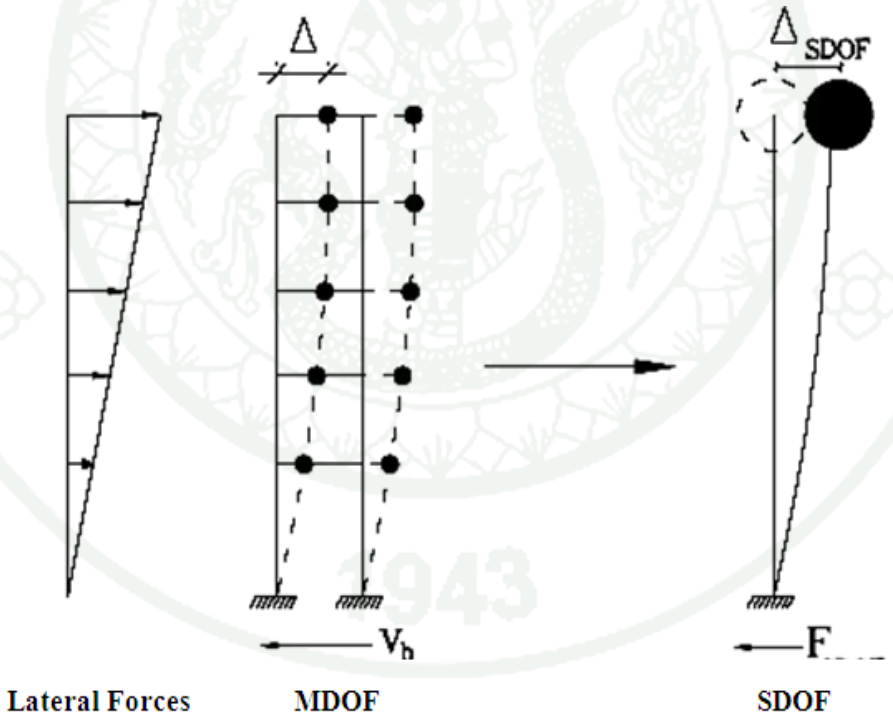

Figure 3 Equivalent SDOF system parameters

Source: Mohamed (2007)

Fajfar 2000 applied Pushover analysis to analyze both a symmetric and an asymmetric model of seven-story reinforced concrete frame-wall building. Pushover

analysis is performed until predetermine displacement is reached at which the seismic performance of the building is evaluated. The target displacement serves as an estimate of the expected global displacement of the building under a design earthquake.

Pushover analysis is perform by subjecting a structure monotonically increasing pattern of lateral forces representing inertial forces which would be experiencing by the structures when subjected to ground motion. Under incrementally increase loads various structural elements yields sequentially. Consequently at each event the structures experience a loss in stiffness. Using pushover analysis, a characteristic non-linear force displacement relationship system can be determined (Fajfar, 2000).

The nonlinear static analysis is mainly a performance evaluation procedure which is used as a tool to obtain further insight into the seismic behavior of structures that cannot be obtained from the elastic static or dynamic analysis. The demand and capacity are the two main key elements for the performance based designed and seismic evaluation of existing buildings. The primary objective of nonlinear static analysis is to obtain estimates of the global lateral strength (capacity), the global displacement (demand), and the failure mechanism of a structure which is likely to experience in an earthquake ground motion. The obtained results are used to assess the integrity of the building system. In addition, this analysis method is also applicable in determining the yielding distribution hierarchy and when it is used together with the demand spectrum, it may be used to predict the maximum deformation in the structure under the seismic action.

The nonlinear static pushover analysis becomes one of the most popular methods of analysis of buildings in the recent times. Linear analysis provides reasonable indication of the elastic capacity of the structures which predicts first yielding occurs. Beyond first yielding, failure mechanism and account for redistribution of forces during progressive yielding can’t be estimated by linearly elastic analysis procedures. Therefore nonlinear analysis procedure can be useful for

the approximation of behavior of the building that actually performs by identifying failure modes and potential for progressive collapse of the building. The use of nonlinear procedure for design and evaluation is an attempt to help engineers for better understanding as how structures will behave when it is subjected to earthquake ground motion, were it is assumed that linearly elastic capacity of the structure is exceeded.

Nonlinear static pushover analysis provides graphical representation of the global force displacement of the structure. It's normally said to be capacity or pushover curve. Nonlinear static pushover analysis has become the most commonly used method to determine the nonlinear behavior of the building structures in the recent years. In this simplified method, a capacity curve is obtained which shows the relation of base shear and roof displacement. This curve represents the behavior of the building structure under increasing base shear forces. As the capacities of the members of the lateral force resisting system exceed their yield limits during the increasing of the base shear forces, the slope of the force-deformation curve will change, and hence the nonlinear behavior can be represented.

The pushover analysis is performed in order to develop the capacity curve or pushover curve of the building to be used for seismic evaluation or performance based design. Pushover analysis can be described as applying lateral loads in patterns that represent the relative inertial forces generated at each floor level and pushing the structure laterally under lateral loads step by step in presence of gravity loads to predetermine displacement is reached. The pushover analysis provides not only the relationship between a base shear and roof displacement normally called as capacity curve of the building but also indicates the inelastic limit as well as lateral loads carrying capacity of the structures. The predetermined initial load pattern is applied incrementally into frame work structures until a plastic collapse mechanism is reached (Tetsuro *et al.*, 2003).

In ATC-40, the capacity curve is normally developed by assuming that the fundamental mode of vibration is predominant which represent first mode of response

of the structures. It is given that the valid fundamental periods of vibration are up to one second. By assuming this, the initial load pattern applied to the structure is in proportion to the product of the mass and the fundamental mode shape.

In the pushover analysis, the structure is loaded until the plastic hinges are enough to create a collapse mechanism or target displacement is attained. The base shear obtained at this target displacement is approximately assumed to be the true lateral strength of the building (Tangsaereemankong, 1998).

The simplified nonlinear analysis, popularly known as pushover analysis uses series of elastic analysis with increment in lateral loads to the structures which finally approximate the capacity of the structure in terms of force-displacement relationship. The lateral forces are applied until the most of the component of the structures are yield or degrade. This process repeats until the whole structure becomes unstable or predetermine target is achieved (Kiattivisanchai, 2001).

In nonlinear static pushover analysis, the magnitude of the structural loading is incrementally increased in accordance with a certain predefined loading pattern. With the increase in the magnitude of the loading, weak links and failure modes of the structure are found at required level. Due to these reasons nonlinear static pushover analysis is an attempt by the structural engineering profession to evaluate the real strength of the structure and it is simple and effective tool for performance based evaluation.

The purpose of the pushover analysis is to evaluate the expected performance of a structural system by estimating its strength and deformation demands for design earthquakes by means of a static inelastic analysis, and comparing these demands to available capacities at the performance levels of interest. The sequence of component yielding, failure and history of formations of hinges in the components can be traced as the lateral loads are monotonically increased (Kunnath *et al.*, 1996). The evaluation is based on an assessment of important performance parameters, including global responses and individual component deformations of the structure. The nonlinear

static pushover analysis can be viewed as a method for predicting seismic force and deformation demands, which accounts in an approximate manner for the redistribution of internal forces occurring when the structure is subjected to inertia forces that no longer can be resisted within the elastic range of structural behavior. The pushover is expected to provide information on many response characteristics that cannot be obtained from an elastic static or dynamic analysis.

5. Capacity Spectrum Method

The capacity spectrum method (CSM) was originally developed by S.A Freeman, 1975. Its concept has been introduced in several US guidelines for seismic evaluation and retrofit of existing buildings such as ATC-40 and FEMA-273. The capacity spectrum method (CSM) is an approximate procedure to analyze the seismic response of a structure with a nonlinear static pushover analysis.

In the Capacity Spectrum Method, the capacity curve is obtained from the Pushover analysis and then transformed to equivalent spectral coordinates. For each point on the capacity curve, the base shear and roof displacement quantities are transformed into equivalent spectral pseudo acceleration and spectral displacement quantities, respectively. This transformed capacity curve is referred to as the capacity spectrum. The target displacement is calculated by finding the intersection between the capacity spectrum and the demand spectrum.

The capacity spectrum method helps to analyze the seismic response of the structure in terms of forces and displacement and permits to describe efficiently the seismic performance of structures. However, this method is well adapted for the analysis of structure where the responses of structures are dominated by fundamental vibration mode (Lee *et al.*, 2005).

The capacity spectrum method requires the construction of capacity curve and seismic demand spectrum plotted in the spectral acceleration and spectral displacement domain referred to as Acceleration-Displacement Response Spectra

(ADRS) format as shown in Figure 4. Capacity spectrum represents the structure's ability to resist the seismic demand. Demand spectrum represents the earthquake ground motion. The intersection of the capacity spectrum and demand spectrum represent the performance point of the structures.

Recently, Mahaney *et al.*, 1993 introduced the Acceleration-Displacement Response Spectra (ADRS) format. This format requires that both the seismic demand spectrum and capacity curves be plotted in the spectral acceleration and spectral displacement domain. The graphical representation of the building response in the ADRS is a great help for the understanding of the analysis results. By using this format, the capacity curve that was typically established from nonlinear static pushover analysis is transformed into capacity spectrum by using the modal participation factor and modal mass coefficient for the first mode of vibration.

The demand spectrum curve is normally estimated by reducing the standard 5% damped design spectrum from Figure 5. On the other hand, the seismic demand spectrum is also transformed from standard S_a versus T format to ADRS format as shown in Figure 6.

The capacity spectrum computed from the nonlinear static pushover analysis is superimposed on the demand spectrum. The performance point is the intersection point between capacity and demand spectrums as shown in Figure 7 and 8.

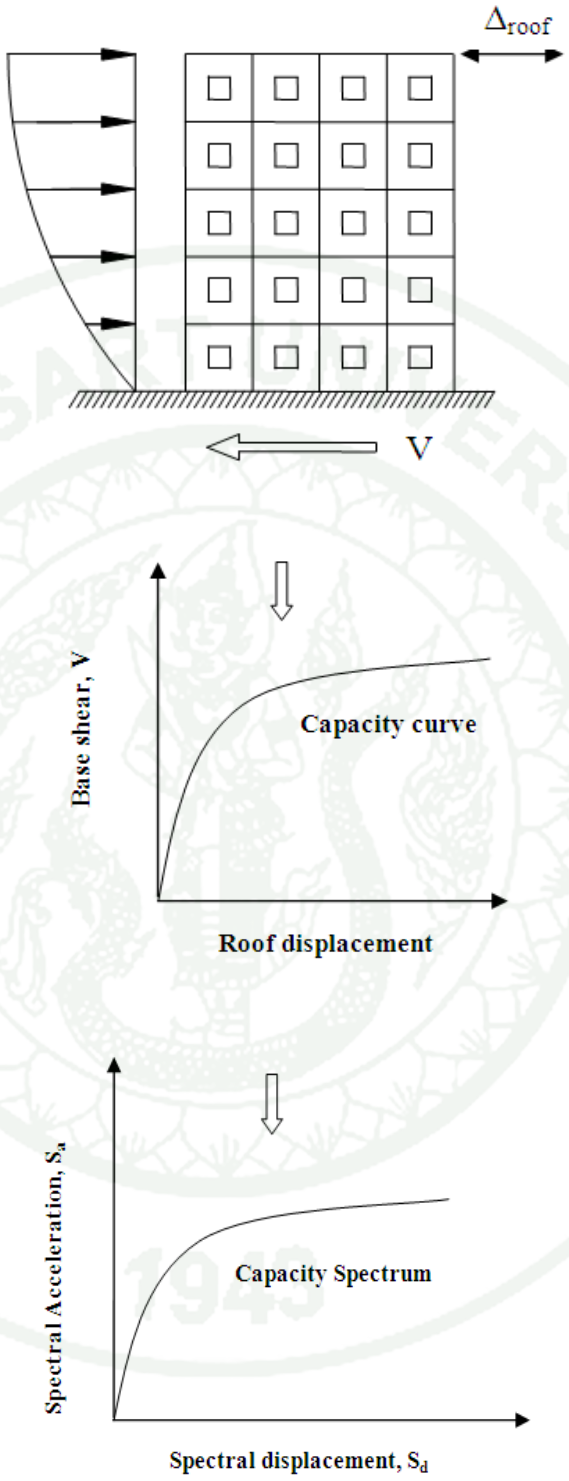

Figure 4 Capacity Spectrum curves as a result of Pushover curve

Source: Phatiwet (2002)

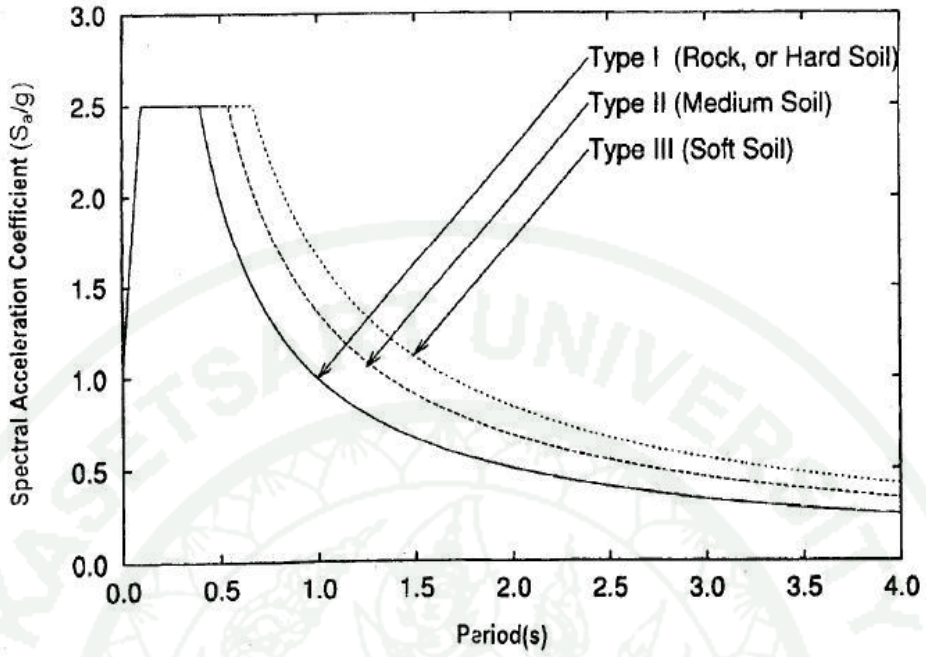

Figure 5 Response Spectrum for 5% damping

Source: IS-1893 part-1(2000)

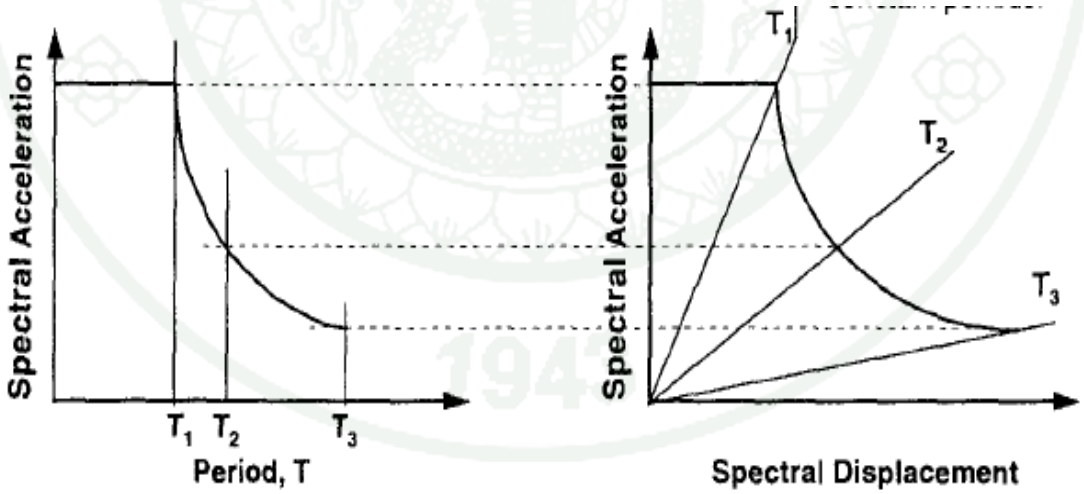

Figure 6 Demand Spectra (a) Standard Format (b) ADRS format

Source: ATC-40 (2000)

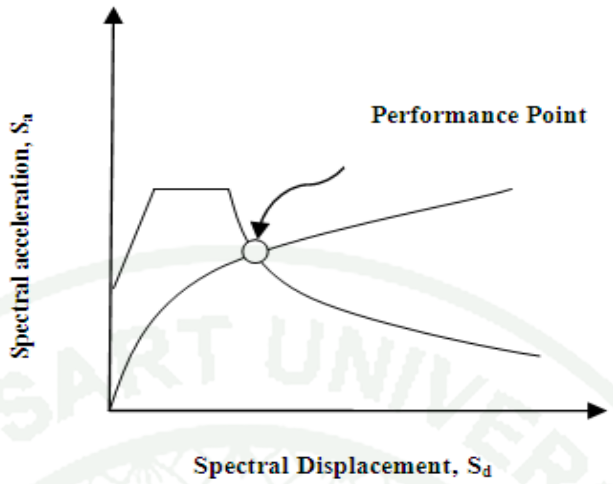

Figure 7 Capacity Spectrum superimposed over demand spectrum in ADRS format

Source: Kiattivisanchai (2001)

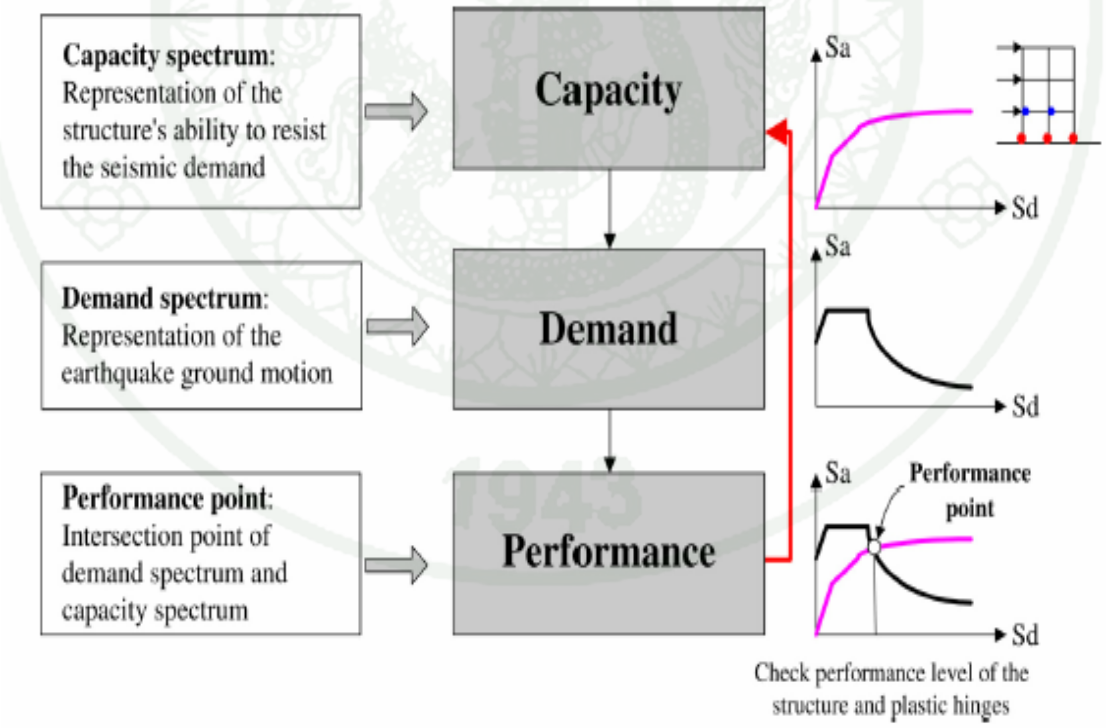

Figure 8 Pushover Analysis procedures

Source: Zou (2005)

6. Acceleration-Displacement Response Spectra (ADRS)

As stated earlier, the application of the capacity spectrum technique requires that both the demand responses spectra and structural capacity (pushover) curve be plotted in the spectral acceleration, S_a and spectral displacement, S_d domain, or so called Acceleration-Displacement Response Spectra (ADRS).

To construct the capacity spectrum, the base shear and roof displacement of capacity curve of the building is converted into spectral acceleration and spectral displacement respectively. Any point and V_{roof}, on the capacity curve is converted to corresponding point S_a and S_d on the capacity spectrum using the Equations as follows:

$$S_a = \frac{V/W}{\alpha_1} \tag{1}$$

$$S_d = \frac{\Delta_{roof}}{PF_1 \phi 1_{roof}} \tag{2}$$

$$PF_1 = \left[\frac{\sum_{i=1}^{N} (w_i \phi_i 1) g}{\sum_{i=1}^{N} (w_i \phi_i 1^2)/g} \right] \tag{3}$$

$$\alpha_1 = \frac{\left[\sum_{i=1}^{N} (w_i \phi_{i1})/g \right]^2}{\left[\sum_{i=1}^{N} (w_i)/g \right] \left[\sum_{i=1}^{N} (w_i \phi_{i1}^2)/g \right]} \tag{4}$$

Where

S_a = Spectral acceleration

S_d = Spectral displacement

PF_1 = Modal mass participation factor for the first natural mode

α_1 = Modal mass coefficient for the first natural mode

W_i / g = Mass assigned to level i

N = Total number of floors of the building

V = Base shear

W = Building dead load weight plus live loads

$\phi_i 1$ = Amplitude of mode 1 in level i

V_{roof} = lateral roof displacement

To compare with the capacity spectrum, every point on a demand spectrum was transformed from the standard S_a versus T format to ADRS format which can be done by using equations as follows:

$$S_d = \frac{S_a T^2}{4\pi^2} \tag{5}$$

In the ADRS format, lines radiating from the origin have constant period as shown in Figure 6. For any point on the demand spectrum in ADRS format, the period T can be computed using the relationship as follows:

$$T = 2\pi\sqrt{\frac{S_d}{S_a}} \tag{6}$$

7. Past studies on seismic evaluation of gravity load designed building

G. Magents and S. Pampanin 2004, had carried out comprehensive experimental-analytical studies on the seismic vulnerability of existing reinforced concrete frame buildings, designed for gravity-loads only as typically found in most seismic prone countries before the introduction of adequate seismic design code provisions, confirmed the inherent weaknesses of these systems, due to inadequate detailing and the lack of capacity design principles. They also noted that controversial effects on the global inelastic mechanism can be expected depending on the infill's properties.

The seismic vulnerability of some frame structures, typical of existing reinforced concrete buildings designed only to carry vertical loads, has been evaluated (Masi, 2003). A simulated design of the structures has been made with reference to the codes, the available handbooks and the current practice at the time of construction. The seismic response is calculated through non linear dynamic analyses. The results showed a high vulnerability for the buildings having irregular infill configuration especially open first storey without infill walls.

Maria *et* al., 2008 did study the vulnerability analysis of gravity load designed reinforced concrete building in Nepal and Italy. In order to reproduce a significant sample of building models, effectively representing the existing building stock, the simulated design was analyzed to a number of buildings defined by Lx-Ly dimensions conveniently by considering variation of geometric, structural configuration, material properties within each building. Push-over analysis along short direction was performed for each one of them as short direction is generally the weaker one for gravity load designed buildings (Mariniello, 2007).

Pichit Phatiwet, 2002 evaluated the seismic performance of gravity load designed building in Bangkok adopting a simplified model of beam-column joint and rigid end offset. The result of the study showed that the lack of transfer reinforcement within the joint in beam-column can lead to brittle shear failure of connections. Also the lateral deformation capacities are greatly reduced.

Lakshmanan, 2006 has evaluated the seismic performance of the buildings in India. Pushover analysis and evaluation of performance of the building using capacity spectrum method was carried out. Evaluation was carried out in accordance with ATC-40, FEMA-356 and IS: 1893, 2002. It was emphasized that the existing procedure is grossly approximate, and hence improving sections of the approach to high levels of accuracy would not necessarily lead to better result.

In 2001, Kiattivisanchai applied the guidelines of ATC-40 and FEMA-273 for evaluating the seismic performance of a typical medium-rise reinforced concrete

building in Bangkok designed by local engineer. A nine story existing gravity load designed reinforced concrete building in Bangkok was chosen as a case study to evaluate the seismic performance of existing reinforced concrete building; and to implement aforementioned seismic evaluation procedures. He used simplified non linear static pushover analysis as an analysis method. In his study, modeling of foundation, and masonry infill walls were emphasized. Also, an approximate method to estimate vertical stiffness of piles using the data compiled by Arworn, 1998 was presented. The evaluation results indicated that the building had sufficient capacity to withstand the highest intensity of earthquake ground motion expected in Bangkok despite the fact that building was designed without any consideration of seismic loading.

8. Brick Masonry Infill Walls

The masonry infill walls are generally used in reinforced concrete frame structures for the functional reasons and normally considered as architectural component by the structural engineers as they are constructed after the frames structures being casted. These walls are built in the vertical plane defined by adjoining pairs of beams and columns. Infill walls are considered to be weak as compared to structural components and they are term as nonstructural components in the building system by structural engineers.

In Bhutan, generally the effect of infill walls on the design of reinforced concrete structures has been ignored. The weight of the infill on the structure has been considered in the structural frame model but not model in the design of building. The model contains only beams, columns and slabs. Therefore in the real behavior of the buildings with infill walls during the earthquake will be different from the case without infill walls (Cagaty, 2004).

In plane strength prediction of infill frames is a complex, statically indeterminate problem. The strength of composite infill frame system is not simply the summation of infill properties plus those of frames (Chaar *et al.*, 2002). Great

efforts have been invested, both experimentally and analytically to better understand and estimate the composite behavior of masonry infill frames. The full-scale experiment of single bay infill frames with brick and clay block was done (Wood *et at*., 1958). The stiffness determination was base on the shearing and bending stiffness of a vertical cantilever was their work. Sachanski, 1960 studied the problems in different manner as adding the shear to be loaded along the faces of the infill. Base on his theoretical investigation, numbers of full-scale test was carried on frame buildings without openings.

Many of the past studies in the literature shows that their experimental testing of infill frames under lateral loads resulted in the specimen deformation shape similar to one illustrated in the Figure 9.

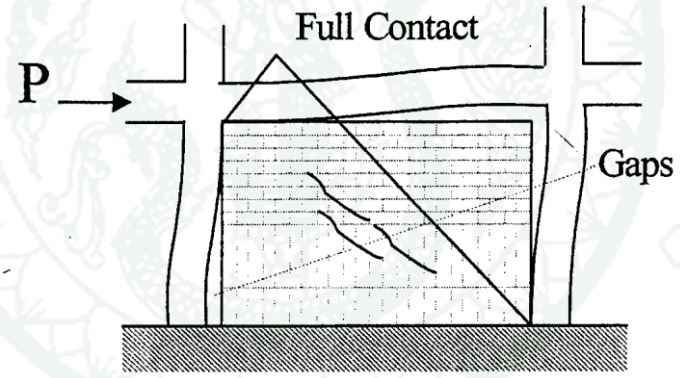

Figure 9 Specimen of deform Shape
Source: Chaar (2002)

During testing of the specimens, the diagonal cracks develop in the centre of the panel and gaps form between the infill and panel on the non-loaded diagonal corners of the specimens, while full contacts was observed in the two loaded diagonal corners. This behavior leads to simplification in infill frame analysis by replacing the masonry infill with an equivalent compressive masonry struts.

The concept of equivalent compressive diagonal strut was first proposed by Holmes (1961) base on series of experiments and analytical investigation carried out on steel infill frames with concrete and masonry. He derived the formula to predict lateral stiffness and strength of infill frame and then proposed the effective width (w) of compressive diagonal strut as one third of the infill diagonal length (d) as given by equation 7.

$$W = \frac{d}{3} \tag{7}$$

Bryan Stafford Smith (1962), in order to determine the lateral stiffness of the infill frames, he made an assumption that infill and frame are not constructed integrally, nor they are bonded together. His main contribution in the world of infill frames studies was that he found the frame gets separated from infill by three-fourth of the length of each unloaded corners of the infill panels. Only one-fourth of frame length remains contact with the infill at each loaded corners of infill panels as shown in Figure 10. From these observation, he drew a conclusion that infill behaves as equivalent structures approximately.

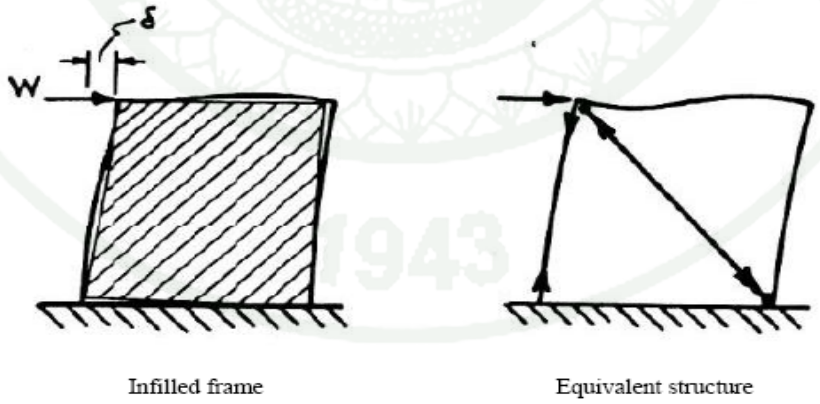

Figure 10 Infill frame and equivalent structures
Source: Smith (1962)

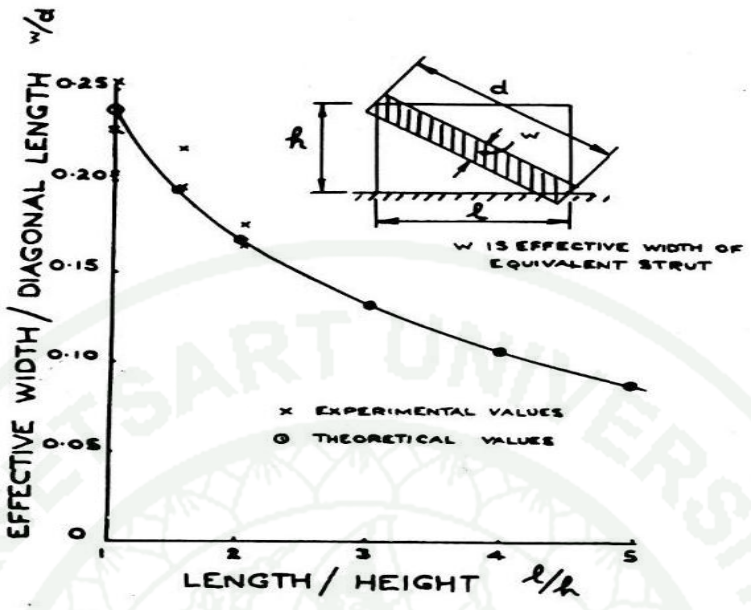

Figure 11 Width of infill wall
Source: Smith (1962)

He developed the relation among, length (*l*), height (*h*), diagonal length (*d*) of infill and effective width of diagonal strut (*w*) which can be replaced over the full infill frames for the prediction of lateral stiffness of the infill frame. This was achieved base on comparing experimental and theoretical analysis results. He found that stress along the loaded diagonal panel increases, resulted in reduce of elastic modulus. Therefore strain got increases and panel becomes more flexible than predicted. The proportionality plot between effective widths of diagonal strut and diagonal length is shown in Figure 11.

In 1966-1967, B.S. Smith had done extensive experiment on small scale frame infill with mortar and developed the equivalent diagonal compressive strut replacing the infill walls to evaluate the lateral stiffness and strength of the infill frame structures. Another model for representing the brick infill panel by equivalent diagonal strut was proposed by Smith and Carter (1969) as given by equations 8 and 10.

$$W = 0.58\left(\frac{l}{h_m}\right)^{-0.445}(\lambda h)^{0.335d}\left(\frac{l}{h_m}\right)^{0.064} \quad (8)$$

Mainstone (1971) observed that unreinforced masonry contains weak shear planes along the bed joints, which may initiates degradation prior to diagonal crushing failure. To evaluate the stiffness on in-plane masonry infill, FEMA-273 adopted the relation proposed by Mainstone as given by equation 9 and 10.

$$\frac{W}{d} = 0.175(\lambda h)^{-0.4} \quad (9)$$

$$\lambda h = hx\sqrt{\frac{E_m t \sin 2\theta}{4E_c I_c h_m}} \quad (10)$$

Pauley and Priestley (1992) had recommended the effective strut width of one quarter of the diagonal length as given by equation 11.

$$W = \frac{d}{4} \quad (11)$$

Where, h is height of column between centre lines of beams, E_c and E_m are young's modulus of frame and infill panel respectively, t is thickness of infill panel, θ is angle of inclination of diagonal strut with the horizontal, I_c is the moment of inertia of column, h_m is the height of infill, w is the effective width of the diagonal strut and d is the diagonal length of infill.

The in-plane lateral forces at low level, the frame and infill wall shows composite behavior along with the boundary elements. When the lateral force increases, the frame tries to deform in a flexural mode as the lateral deformation increases. On the other hand infill wall panel deforms in shear mode which exhibits the separation between infill wall and surrounding frame at the unloaded corners and

development of diagonal compression strut along the loaded corners as shown in Figure 12.

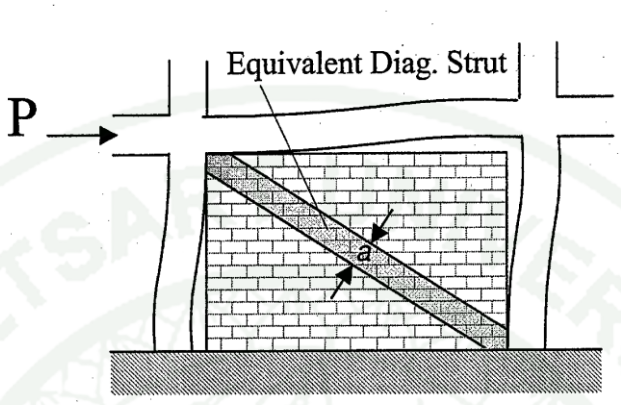

Figure 12 Equivalent diagonal strut
Source: Chaar (2002)

In case of partially infill frame shown in Figure 13, to determine the effective width of equivalent strut, the same equation 9 and 10 can be used, but the reduced column length (L_{column}) is equal to the un-braced opening length for the windward columns, while (L_{column}) for the leeward's sides is defined as usual should be used in the equations.

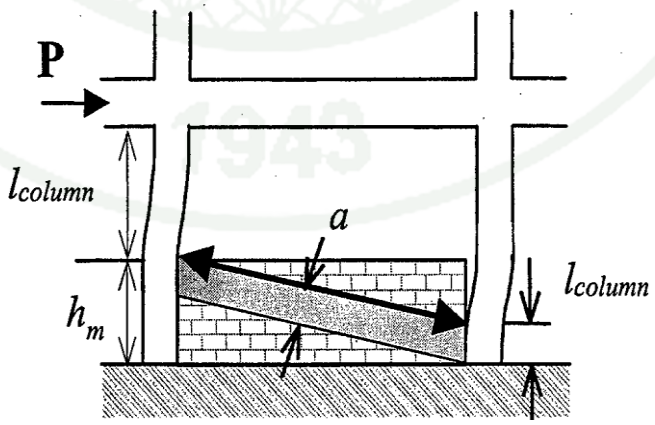

Figure 13 Partially Infill Frame
Source: Chaar (2002)

The presence of opening in the infill panel found to be adversely affecting the lateral stiffness of the infill frames, especially when position of the opening moves towards the compression diagonal (Mallick and Garg, 1977). They recommended that door location can be best suited in the centre of the lower half of the panel and window opening in the mid-height of the left or right of the panel near to the vertical edge of the panel as possible. The opening in the infill panel contributes large deductions on the strength and stiffness of the infill frame by imposing early cracks usually on the top corners of the openings (Liauw, 1979).

The openings in unreinforced masonry infill walls creates more room for desirable cracking pattern than the extensive bed joint cracking that occurs in the full panel infill walls. For the infill panels with openings, multi-strut configuration can be used to capture the boundary conditions generated by the openings (Buonopane, 1999) as shown in the Figure 14.

Mehmet and Altin, 2006 found that the aspect ratio of the infill wall increases, the lateral strength and rigidity increases significantly in the case reinforced concrete frame with reinforced concrete partially infill walls. They also observed that placement of configuration of partially infill walls in the infill frame was not so much effective on the lateral strength but was very effective on the lateral stiffness of the specimens.

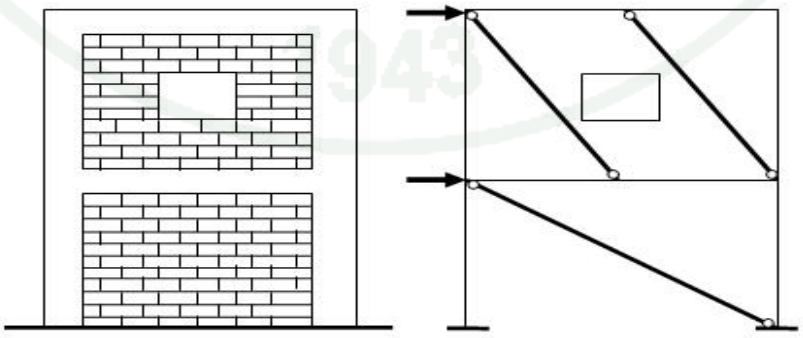

Figure 14 Multi-diagonal strut mechanisms for infill with opening
Source: Buonopane (1999) and Shrestha (2008)

9. Modes of failure of infill frames

Many of the past researchers observed that a separation between the infill wall and the frame element occurs when the infill frame is subjected to horizontal load at the top of the frame. Normally the separation occurs at early stages of the loading along the unloaded corners at the joint of the bottom beam and the compressed column as shown in Figure 15. The infill wall along the compressed diagonal gets stressed, while remaining portion of the wall receives less stress.

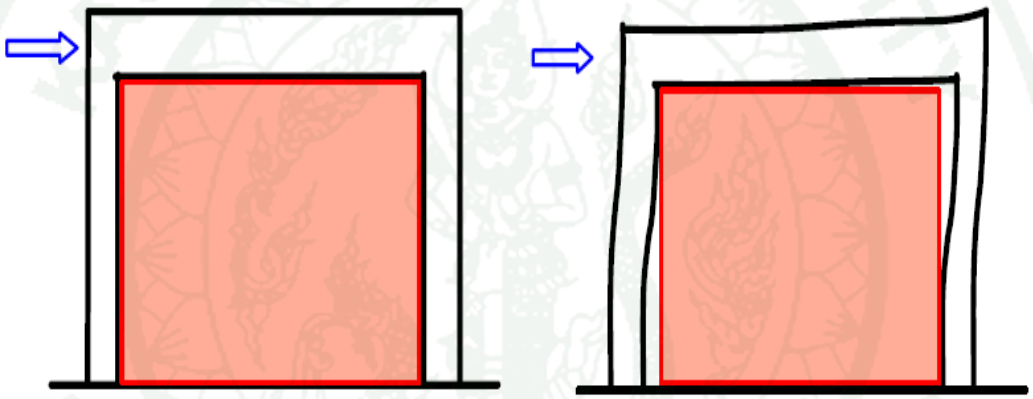

Figure 15 The infill frame subjected to horizontal force
Source: The Indian concrete journal (2004)

When the imposed horizontal force increases, at one point the infill frames structures will attain the maximum shear resistance. Beyond which the structure will undergo following failure mechanisms:

1) Compression failure mechanisms
2) Shear failure mechanisms
3) Tension failure mechanisms

9.1 Compression failure

Basically this compression failure prevails in the case of weaker frames in which the structural elements can't transfer considerably larger amount of forces to the compressed diagonal of the infill walls. Therefore, local crushing of the masonry or mortar in one of the compression corners of the infill wall as shown in Figure 16.

9.2 Shear failure

A masonry infill panel fails due to horizontal sliding shear along the mortar joints (Figure 10.b) when the masonry infill wall is weaker as compare to surrounding structural frame elements (Zarnic and Tomazevic, 1985).

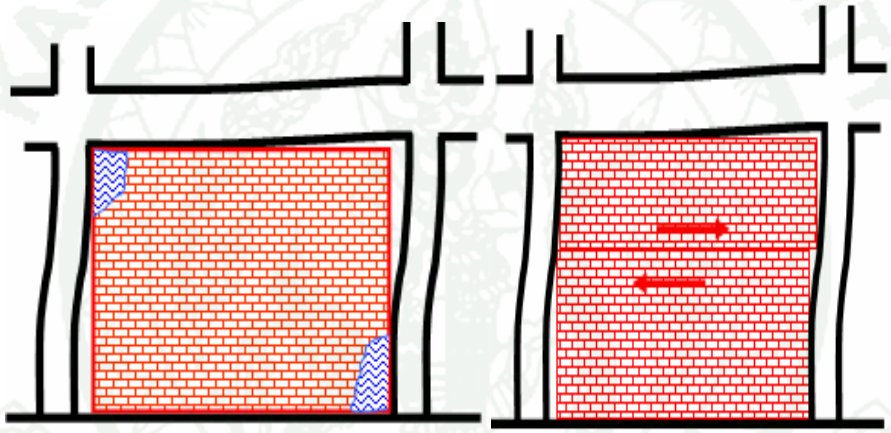

a. Local crushing of masonry b. shear failure

Fugure 16 Shear failure mechanism

Source: The indian concrete journal (2004)

9.3 Tension failure

The tension failure of the infill frame structure occurs either by failing of masonry infill or by surrounding frame element. The masonry diagonal tension failure also occurs in case of weak infill. The structural frame element especially column fails near the beam-column joints due to poorly design infill frame as shown in Figure 17. When the surrounding frame is strong enough, very large amount of forces imparts to the compression diagonal until the diagonal crack initiates within the infill

panel. As the shear force increases, these diagonal cracks propagate towards the central region of the infill wall (Mainstone, 1971).

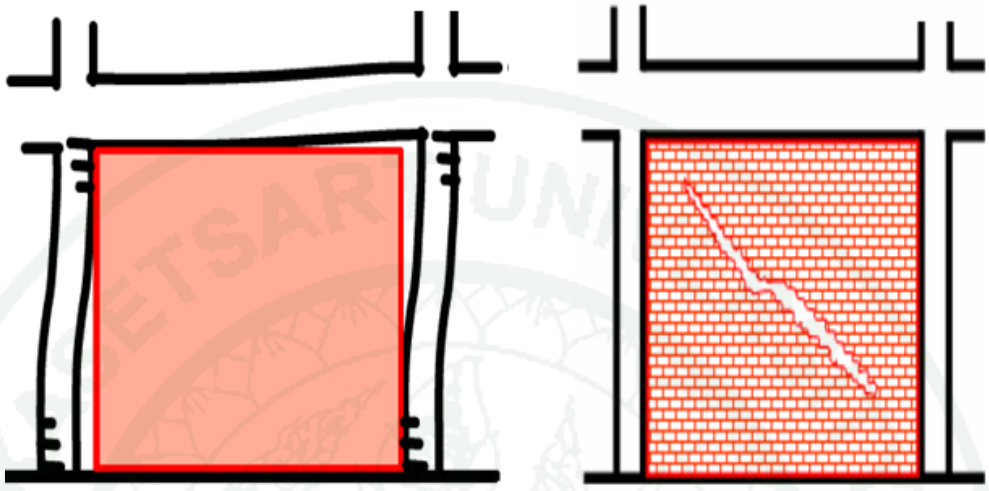

a. Column tension failure b. Diagonal tension failure

Figure 17 Tension failure mechanisms
Source: The Indian concrete Journal (2004)

To evaluate the lateral capacity and seismic performance of reinforced concrete building it is very much required to include the effects of masonry infill walls in the analytical modeling of buildings. Moreover by ignoring the infill walls in the analysis and design of the building structures may lead to substantial inaccuracy in predicting the lateral stiffness, strength and ductility of the structures. The interaction between infill walls and bounding frames may or may not effective to the performance of the building structures.

10. Foundations

A foundation (also called a groundsill) is a structure that transfers loads to the earth. Foundation systems for buildings can in some cases be complex. For the purpose of simplicity, foundations are generally broken down in to three categories and they are considered in the standard guidelines like FEMA-273, FEMA- 450 and ATC-40. They are as follows:

1) Shallow foundations
2) Deep foundations
3) Combination of shallow and deep foundation

10.1 Shallow foundations

These types of foundations are so called because they are placed at a shallow depth relative to their dimensions beneath the soil surface. Their depth may range from the top soil surface to about 3 times their breadth.

A shallow foundation is a type of foundation which transfers building loads to the earth very near the surface, rather than to a surface layer or a range of depths as does a deep foundation. Shallow foundations include spread footing foundations, mat-slab foundations, and slab-on-grade foundations. Shallow foundations are normally isolated or continuous spread footing or large mats that are vertically supported by bearing directly on the soil. When compared with deep foundations, they relatively flexible in resisting vertical and rotational actions.

10.2 Deep foundations

The most common of these types of foundations are piles. They are called deep because they are embedded very deep relative to their dimensions into the soil. Their depths may run over several 10s of meters. They are usually used when the top soil layer have low bearing capacity.

A deep foundation is a type of foundation distinguished from shallow foundation by the depth they are embedded into the ground. There are many reasons a geotechnical engineer would recommend a deep foundation over a shallow foundation, but some of the common reasons are very large design loads, a poor soil at shallow depth, or site constraints (like properties lines). There are different terms used to describe different types of deep foundations including piles, drilled shafts, caissons and piers. The naming conventions may vary between engineering

disciplines and firms. Deep foundations can be made out of timber, steel, reinforced concrete and pre-tensioned concrete. Deep foundations can be installed by either driving them into the ground or drilling a shaft and filling it with concrete, mass or reinforced. Most deep foundation elements are driven piles of steel or concrete or drilled cast-in-place concrete piers. These components rely on friction or end bearing for downward vertical support. Piers and piles are capable of significant resistance to uplift provided that they are adequately tied to the structures. Although deep foundations are relatively stiff and strong, this does not mean that foundation movements will not affect the structural response.

10.2 Combine of shallow and pile foundation

Combined systems of shallow and deep elements can be sensitive to foundation effects because of the inherent differences in strength and stiffness, particularly in the inelastic range. When the shallow footing beneath a shear wall begins to rock, a significant redistribution of load can ensue if other walls are supported on deep elements.

Foundation stiffness and strength influence the seismic performance of a structure. The structural engineers must include the effects of foundation in the analysis of model for the evaluation and retrofit of an existing building. In many instances the expert assistance from a geotechnical engineer is essential. Geotechnical engineers must keep in mind that stiff and strong is not necessarily better than flexible and weak. The very reason is revealed from Figure 18. Soft-weak assumptions for soils properties are not always conservative for the structures (ATC-40).

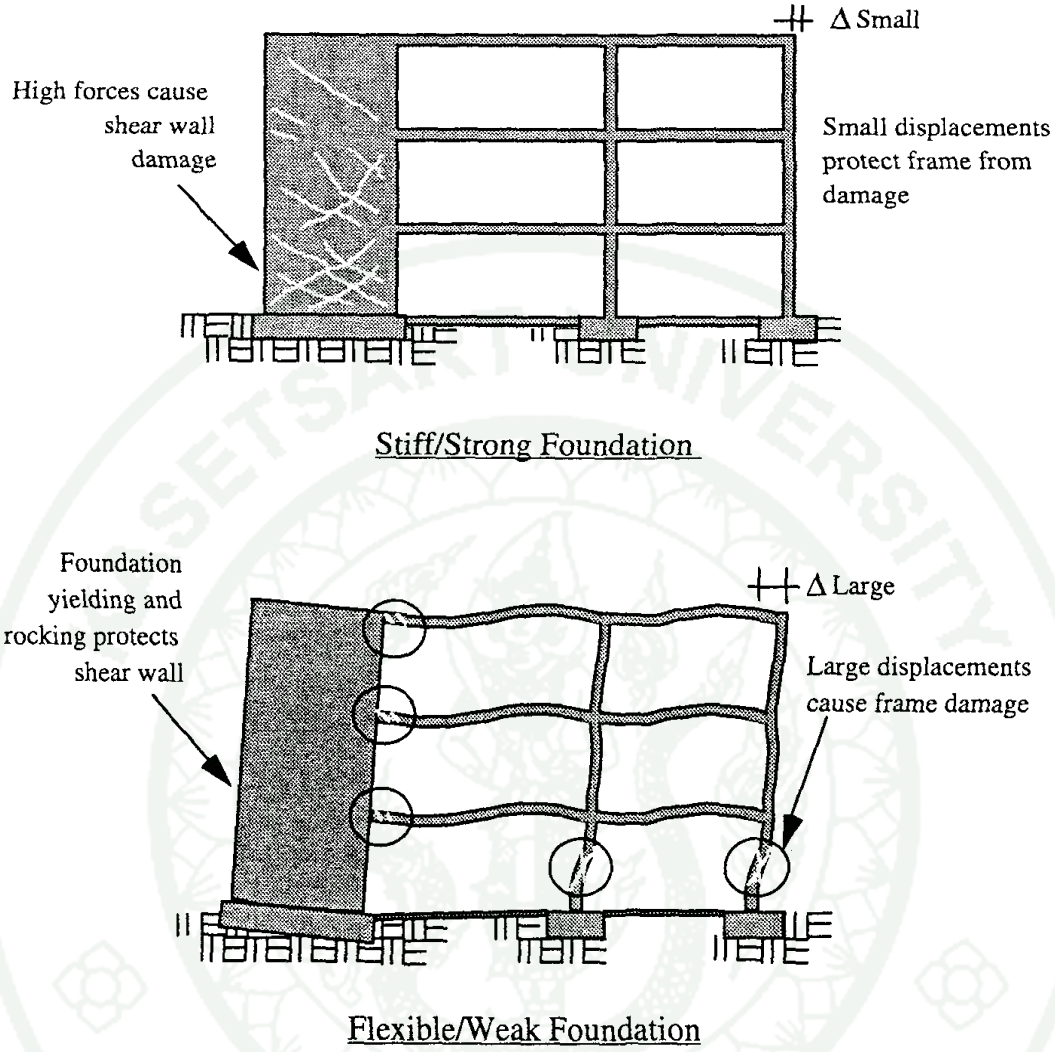

Figure 18 The foundation stiffness and strength affect various structural components
Source: ATC-40 (2000)

The shallow foundation in general can be modeled either by uncoupled component Model or Winkler component Model as shown in Figure 19. Most shallow bearing footings are stiff relative to the soil upon which they rest. For simplified analysis uncoupled model may be sufficient for shallow foundation (FEMA-273).

The three equivalent spring constants may be determined using conventional theoretical solutions for rectangular plates in terms of an equivalent circular radius as the details are given in FEMA-273. For more complex analysis a finite element

representation of linear or nonlinear foundation behavior may be accomplished using Winkler component models. Distributed vertical stiffness properties may be calculated by dividing the total vertical stiffness by area. Similarly, the uniformly distributed rotational stiffness can be calculated by dividing the total rotational stiffness of the footing by the moment of inertia of the footing in the direction of loading (ATC-40).

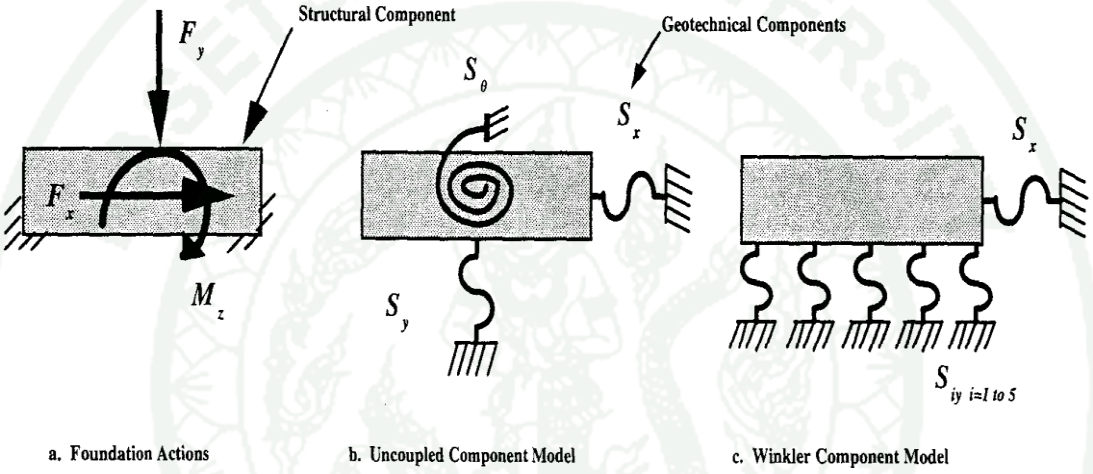

Figure 19 General Shallow Foundation Element Models
Source: ATC-40 (2000)

11. Nonlinear Behavior of Structural and Non-structural Elements

The nonlinear behavior of a building structure depends on the nonlinear responses of the elements that are used in the lateral force resisting system (Mehmet, 2007). Therefore, before applying any nonlinear analysis method on a building structure, the nonlinear behavior of such elements must be clearly described and evaluated. The nonlinear static and dynamics analysis tries to capture the strength and stiffness degradation of the building as they are damaged.

Generalized load deformation relationship given in FEMA-356 when the structural members exhibiting nonlinear behavior as shown in Figure 20. In this figure Q_c refers to strength of the component and Q refers to the demand imposed by the

earthquake. The linear response of load deformation relation is defined till point B. After point B, still linear response is observed even the member get yields but with reduced stiffness till point C. At point C there observed an abrupt reduced in load resistance of the member as graph drops to point D represent initial failure of the component. It may be associated with phenomenon such as fracture of longitudinal reinforcement, spalling of concrete or sudden shear failure. But still residual resistance is observed until point E which represent the components have lost the lateral load resistance but still capable of sustaining gravity loads. Point E is the maximum deformation capacity.

Deformation beyond these limits should not be permitted because gravity load can no longer be sustained. The above mentioned nonlinear response of the structural members is called hinge property which can be defined symmetrically in order to incorporate reversal actions in the calculations.

In ATC-40 and FEMA-356 provides the values of parameters A, B, and C during the modeling of nonlinear response of the elements. The acceptance criteria depending up on the plastic hinge rotations by considering different performance levels are also given in ATC-40 and FEMA-356.

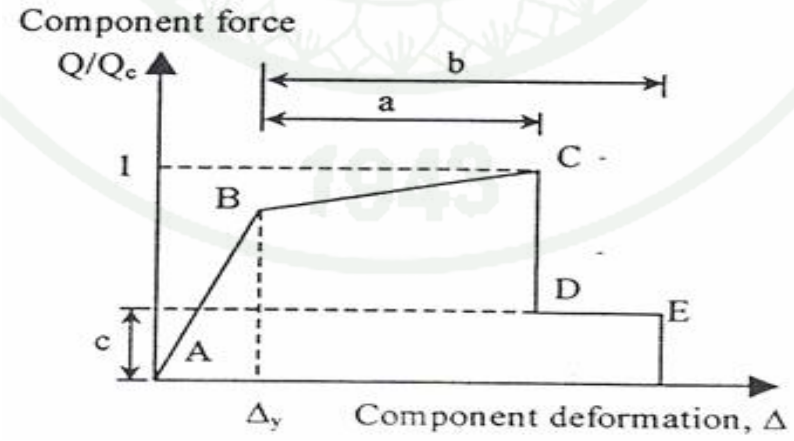

Figure 20 The generalized load deformation for nonlinear behavior of structure.
Source: FEMA-356

12. Component initial stiffness

To evaluate the lateral capacity of concrete frame structures, it is important that the distribution of component forces be based on realistic stiffness values applying close to the component yield force in order the ensure that the hierarchy of formation of component yield is correct (Kiattivisanchai, 2001). However, it is impractical to evaluate the properties of several cross sections in each component in the multistory buildings. Therefore the effective initial stiffness recommended in ATC-40 as shown in Table 1 was adopted in this study.

Table1 Effective initial Stiffness Values

Component	**Flexural Rigidity**	**Shear Rigidity**	**Axial Rigidity**
Beams-nonprestressed	$0.5E_c I_g$	$0.4E_c A_w$	$E_c A_g$
Beams-prestressed	$E_c I_g$	$0.4E_c A_w$	$E_c A_g$
Columns in compression	$0.7E_c I_g$	$0.4E_c A_w$	$E_c A_g$
Columns intension	$0.5E_c I_g$	$0.4E_c A_w$	$E_c A_g$
Walls-uncracked	$0.8E_c I_g$	$0.4E_c A_w$	$E_c A_g$
Walls-cracked	$0.5E_c I_g$	$0.4E_c A_w$	$E_c A_g$
Flat slabs-nonprestressed	-	$0.4E_c A_g$	
Flat slabs-prestressed	-	$0.4E_c A_g$	

Source: FEMA-273

Note: I_g for T-beams may be taken as twice the values of I_g of the web.

For shear stiffness, the quantity $0.4E_c$ has been used to represent the shear modulus G

13. Material Models

13.1 Concrete

Two parameters of concrete are compressive strength and modulus of elasticity. The compressive strength of concrete is usually obtained from cylinder with height to diameter ratio of 2. The typical stress-strain behavior of concrete loaded in uniaxial compression is nonlinear. The curves are almost linear up to about one-half the compressive strength. The strain at maximum stress is approximately 0.002. Idealized stress-strain curve of concrete in uniaxial compression is shown in Figure 21. The modulus of elasticity of concrete is generally determined by short term loading test by secant modulus at stress of approximately 0.5 f_c'. Besides, ACI 318-2002 recommends using Equation 12 for the modulus of elasticity of concrete.

$$E_c = W_c^{1.5} x 0.043 \sqrt{f_c'} \quad MPa \tag{12}$$

Where, W_c is the unit weight of concrete in Kg/m^3. For normal weight concrete, ACI-318-2002 recommends to take the modulus of elasticity of concrete using equation 13.

$$E_c = 4700 \sqrt{f_c'} \quad MPa \tag{13}$$

Modulus of elasticity of concrete as per Indian Standard, (IS 456:2000) recommends to use equation 14.

$$E_c = 5000 \sqrt{f_c'} \quad MPa \tag{14}$$

In this study, the modulus of elasticity of concrete recommended from Indian standard was used.

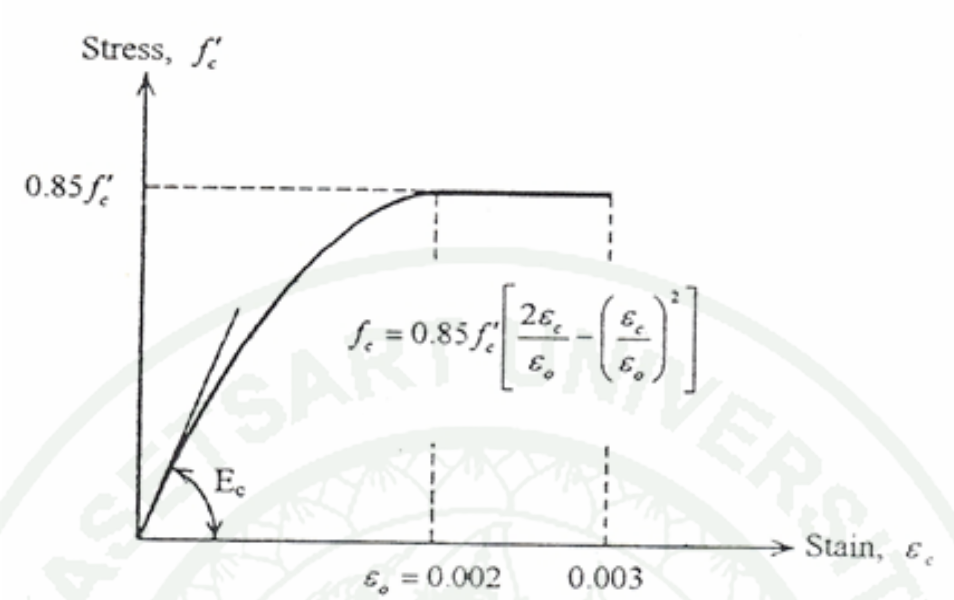

Figure 21 Idealized Stress-Strain Curve of Concrete in axial compression
Source: Phatiwet (2002)

13.2 Reinforcement

Typical stress-strain curves for steel bar used in reinforced concrete construction are obtained from bar loaded monotonically in tension. The curves exhibit an initial linear elastic portion, a yield plateau, a stain hardening range in which stress again increases with strain, and finally a range in which stress drops off until fracture occurs. Generally, the stress-strain curves for steel in tension and compression are assumed to be identical. The slope of the linear elastic portion of the curve gives the modulus of elasticity of the steel. The modulus of elasticity of the steel reinforcement E_s is generally taken as 2.0×10^5 MPa (IS: 456, 2000).

The stress at yield point, referred to as yield strength is a very important property of steel reinforcement. The specified yield strength normally refers to a guaranteed minimum. The actual yield strength of the steel is usually higher than the specified value.

14. Modeling of Beams

Beams have been modeled explicitly by the line elements having linear elastic properties along the length with nonlinear moment hinges at the locations at which potential yielding can occur along the beam span in order to represent the flexural plastic hinges. The plastic hinges that used to represent the flexure behavior of the beam have the moment-rotation relationship as show in Figure 22. The coordinates of the point at B gives the yield moment and yield rotation of the beam when the reinforcement bar in the beam attains the first yielding point. At point C, the moment rotation relationship which shows correspond to expected flexural strength that the member is likely to experience over the range of deformation. The plastic hinge rotation capacity at point C and E can be derived either from experiments or rational analysis.

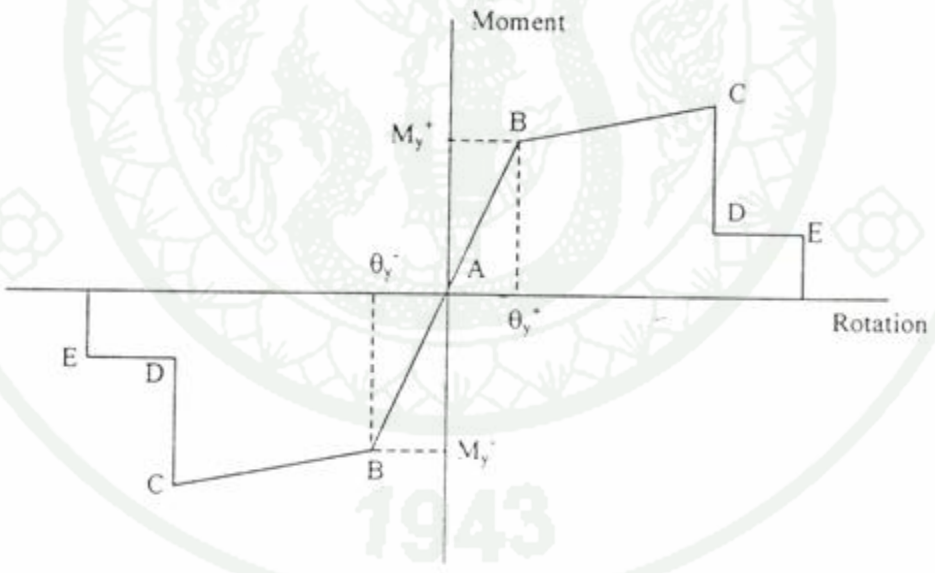

Figure 22 Moment rotation relation for moment hinges used in pushover analysis
Source: Kiattivisanchai (2001)

However the plastic hinge rotation capacity and acceptance criteria for plastic rotation in the reinforced concrete beam is recommended in ATC-40 and FEMA-356 Therefore these values were used in this study. Such type of modeling approach was

adopted by Kiattivisanchai, 2001, Phatiwet, 2002, and Lakshmanan, 2006 by using SAP2000 for the seismic evaluation of existing building. The plastic hinge rotation capacity recommended as par ATC-40 and FEMA-356 are shown in tables 2.

Table 2 Modeling parameter for nonlinear procedure-reinforced concrete beams

			Modeling Parameters [3]		
			Plastic Rotation Angle (rad)		Residual Strength Ratio
Component Type			a	B	C
1. Beams controlled by flexure [1]					
$\frac{\rho-\rho'}{\rho_{bal}}$	*Transverse Reinforcement*	$\frac{V}{b_w d\sqrt{f_c'}}$ [4]			
≤ 0.0	C	≤ 3	0.025	0.05	0.2
≤ 0.0	C	≥ 6	0.02	0.04	0.2
≥ 0.5	C	≤ 3	0.02	0.03	0.2
≥ 0.5	C	≥ 6	0.015	0.02	0.2
≤ 0.0	NC	≤ 3	0.02	0.03	0.2
≤ 0.0	NC	≥ 6	0.01	0.015	0.2
≥ 0.5	NC	≤ 3	0.01	0.015	0.2
≥ 0.5	NC	≥ 6	0.002	0.01	0.2
2. Beams controlled by shear [1]					
Stirrup spacing ≤ d/2			0.0	0.02	0.2
Stirrup spacing > d/2			0.0	0.01	0.2
3. Beams controlled by inadequate development or splicing along span [1]					
Stirrup spacing ≤ d/2			0.0	0.02	0.0
Stirrup spacing > d/2			0.0	0.01	0.0
4. Beams controlled by inadequate embedment into beam-column joint [1]					
			0.015	0.03	0.2

Source: FEMA-356

15. Modeling of Columns

Modeling of columns are done as similar manner to that of beams to adequately represent important characteristics of reinforced concrete column

components subjected to gravity and lateral loadings. Multiple failure modes, stiffness and strength degradation are considered. Columns are modeled as line element having linear elastic properties along its length with nonlinear moment-rotation hinges at the ends. However, there are significant axial force variations under the action of earthquake load that affect the variation of stiffness and strength properties of column components. So, the flexural yielding moment will depend mainly on the axial force level. Therefore, the interaction diagram showing the relationship between axial force and the flexural yielding is important to be considered. Under each flexural yielding moment, the properties of nonlinear moment-rotation hinges of column components will be the same as that of beam components. In addition, ATC-40 recommends that the plastic hinge rotation capacities of reinforced concrete column considering the design shear force level as shown in Table 3 were adopted in this study.

The flexural strength of column components can be calculated using the same procedures and assumption as in beam components by considering axial force levels as shown in Figure 23. In this relationship between flexural yielding moments and axial force, point A represents pure axial compression where concrete in compression reaches its ultimate compressive strain, ε_{cu} set at 0.003. Point B corresponds to crushing of concrete at one face and zero tension at another. Point C corresponds to a strain distribution with a maximum compression strain ε_{cu} on one side of section and tensile strain ε_y, the yielding strain of reinforcement at the level of tension steel. This represents balanced failure in which crushing of concrete and yielding of tension steel develop simultaneously. Point D represents pure bending where axial load equal to zero and the calculation of flexural strength of column at this point is exactly the same as beams. Point E represents pure axial tension where all reinforcements reach their yielding strain.

Table 3 Modeling parameters for nonlinear procedure-reinforced concrete column

			Modeling Parameters [4]		
			Plastic Rotation Angle	Residual	Strength
Component Type			A	B	C
1. Columns controlled by flexure [1, 3]					
$\frac{P}{A_g f_c'}$ [5]	*Transverse Reinforcemen*	$\frac{V}{b_w d\sqrt{f_c'}}$ [6]			
≤ 0.1	C	≤ 3	0.02	0.03	0.2
≤ 0.1	C	≥ 6	0.015	0.025	0.2
≥ 0.4	C	≤ 3	0.015	0.025	0.2
≥ 0.4	C	≥ 6	0.01	0.015	0.2
≤ 0.1	NC	≤ 3	0.01	0.015	0.2
≤ 0.1	NC	≥ 6	0.005	0.005	-
≥ 0.4	NC	≤ 3	0.005	0.005	-
≥ 0.4	NC	≥ 6	0.0	0.0	-
2. Columns controlled by shear [1, 3]					
Hoop spacing ≤ d/2, or $\frac{P}{A_g f_c'}$ [5] ≤			0.0	0.015	0.2
Other cases			0.0	0.0	0.0
3. Columns controlled by inadequate development or splicing along the clear height					
Hoop spacing ≤ d/2			0.01	0.02	0.4
Hoop spacing > d/2			0.0	0.01	0.2
4. Columns with axial load exceeding $0.70P_o$ [1, 3]					
Conforming reinforcement over the entire length			0.015	0.025	0.02
All other cases			0.0	0.0	0.0

Source: FEMA-356

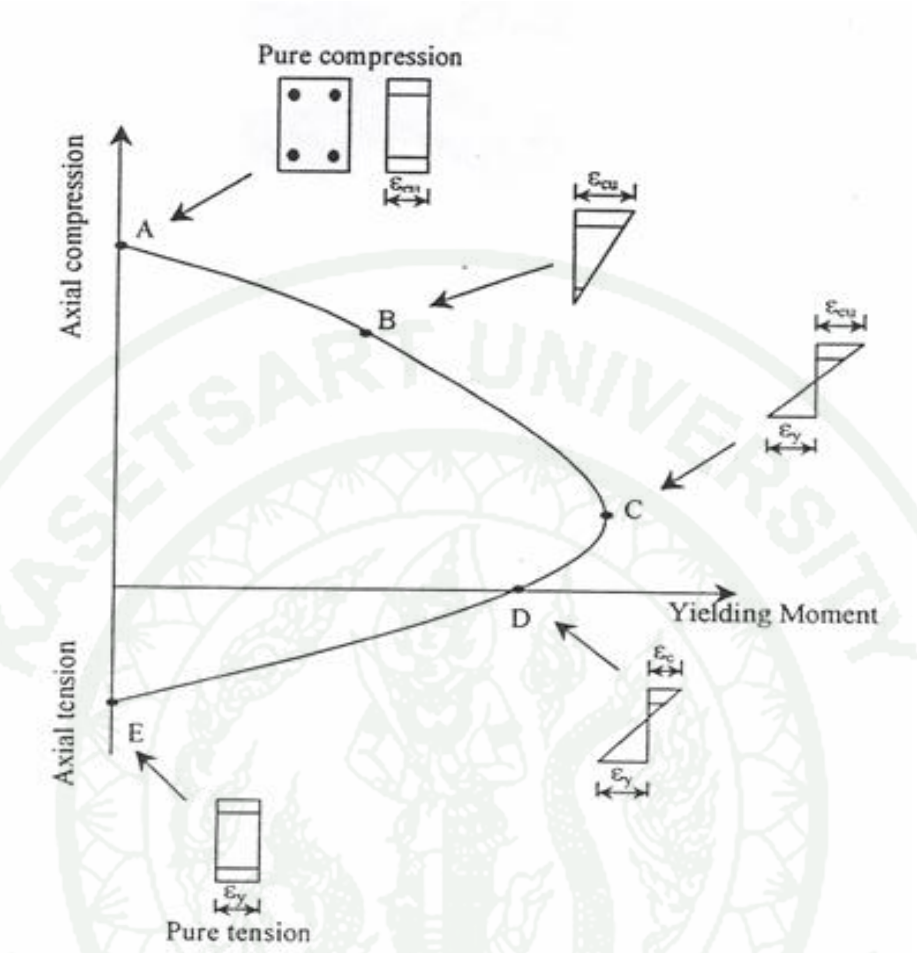

Figure 23 Strain distributions corresponding to points on Interaction Diagram
Source: Phatiwet (2002)

16. Modeling of masonry walls

In Bhutan most of the masonry infill walls are constructed by using burnt clay with mortar. Basically there are three important mechanical properties of the masonry infill wall used to calculate stiffness and strength of infill panel which included compressive strength, modulus of elasticity and shear strength (Hossien and Toshimi, 2004). The compressive strength of the masonry infill wall unit referred to as prism f'_{me}, compressive unit of brick unit f'_{br} and modulus of elasticity, E_{me}.

There are several potential failure modes for infill masonry walls come across from past studies. Firstly horizontal sliding shear failure of masonry walls, second is the compression failure of diagonal strut, third is the diagonal tensile cracking which does not generally constitute a failure condition, as higher lateral forces can be supported, and lastly the tension failure mode (flexural) which is not usually a critical failure mode for infill wall (Paulay and Priestley, 1992).

The Shear strengths obtained from the first and second failure mode for each infill panel are critical types of failure modes and minimum value of the two should be considered for the calculation of shear strength of the infill walls (Hossien and Toshimi, 2004).

If the sliding shear failure of the bed joints in masonry infill occurs, the equivalent structural mechanism changes from the diagonally braced pin-jointed frame to the knee-braced frame which significantly alter the nature of interaction between the frame and infill panel by reducing the effectiveness of diagonal strut and producing large local forces on frame elements as shown in Figure 24. The equivalent diagonal strut compression force *Rs* to initiate horizontal shear sliding depends on the shear friction τ and aspect ratio of the panel. The Mohr-Coulomb failure criteria can be applied to assess the maximum shear strength for un-crack masonry is given by equation 15.

$$\tau = \tau_0 + \mu_f f_m \tag{15}$$

In 1992 Priestley and Pauley recommends the average values of cohesive strength capacity of mortar beds, τ_o of 4 % of masonry compressive strength and typical value of coefficient of sliding friction along the bed join, μ_f is 0.5. They also discussed the vertical compressive force or stress, f_m across potential sliding plane which is given by vertical component of the strut force divided by area of sliding plane.

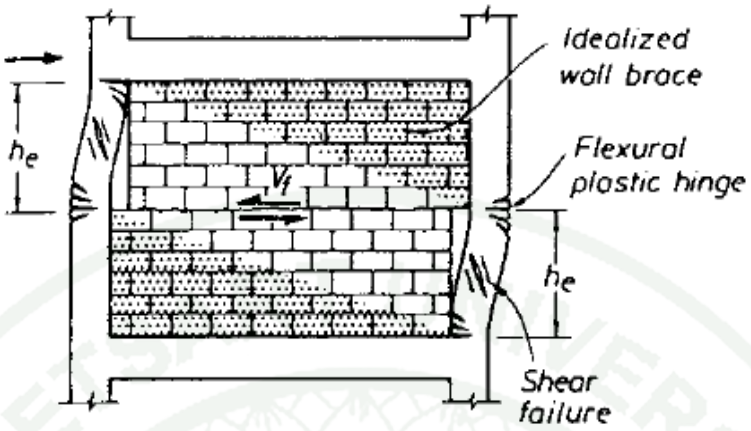

Figure 24 Knee braced frame model for sliding shear failure of masonry infill
Source: Priestly and Pauley (1992)

16.1 Equivalent Strut Model

The concept of equivalent compressive diagonal strut was proposed by so many researchers base on series of experiments and analytical investigation. The proposed relation to evaluate the stiffness on in-plan masonry infill by Mainstone (1971) is adopted in FEMA-273. Base on his proposal, the equivalent diagonal compression strut width of solid unreinforced masonry infill panel prior to cracking is given by equation 16 and the parameter (λ) is given in equation 17.

$$a = 0.175(\lambda h)^{-0.4} d_m \tag{16}$$

$$\lambda = \left[\frac{E_{me} t_{inj} \sin 2\theta}{4 E_{fe} I_{col} h_{\inf}} \right]^{1/4} \tag{17}$$

Where, h_{col} is height of column between centre lines of beams, E_{fe} and E_{me} are young's modulus of frame and infill panel respectively, t_{inf} is thickness of infill panel, θ is angle of inclination of diagonal strut with the horizontal, I_{col} is the moment of

inertia of column, h_{inf} is the height of infill, a is the effective width of the diagonal strut and r_{inf} is the diagonal length of infill as shown in Figure 25.

In FEMA-273 and FEMA-356 has recommended that infill masonry can be modeled as equivalent diagonal strut in which the stiffness contribution of infill wall is represented by diagonal compression strut base on relation proposed by Mainstone (1971). The thickness of the equivalent compression strut is identical to that of the wall thickness. The width of the equivalent diagonal compression strut for solid unreinforced masonry infill panel prior to cracking is given by equation 16.

Kiattivisanchai, 2001 and Phatiwet, 2002 has modeled the masonry infill following the guidelines given in FEMA-273 and FEMA -356 by considering the important properties like compressive strength, modulus of elasticity and the shear strength that affects the behavior of masonry wall.

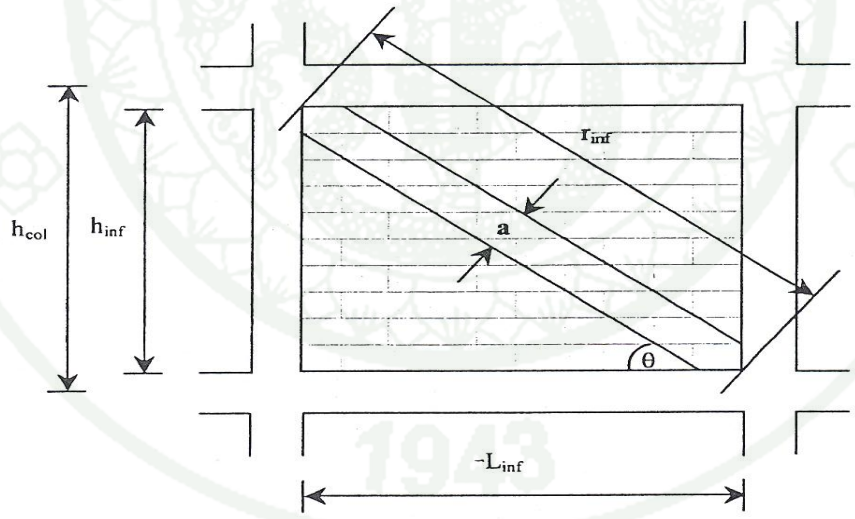

Figure 25 Equivalent diagonal strut compression models
Source: Phatiwet (2001)

In order to determine expected compressive strength of strut R_s, the expected shear strength V_{ine} (shear failure) and compression failure Vc is compared. The expected shear strength or the horizontal lateral load required to reach the infill shear

strength V_{ine} was calculated as the product of the net horizontal area of the infill wall panel, A_{inf}. Similarly *Vc* can be determined from equation 19. And the smaller value of the two is considered to determine the expected compressive strength of strut. But the sliding shear failure is control over compression failure from past research and experimental studies. The axial compression strength of the equivalent strut Rs was obtained by solving equations 18 and 20 simultaneously and desired equation 21 was obtained.

$$V_{ine} = \tau_0 A_{\text{inf}} + \mu_f f_m \tag{18}$$

$$V_c = axt_{\text{inf}} f_m^{'} \cos\theta \tag{19}$$

$$V_{ine} = R_s \cos\theta \tag{20}$$

Where,

$$A_{\text{inf}} = L_{\text{inf}} xt_{\text{inf}}$$

$$f_m = \frac{R_s \sin\theta}{A_{\text{inf}}}$$

$$\sin\theta = \frac{h_{\text{inf}}}{r_{\text{inf}}}$$

$$\cos\theta = \frac{L_{\text{inf}}}{r_{\text{inf}}}$$

$$R_s = \frac{\tau_0 r_{\text{inf}} t_{\text{inf}}}{\left[1 - \mu_f \tan\theta\right]} \tag{21}$$

The axial yield deformation can be used directly from the axial stiffness of strut and compressive strength of the equivalent diagonal strut R_s.

In SAP 2000 has a provision to model the equivalent diagonal compression strut as axial element having a linear hinge along its length. The plastic hinges in

column should capture the interaction between axial load and moment capacity. Hinges in beams needs only characterized the flexural behavior of the members.

The equivalent strut, however only needs hinge that represent the axial load. The hinges should be placed at the mid span of the members (Al Chaar 2002). In general, the minimum number and type of plastic hinges needed to capture the inelastic action of infill frames are show in Figure 26.

According to Hossein and Toshimi (2004) the lateral force-displacement relation for infill wall are defines by a series of straight line segments shown in Figure 27. The initial stiffness (K_0) can be obtained by equations 22 and 23.

$$K_0 = \frac{2V_m}{U_m} \tag{22}$$

$V_m = V_{ine}$ (Sliding shear failure is control)

$$U_m = \frac{\varepsilon_m' r_{\inf}}{\cos\theta} \quad \text{(Hossien and Toshimi, 2004)} \tag{23}$$

Where, U_m = Maximum displacement at the maximum lateral force

ϵ'_m = Masonry compression strain at maximum compressive stress.

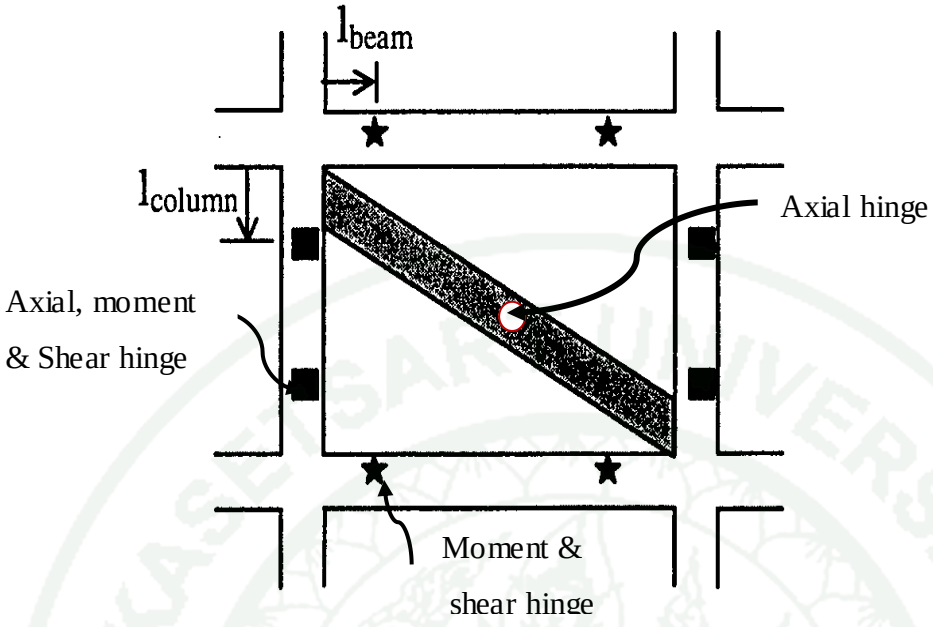

Figure 26 Plastic hinge placements

Source: Chaar (2002)

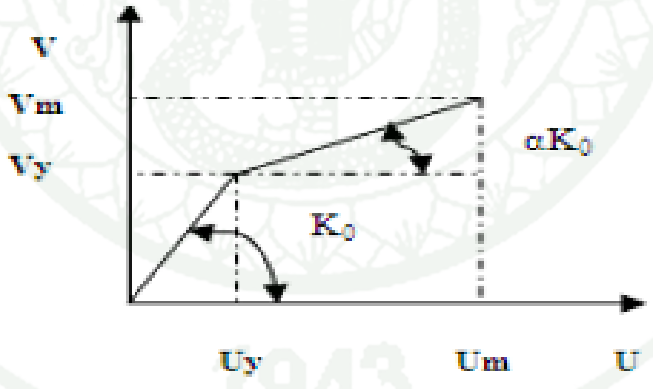

Figure 27 Force-Displacement relations of infill walls

Source: Hossien and Toshimi (2004)

Table 4 Force-Displacement relations and acceptance criteria for masonry infill

$\beta = V_{fre} / V_{ine}$	$L_{\inf} / h_{\inf}$	C	d (%)	e (%)	Acceptance Criteria	
					LS (%)	CP (%)
	0.5	n.a.	0.5	n.a.	0.4	n.a.
$0.3 \leq \beta < 0.7$	1.0	n.a.	0.4	n.a.	0.3	n.a.
	2.0	n.a.	0.3	n.a.	0.2	n.a.
	0.5	n.a.	1.0	n.a.	0.8	n.a.
$0.7 \leq \beta < 1.3$	1.0	n.a.	0.8	n.a.	0.6	n.a.
	2.0	n.a.	0.6	n.a.	0.4	n.a.
	0.5	n.a.	1.5	n.a.	1.1	n.a.
$\beta \geq 1.3$	1.0	n.a.	1.2	n.a.	0.9	n.a.
	2.0	n.a.	0.9	n.a.	0.7	n.a.

Source: FEMA-273

V_{ine} =Expected infill shear strength

V_{fre} =Expected storey shear strength of bare frame.

Note: Interpolation is permitted between table values.

17. Modeling of foundation

To evaluate the lateral strength and behavior of the buildings under seismic loading many factors are normally left in the analysis which is required to be done in the analytical model. In this study the shallow foundation modeling was considered since selected building has isolated footing. For simplified analysis, an uncoupled component modeling as recommended in FEMA-273 was adopted as shown in Figure 28.

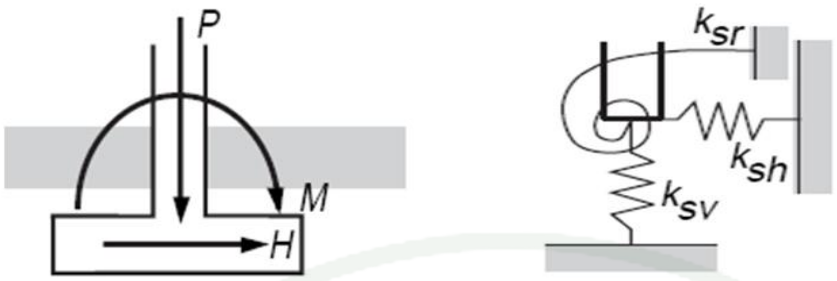

(a) (b)

Figure 28 Foundation load (a) and uncoupled component model (b).

Source: FEMA-273

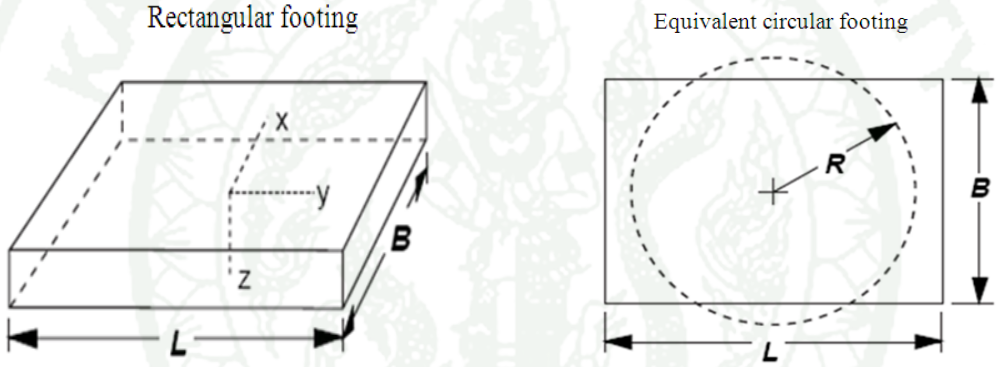

Figure 29 Radii of circular footings equivalent to rectangular footing.

Source: FEMA-273

The spring constants for shallow foundation are obtained by modifying the solution for circular footing shown in Figure 29 and given by equation 24.

$$K = \alpha\beta K_0 \tag{24}$$

Where

α = Foundation Shape correction factor

β =Embedment factor

K_0 = Stiffness coefficient for the equivalent circular footing

The stiffness parameters for shallow bearing foundation such as shear modulus G for a soil is related to Young's modulus of elasticity E and Poisson's ratio V by the relationship given in equation 25.

$$G = \frac{E}{2(1+v)} \tag{25}$$

The radius of equivalent circular footing and stiffness coefficient can be calculated from the formulae given in table 5.

Poisson's ratio may be assumed as 0.25 for rock, stiff clay and nearly dry sand (ATC-40). Young's modulus of elasticity for medium normally consolidated sand ranges in between 20000-40000 *KPa*. Embedment factor and Foundation Shape correction factor can be obtained from Figures 30 and 31.

Table 5 Equivalent radius (R) and stiffness coefficient (K_0)

	R	K_0
Rotation	$R = \left[\frac{B^3 L}{3\pi}\right]^{1/4}$	$K_0 = \frac{8GR^3}{3(1-v)}$
Translation (Vertical)	$R = \left[\frac{BL}{\pi}\right]^{1/2}$	$K_0 = \frac{4GR}{(1-v)}$
Translation (Horizontal)	$R = \left[\frac{BL}{\pi}\right]^{1/2}$	$K_0 = \frac{8GR}{(2-v)}$

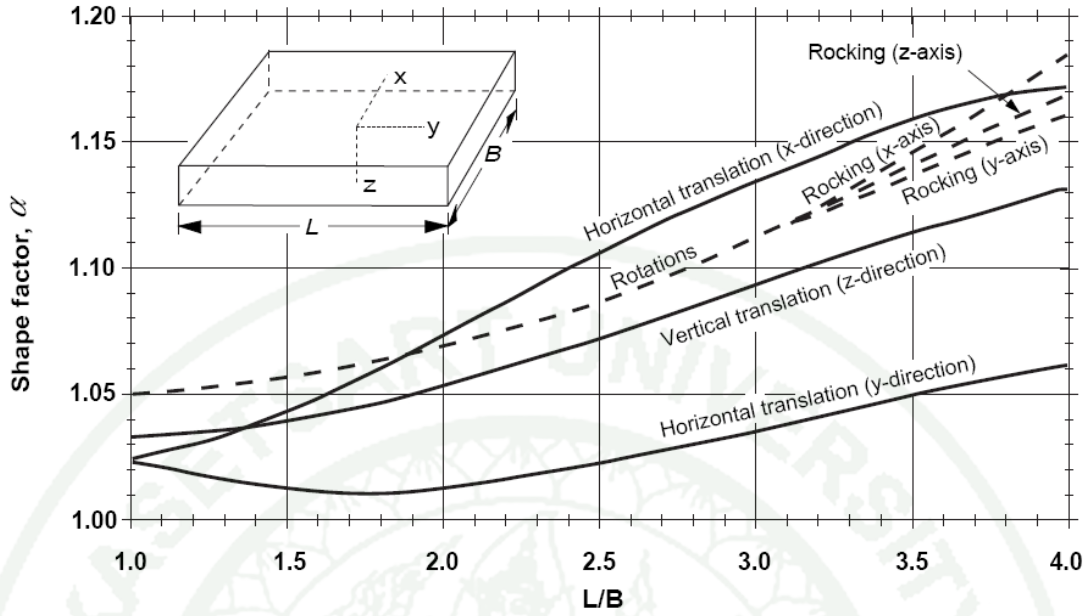

Figure 30 Foundation shape correction factor.

Source: FEMA-273, 2003

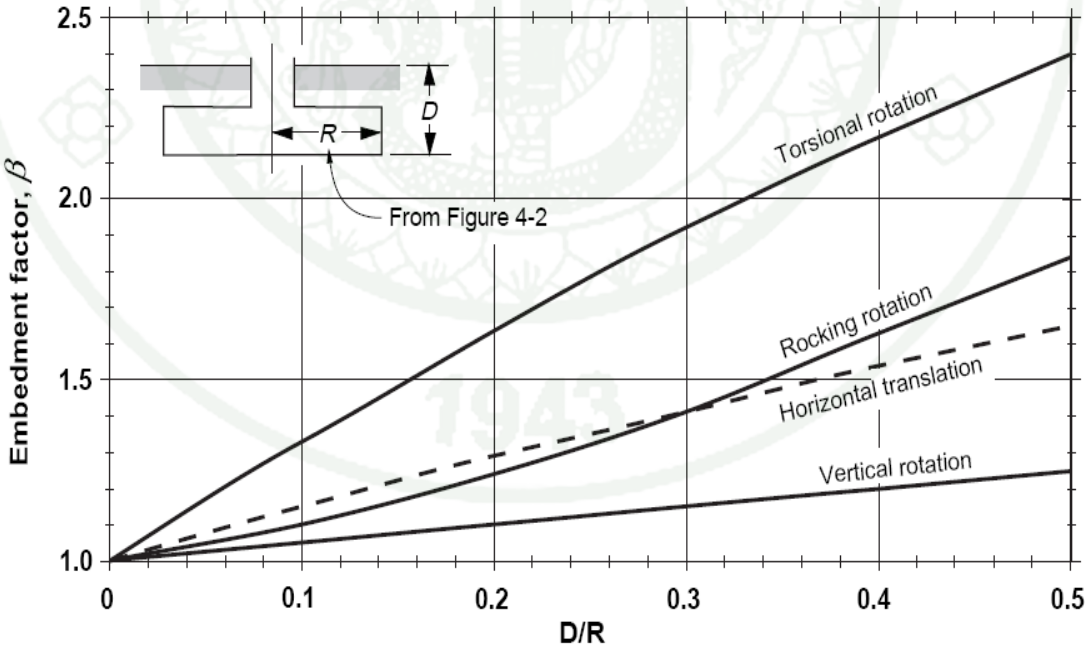

Figure 31 Embedment correction factors.

Source: FEMA-273, 2003

RESEARCH METHODOLOGY

1. General

In order to carry out the seismic evaluation of gravity load design building in Bhutan, literature review on the related subjects was done to gain the in-depth knowledge to carry out the present study. Besides several relevant building design codes and standard seismic evaluation guidelines like ATC-40, FEMA-273 and 356 were studied minutely to be able to adopt in this study. Never the less, the modeling techniques of structural components, nonstructural component and material modeling were reviewed thoroughly from the past studies. Nonlinear static pushover analysis and capacity spectrum methods were adopted as a method of analysis in this study.

In the subsequent section, selection of building, description of models, modeling assumptions, application of loads on the structure, numerical modeling of building, hinges properties, analysis of building and finally seismic performance evaluation of building are presented herein.

2. Selection of building

To evaluate the seismic performance of existing building, the five storey reinforced concrete building having typical layout plan with dimensions of 18.15m x 8.45m representing the buildings in Bhutan was selected and shown in Figure 32. This selected building is typical gravity load designed of low-rise reinforce concrete building. The live loads have been assumed as 4 KN/m^2 as prescribed for residential buildings. The storey height of the models is 3.2m for all floor levels and span lengths can be acquired from the plan. This building is use as residential purpose and located in high seismicity region which was designed without seismic provision as most of the buildings in Bhutan are constructed prior to the introduction of seismic design concepts.

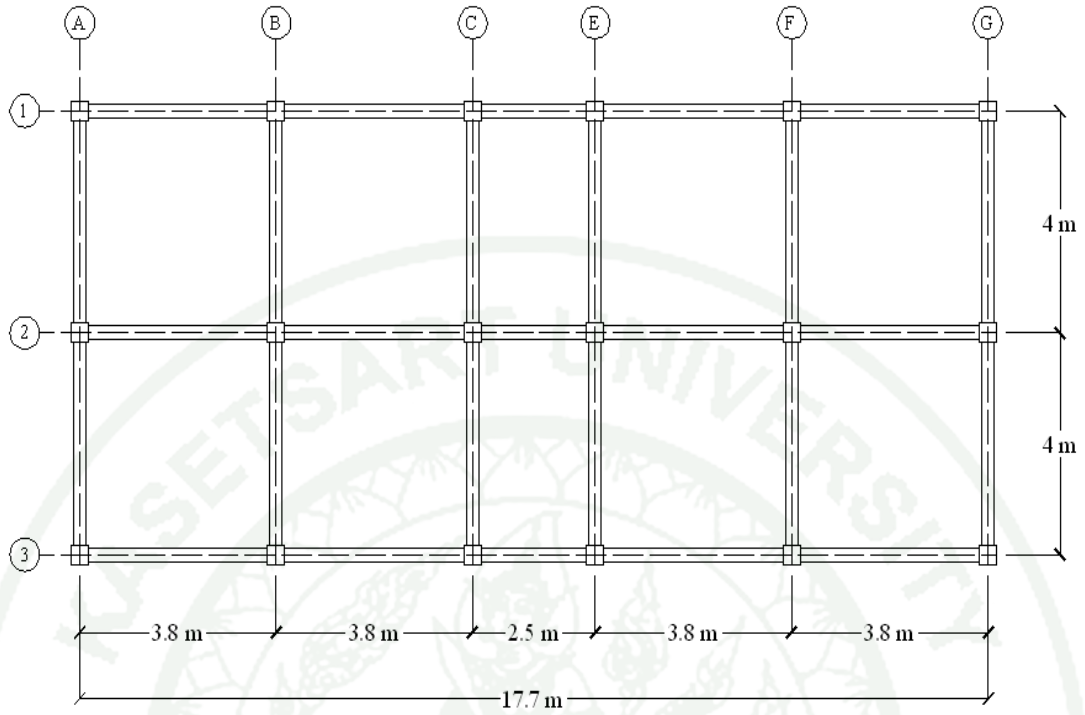

Figure 32 Typical Building lay out plan.

3. Description of models

The typical planer frame with multistory masonry infill reinforced concrete (RC) frame building of five storey which is composed of two bays in the weak direction (Grid along B) and five bays in the strong direction (Grid along 2) was considered in this study. Based on the review of architectural layouts and structural framing plans of masonry infill reinforced concrete frame buildings constructed in Bhutan, the practically relevant and prevailing structural configurations of planner masonry infill reinforced concrete frames were identified for the nonlinear static pushover analysis in this study and it is shown in Figures 33.

Tables 6, 7 and 8 present the material properties, typical dimensions, reinforcement details for structural members and designed parameters for masonry infill walls for the existing as well as newly designed building.

Table 6 Materials properties for different structural RC frame members

Characteristic compressive strength of concrete (*MPa*)	Ultimate tensile strength of main steel (*MPa*)	Ultimate tensile strength of distribution steel (*MPa*)
15	250	250

Table 7 Reinforcement details and typical dimension for RC frame members

Structural members	Longitudinal reinforcement	Transverse reinforcement	Column-size (mm)	Beam-size (mm)
C1	8#25ø	8@100mmc/c	350x350	
C2	8#22ø	8@100mmc/c	350x350	
C3	8#22ø	8@100mmc/c	300x300	
B	2#16,18ø Top	2#18 ø Bottom	8@100mmc/c	500x250
Newly Design sections				
C1 and C2	Same sections and reinforcements to existing building			
C3	8#20ø	8@100mmc/c	300x300	
B	2#16,14ø Top	2#16 ø Bottom	8@100mmc/c	400x250

Table 8 Materials properties and design parameters for masonry infill

Masonry compression strength *(MPa) f'm*	Masonry compression strain ($\varepsilon_m^{'}$)	Coefficient of friction (μ)	Thickness of masonry infill (mm)	Density of infill *(kN/m^3)*	Modulus of elasticity *(MPa) 550f'm*
3	0.002	0.3	125	20	1650

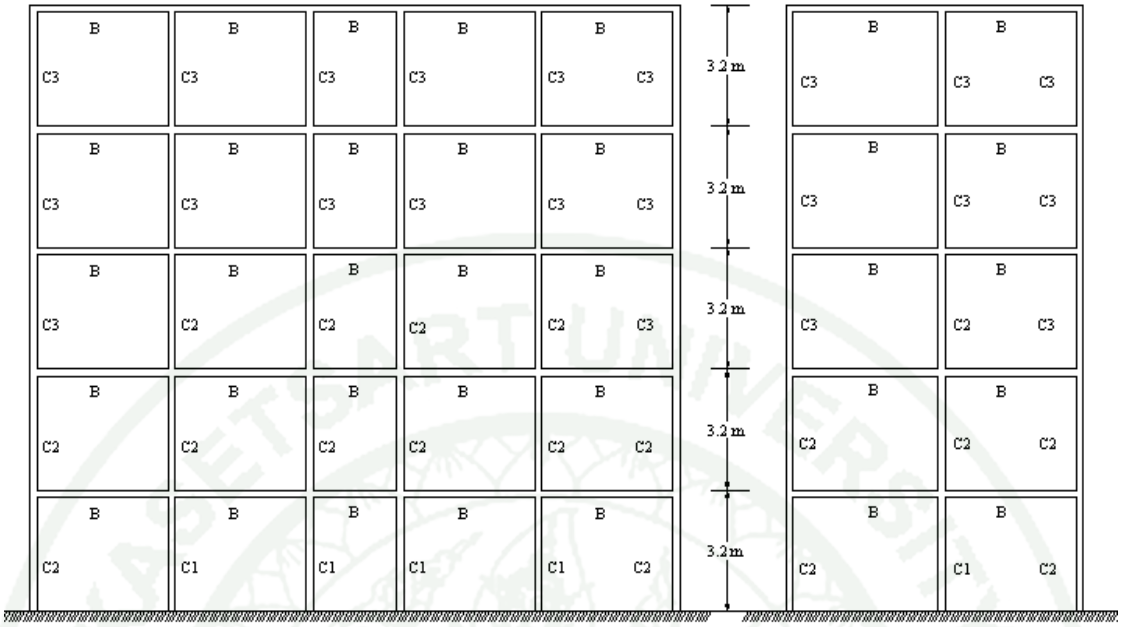

(a) Bare Frame (X) (b) Bare Frame (Y)

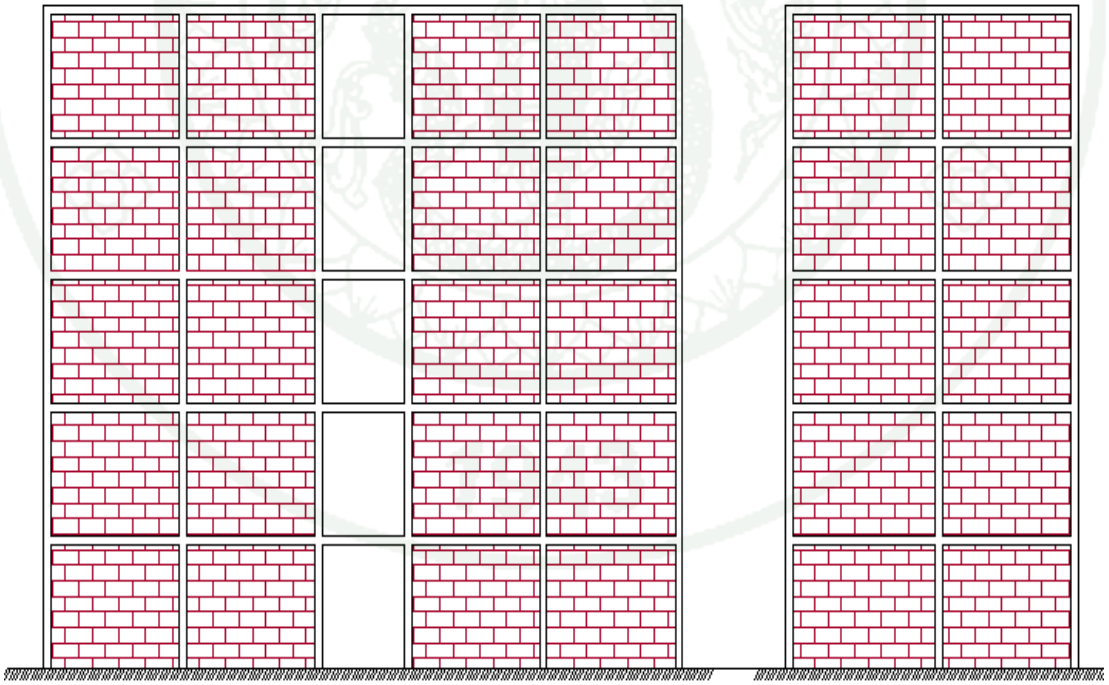

(c) Infill Frame (X) (d) Infill Frame (Y)

Figure 33 Layout of Frame models

4. Modeling Assumptions

The following assumptions were made in creating models of building for seismic evaluation in this study.

1. Diaphragm was assumed to be rigid. That is, the floor was assumed to be rigid in the plane of diaphragm but flexible in bending. In other words, all the horizontal components displacements at the same floor level were assumed to be identical.
2. Lateral load is assumed to be acted only at floor level.
3. Joints are assumed to be rigid.
4. Footings are assumed to be fixed.

5. Application of loads on the structure

5.1 Gravity loads

The vertical design loads of the two dimensional analytical models was calculated from three dimensional frames. The sum of the vertical loads from the slabs are calculated (as per IS-code 456-2000 slab load distribution) as a uniformly distributed load over the normal story beams. These mentioned loads cover only dead loads but live load are also calculated as similar procedures from the given live load intensity for the residential building. In this study live load intensity was taken as 4 KN/m^2 throughout the floor levels. It should be noted that SAP2000 analysis program automatically estimates its own weight of the structural elements depending on sections provided and include in the elastic analysis.

5.2 Lateral loads

In evaluating the lateral capacity of the buildings, the magnitude of the applied load is not known in advance. Moreover, the structure is expected to lose strength or become unstable under seismic loading. In this case displacement control analysis option is more convenient for applying lateral force to the structures. In IS-code 1893-

2000, maximum roof displacement is given as 0.04H, where H is height of building and this was adopted in this study.

There are several load patterns can be used in the pushover analysis. Generally, the lateral load is intended to represent the distribution of lateral inertia forces that can act on the building during earthquake. In this study inverted triangular load pattern was used which is recommended in FEMA-356 guidelines base on assumption that fundamental mode of vibration is the predominant response of the structures.

6. Numerical Modeling of the Building

The structural analysis program SAP2000 is a software package from Computers and Structures, which is based on the finite element method for modeling and analysis. It has the capability of designing and optimizing building structures. Among the features introduced by the analysis engine of SAP2000 are Eigen value analysis, static and dynamic analysis, linear and nonlinear analysis, and pushover analysis. The analytical modeling used in this software is the member type model which means that beams or columns are modeled using single element. The inelasticity formed in these single elements is assumed to be concentrated at the ends and which is the case for the behavior of building elements during earthquake excitation. The hysteretic response of the concentrated plasticity at the ends of a member can be described by a moment curvature relationship.

A variety of cross sections are available in SAP2000 element library. These sections include regular sections as used for modeling of beams, columns and equivalent diagonal strut of masonry infill panels for the reinforced concrete buildings. Beams and columns were modeled as line elements as stated in the previous section under modeling discussion of structural components. All the members were modeled as reinforced concrete elements except diagonal strut with sections given in the design for the nonlinear analysis. The considered mass includes dead load and 25 percent of live load intensity (4 KN/m^2) in the design.

7. Frame Hinge Properties

SAP2000 introduces the capability of providing plastic hinges at discrete user defined hinges along the clear length of a frame element. The plastic hinge represents the post-yield behavior in one or more degree of freedom. Uncoupled moment, torsion, axial force and shear hinges are available to be modeled along the frame element. More than one type of hinges can exist at the same location, for example, the user might assign both M3 (moment) and V2 (shear) hinge to the same end of a frame element.

Default hinge properties are provided based on FEMA-356 criteria. Hinge length is the distance over which the plastic strain or plastic curvature is integrated. The standard guidelines like FEMA-356 give some recommendations for hinge length. Typically this length is taken as a fraction of the element length, and is often in the order of the depth of the section, particularly for moment-rotation hinges. Hinge length can be used to obtain full nonlinear behavior all over the total element length. This can be achieved by inserting a specified number of hinges each has a specified length such that the number of hinges times the hinge length gives the total length of the element. In this study, the potential plastic hinges are located at the ends of the element, since this is the location of the maximum straining actions for beams and columns but for equivalent diagonal strut, hinge location is at the mid span of length as the straining acting is more in that portion.

The plastic deformation curve is a force-displacement (moment-rotation) curve that gives the yield value and the plastic deformation following yield. This is done in terms of a curve with values at five points, A-B-C-D-E, as shown in Figure 34. The user can specify a symmetric curve, or one that differs in the positive and negative direction.

The plastic deformation curve is characterized by the following points:

1. Point A represents the origin.

2. Point B represents the yielding state. No deformation occurs in the hinge up to point B. Only the plastic deformation beyond point B will be exhibited by the hinge.
3. Point C represents the ultimate capacity for pushover analysis.
4. Point D represents the residual strength for pushover analysis.
5. Point E represents total failure.

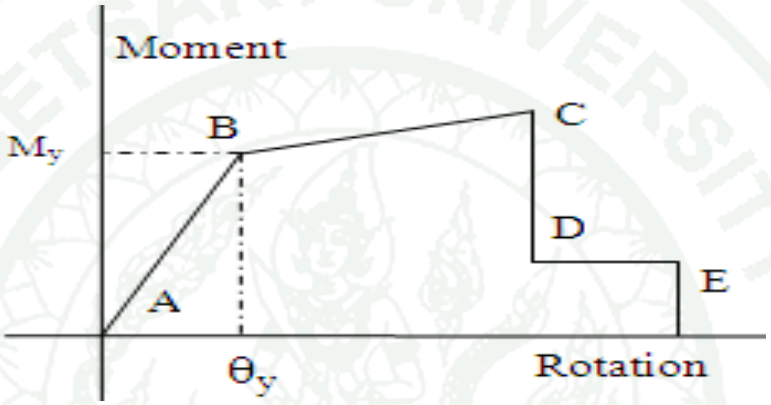

Figure 34 Moment-Rotation relation for plastic hinges
Source: FEMA-356

Prior to reaching point B, the deformation is linear and occurs in the frame element itself, not the hinge. Plastic deformation beyond point B occurs in the hinges in addition to any elastic deformation that may occur in the element. When the hinge unloads elastically, it does so without any plastic deformation, i.e., the unloading path is parallel to line A-B.

The plastic hinge rotation capacity for reinforced concrete members at point B can be obtained from equation 26 (Das and Murty, 2004) and for steel elements from equations 27 and 28 (FEMA-356). The plastic hinge rotation capacities at point C, D and E can be derived from experimental or from the rational analysis using realistic material stress-strain relations.

$$\theta_y = \frac{M_y(L/2)}{4EI} \tag{26}$$

$$\theta_y = \frac{ZF_{ye}l_b}{6EI_b} \quad \text{(For-beam)} \tag{27}$$

$$\theta_y = \frac{ZF_{yc}l_c}{6EI_c}\left[1-\frac{P}{P_{ye}}\right] \text{(For-column)} \tag{28}$$

Where, M_y is yield moment, L is length of the member, E is the modulus of elasticity, θ_y is yield rotation. l_b is the beam length, l_c is the column length, and I_b and I_c is the moment of inertia of beam and column respectively. Z is the plastic section modulus; F_{ye} is the expected yield strength. P is the axial force in the member at the target displacement for nonlinear static analyses, and P_{ye} is the expected axial yield force of the member.

When default hinge properties are used, the program automatically uses the yield values. These values are calculated based on the frame section properties and the yield stress provided for the element material. In FEMA-356 and ATC-40 also recommended the plastic hinge rotation capacities of reinforced concrete beams and columns at point C, D and E.

In this study, three types of hinges were used to simulate the plastic hinge formation through the nonlinear behavior of the structure. The first is the axial and moment hinge which was assigned to the column elements base on FEMA and ATC-40 recommendations. The second type is the moment hinge which was assigned to the beam elements base on FEMA and ATC-40 tables. The third type of hinge is the axial hinge which was assigned to diagonal strut which is also based on FEMA and ATC-40 recommendations. In this study, all the beams, columns and equivalent diagonal struts are regular in shapes, because as the programs requires the shape of reinforce concrete members should be rectangular or square or circular.

8. Static Pushover Analysis in SAP2000

SAP2000 provides the following tools needed for pushover analysis:

1. Material nonlinearity at discrete, user-defined hinges in frame elements. The hinge properties are created based on pushover analysis regulations found in performance-based guidelines. Default hinge properties are provided based on criteria given in FEMA-356.
2. Nonlinear static analysis procedures that allow displacement control, so that the structure can be pushed to a desired target displacement.
3. Display capabilities in the graphical user interface to generate and plot pushover curves, including demand and capacity curves in spectral ordinates.
4. Capabilities in the graphical user interface to plot and get information about the state of every hinge formed at each step in the pushover analysis.

The following are the general sequence of steps involved in performing nonlinear static pushover analysis using SAP2000 in the present study:

1. The model of the structure is to be created.
2. Frame elements are adequately defined. For reinforced concrete elements, the appropriate reinforcements are provided for the cross sections.
3. Frame hinge properties are defined and assigned to the frame elements.
4. Load cases that are needed for use in the pushover analysis are defined, these loads cases includes:
   I. Gravity loads and other loads that may be acting on the structure before the lateral seismic loads are applied.
   II. Lateral loads that will be used to push the structure.
5. Pushover analysis cases are set to run.
6. At last step, SAP2000 software plots the pushover curve (base shear versus roof displacement), demand curve, performance point and the deformed shape showing the hinge states of the building.

9. Analysis of Buildings

Nonlinear static pushover analysis by using SAP2000 was carried out on two dimensional frames to obtain the lateral capacity and performance point of the building. This was done along both the principal directions considering with and without infill walls. Furthermore, the parameters that affect the lateral capacity of the building were investigated by considering only in weak direction of the building frame. This was done by varying thickness of infill wall, varying compressive strength of concrete and varying yield strength of reinforcement by keeping all other parameters constant.

The building was pushed laterally with monotonically increasing lateral loads in step by step until plastic collapse mechanism is obtained on the base shear and roof displacement plot. The pushover curve which plots base shear coefficient versus roof displacement of the building represents the inelastic limit as well as lateral load carrying capacity of the structures under earthquake excitation. The change in slope of the pushover curve indicates the yielding of components and when pushover curves drops vertically indicates the failure of components of the building as shown in Figure 35. Where IO, LS and CP stand for immediate occupancy, life safety and collapse prevention respectively. We shall present to this curve in the progression of hinges in the element.

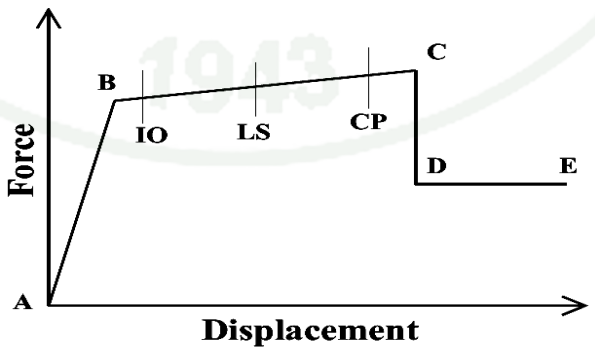

Figure 35 Load–deformation (Pushover) curve

Source: Ashraf and Stephen (1998)

10. Seismic Performance Evaluation of Building

In this study capacity spectrum method was used to evaluate the seismic performance of the selected building. The capacity curves of the building obtained from pushover analysis were converted to capacity spectrum curve which is plotted between spectral acceleration (S_a) and spectral displacement (S_d). The demand curve was generated in accordance with IS:1893, 2000 which is a standard S_d versus T, periods for 5 percent critical damping for reinforced concrete frame structures considering seismic zone V, zone factor, Z=0.36, importance factor, I=1 and response reduction factor, R=3. Medium soil type was adopted as recommended by Bhutan building code of practice. The bearing capacity of 170 KN/m^2 for medium soil was considered. The Young's modulus of elasticity of soil was assumed as 40000 KPa for medium normally consolidated, Poisson's ratio, v=0.25 for stiff clay and nearly dry sand during the modeling of shallow foundation in this study. The standard demand curve was converted to acceleration displacement response spectra format as S_a versus S_d in accordance to IS-1893, 2000.

The capacity and demand spectra in acceleration displacement response spectra format is superimposed to get performance point. Performance point represents the dynamic equilibrium which implies that the lateral load resisting capacity of the building equals the demand levels resulting from the earthquake ground motion.

RESULT AND DISCUSSIONS

1. General

The general information required for the seismic evaluation of gravity load designed building was discussed in the earlier sections. Base on these theoretical concepts, the nonlinear static pushover analysis was executed to the selected reference building frame models along both major directions and their analysis results are illustrated in this section.

In the succeeding sections, results of the pushover analysis in terms of capacity curves, performance points of the building and the results of the parametric study on the effect on lateral capacity of the building due to variation of compressive strength of concrete, yield strength of reinforcement bar, variation in infill wall thickness and finally effects due to shallow foundation modeling are available herein.

2. Pushover Analysis Results

2.1 Notation

The lateral capacity of the building is presented by capacity curve which plot between the normalized base shear versus roof displacement. From the very curve, the significant events in the progressive lateral response of the building are depicted on the curve. Due to the constrain space available to be described the response of the structure during the pushover analysis, the general format citing a particular event can be noted as *AA-AA[A]*. Where, the first two characters represent damage type of building component. The next two characters represent component name. The last digit indicates the location of the component in the structures. For an example, flexural yielding of column (*C1*) at first floor will be represented as *FY-C1[1]*.

In addition to this, basically three to four events (Event [1] to Event [4]) are cited for the discussion of important stages to be noted from the capacity curves of the building in this study. In general, these events are reflected on the capacity curve to mark the important stages of the component underwent either flexural yielding (FY) or flexural failure (FF) during the pushover analysis.

For the bare frame, generally the events are labeled from event one (Event [1]) to event there (Event [3]). The first event, Event [1] indicates the first failure of any structural component either beams or columns in the building are referred in the discussion of the results in this study. The second event, Event [2] shows the stage of change of failure component either from beams to columns or marked the stage were abrupt decrease in lateral load carrying capacity of the building has occurred and that can be brought to the notice of the reader at first glance. The third event, Event [3] depicts the final stage of the structural or non-structural components of the building when the building is push until predetermined target displacement is achieved.

In the case of infill frame, events are cited form first event, Event [1] to fourth event, Event [4]. The first event, Event [1] reveals the failure of brick wall (F-BW) and the remaining events are resemble to that of event cited for the bare frame in the discussion of results in this study. This can be brought to the meaning more vividly while reading through the pushover curves as discussed in the succeeding sections.

2.2 Capacity curve of the building

Nonlinear static pushover analysis has been performed using two dimensional frames in both principal directions. The capacity curves are plotted between normalized base shear versus roof displacements and their failure mechanism are presented. To investigate the effect of infill walls, building without and with infill walls with fixed support condition was analyzed. Furthermore, to investigate the effect on lateral capacity of the building, two dimensional frames along Y-direction was analyzed by varying the compressive strength of concrete, yield strength of the reinforcement steel, thickness of the infill walls and modeling shallow foundation as

uncouple component model. The capacity curves obtained from the analysis results for different conditions are presented herein.

2.2.1 Capacity curve of the building along weak direction

The capacity curve of the building frame without infill under consideration (Y-direction) is shown in Figure 36. This curve depicts the sequence of flexural yielding (FY) and flexural failure (FF) of elements for the selected building. The capacity curves shows they are initially linear but start to deviate from linearity as the structural component undergoes inelastic actions. When the building is push enough in to the inelastic region, the curve become linear again with a lesser slope until ultimate lateral strength is achieved.

The Flexural yielding of the structural component starts from beam and then to column as indicated by hinges formation. It can be seen from this curve, Event [1] that the lateral capacity of the building starts dropping down at first point when the beam at third floor, B [3] undergoes flexural failure. It is also seen that the capacity curve continue to dropped down in step wise step as other structural components such as beams B [2] and columns C1 [1] fails. The overall capacity falls down sharply when columns at first floor level, C1 [1] and C2 [1] are collapsed in the progression of pushing the structure until predetermine estimated displacement; Event [3] is reached.

These events are clearly figured out from the damage distribution and failure mechanism of the selected frame model through hinges formation. The plastic hinges formation for the model can be obtained for three different events, Event [1] to Event [3] as shown in Figure 37.

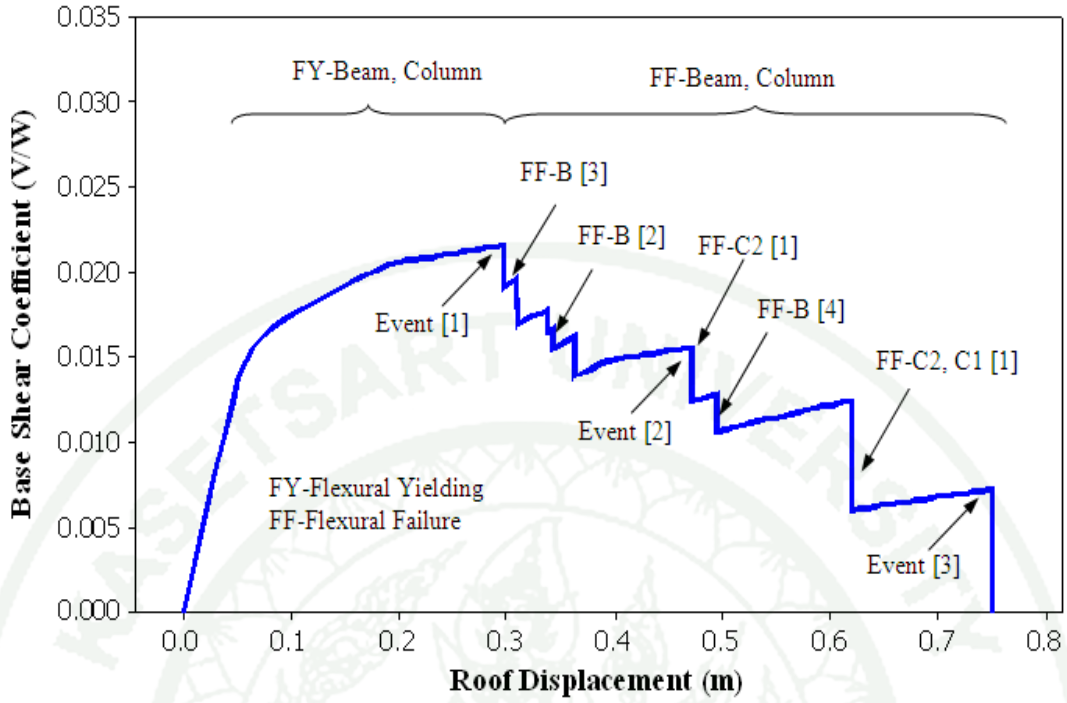

Figure 36 Capacity curve of the building without infill walls (Y-direction)

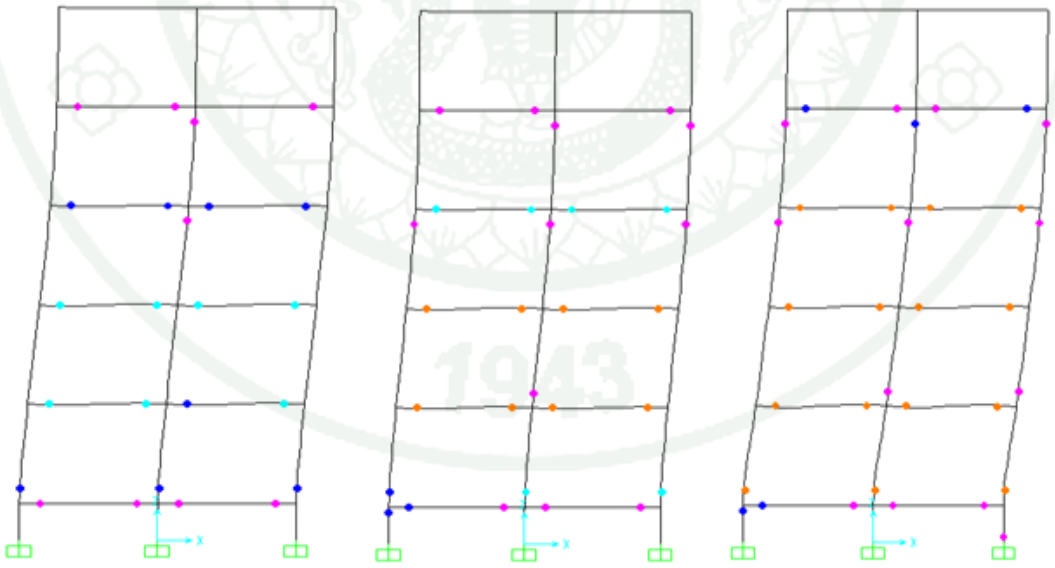

Event [1] Event [2] Event [3]

Figure 37 Damage distribution and failure mechanism of Bare Frame (Y-Direction)

The capacity curve of infill frame modeled by replacing the infill panel as equivalent diagonal strut along Y-direction is shown in Figure 38. The response of the building frame is linear until yielding of equivalent diagonal strut occurred. The capacity curve increases with reduced slope until ultimate lateral capacity of the building is achieved. In this case, the failure of components initiates from brick wall. The equivalent diagonal strut fails before ultimate lateral capacity of the building is reached and it can be seen from Event [1]. This is because masonry infill wall is very weak as compare to structural components.

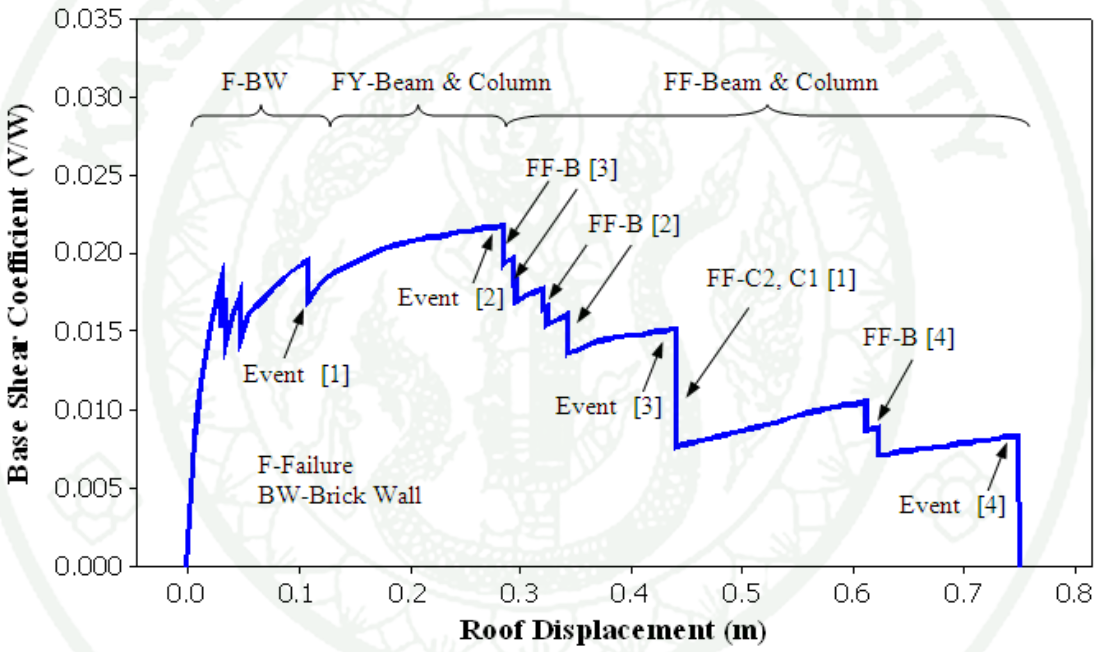

Figure 38 Capacity curve of the building with infill walls (Y-direction)

The lateral capacity dropped down due to collapse of beam at third floor B [3] at first point as similar to that of bare frame. The beam at fourth B [4] and second B [2] floor level fails in step wise step. When columns at first floor level C2 [1], C1 [1] are collapsed the lateral capacity of the building falls down penetratingly. The sequence of flexural yielding (FY) and flexural failure (FF) of components are reflected in Figure 39 where it can be traced out through formation of hinges of the member individually.

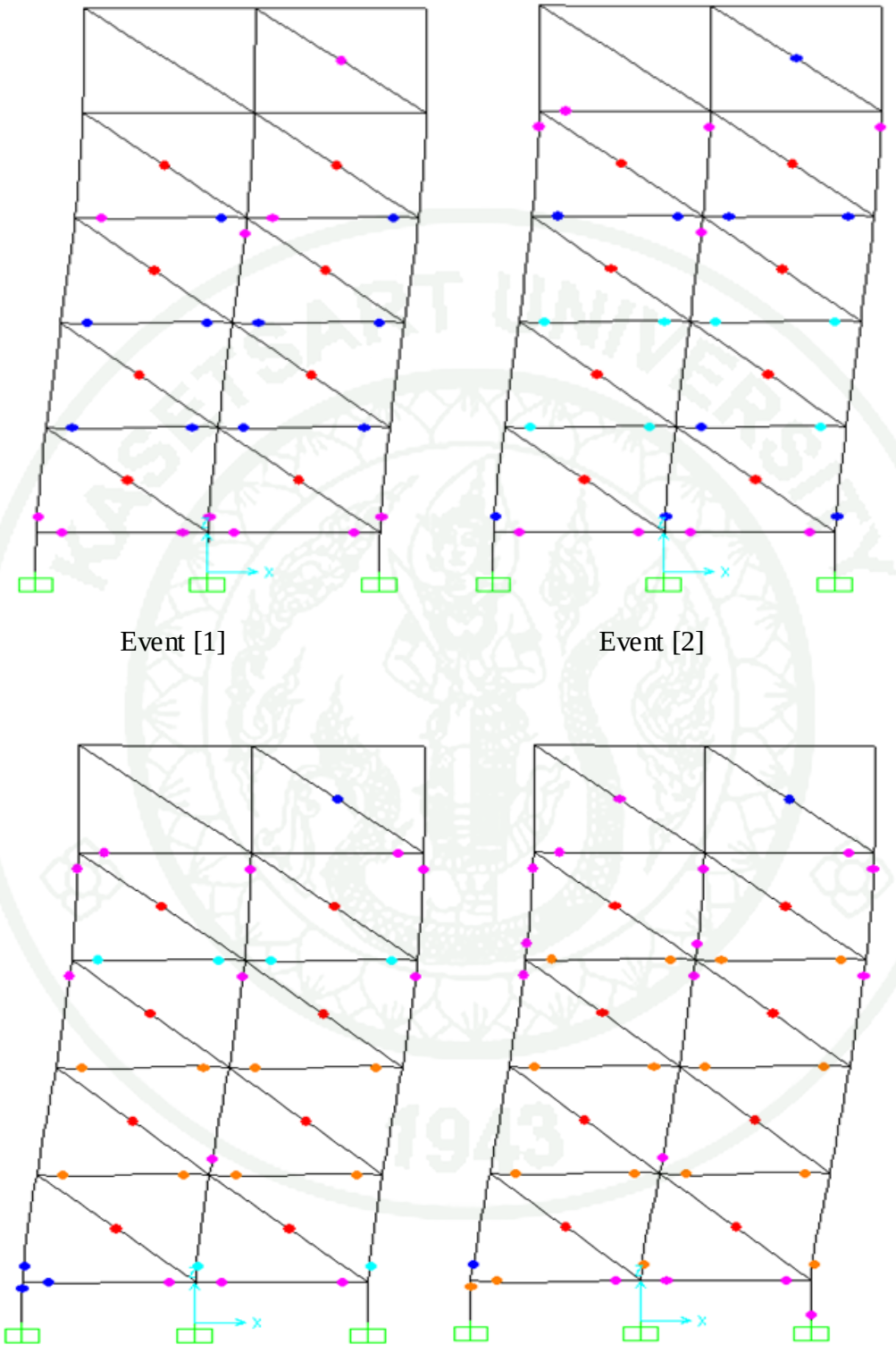

Figure 39 Damage distribution and failure mechanism of Infill Frame (Y-Direction)

2.2.2 Capacity curve of the building along strong direction

The capacity curve of the building without infill wall along X-direction is shown in Figure 40. The capacity curve of the building shows straight line until yielding of beams and columns are exhibited. The lateral capacity increases with the lesser gradient until failure of members occur after yielding of members such as beams at second and third floor level and columns at first floor level. The building frame along X-direction also demonstrated the similar sequence of failure of the members to that of frame along Y-direction.

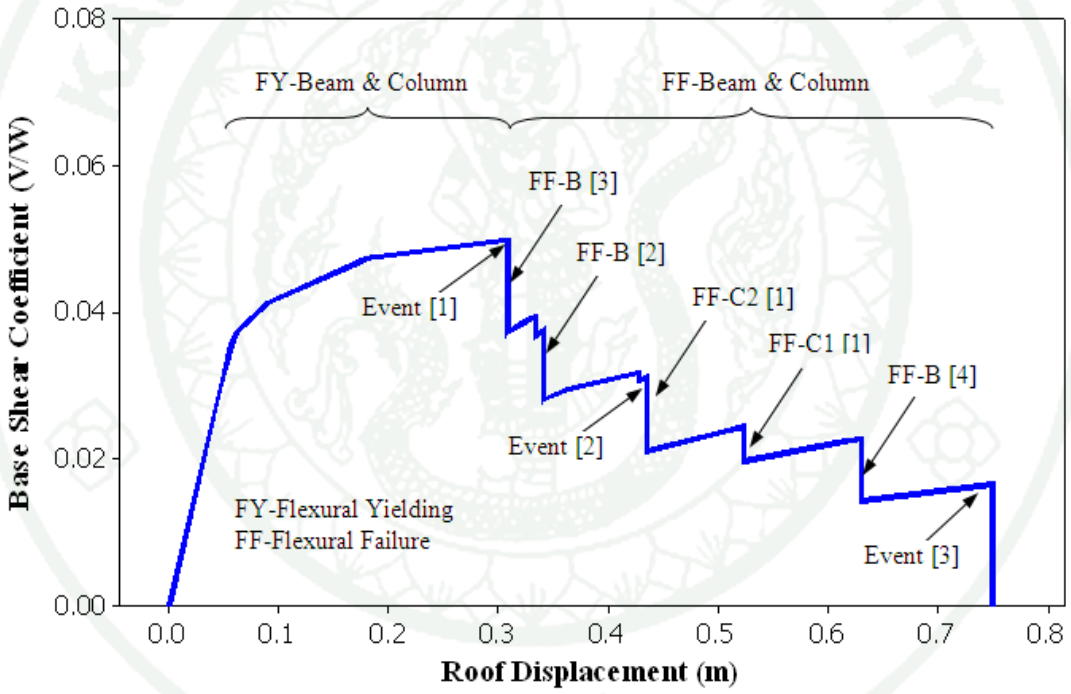

Figure 40 Capacity curve of the building without infill walls (X-direction)

The lateral capacity of the building dropped down due to collapsed of beams at third floor B [3] and followed by beam at the second floor B [2]. Subsequently columns at first floor C2 [1], C1 [1] levels and beams at the fourth floor B [4] level fails when building is sufficiently pushed till predetermined target displacement is attained. These collapse mechanisms, sequence of yielding and failure of individual members are shown in Figure 41 through hinge formation.

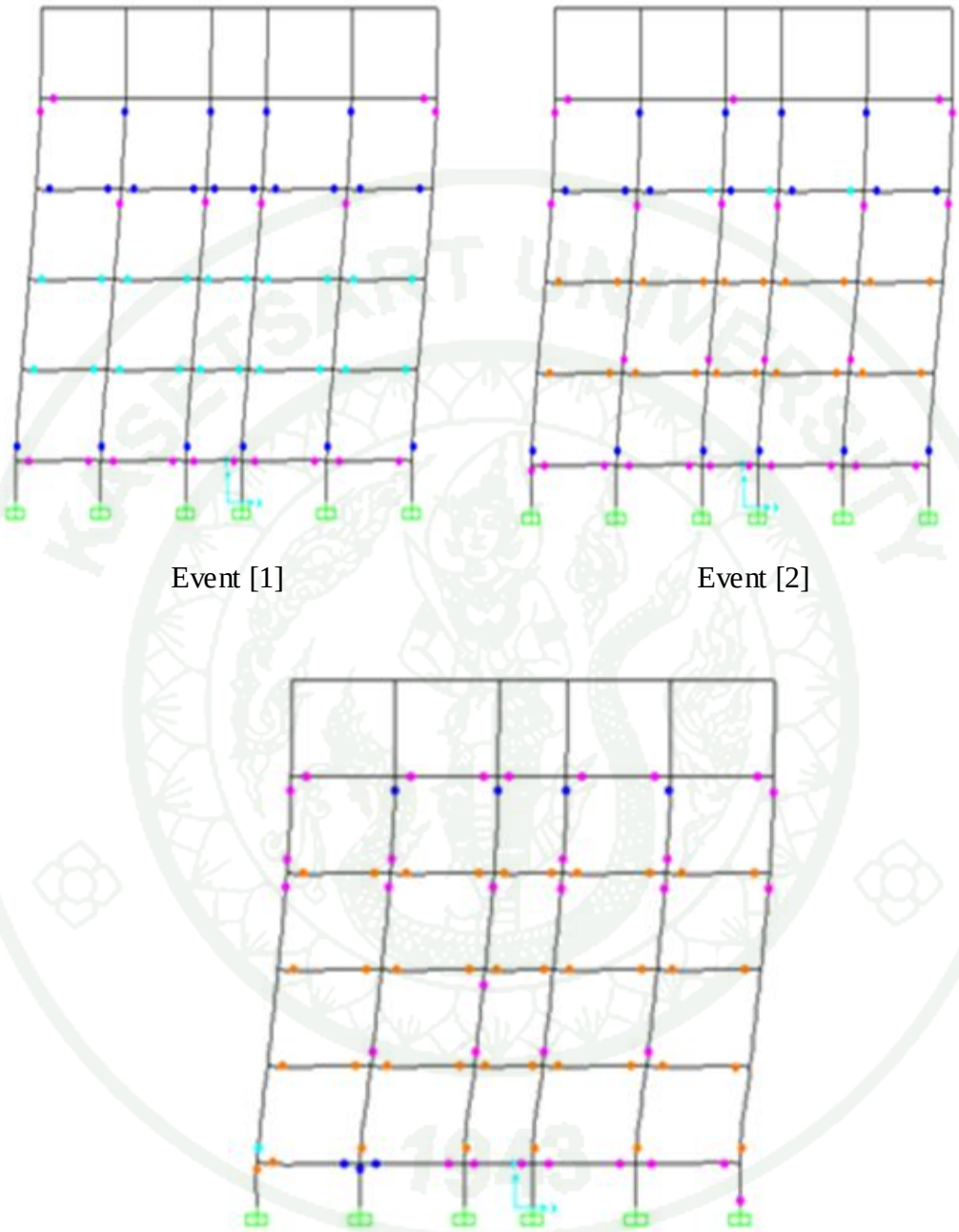

Figure 41 Damage distribution and failure mechanism of Bare Frame (X-Direction)

The capacity curve of the building in presence of infill wall along strong direction is illustrated in Figure 42. The nature of the curve is very similar to that of

infill frame along weak direction as shown in Figure 38. The capacity curve shows linear response of lateral load deformation relation until failure of brick walls begins. After failure of brick walls, still linear response is observed due to yielding of structural components but with reduced stiffness until the point where beam at third floor level B [3] under goes flexural failure.

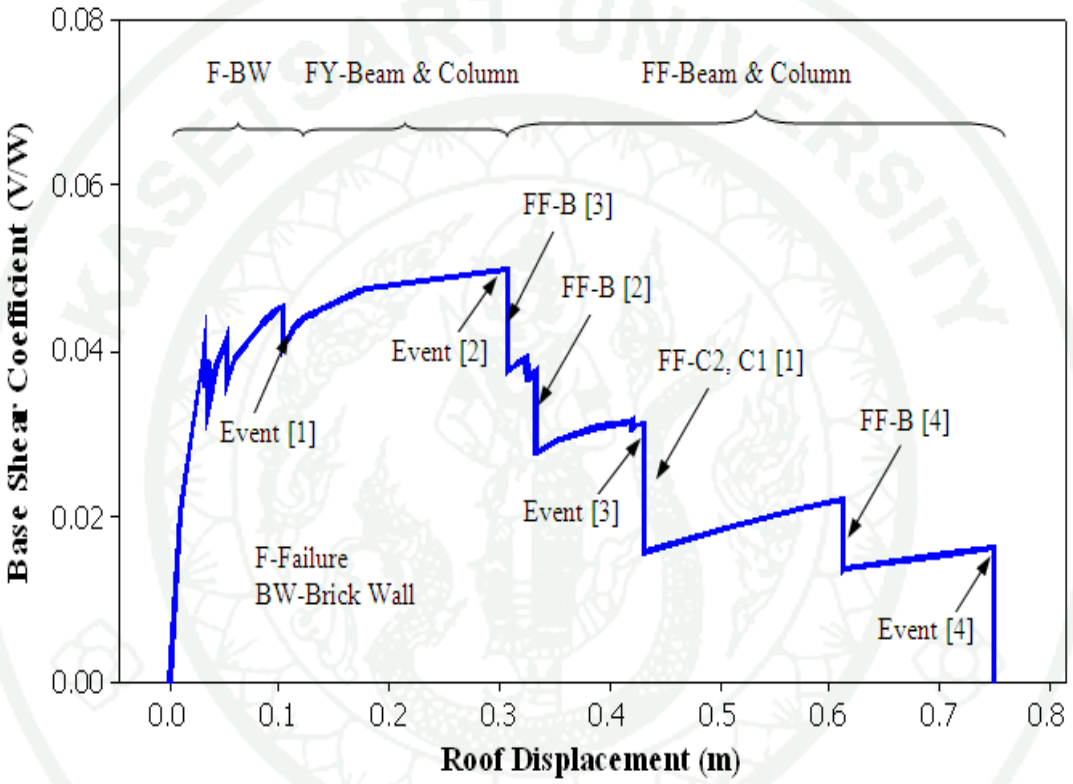

Figure 42 Capacity curve of the building with infill walls (X-direction)

It was also observed that after failure of brick infill walls, failure sequence of structural components shows all most identical nature to that of bare frame in the same direction. The sequence of individual component yielding and failure can be traced out from the capacity curve and its results can be noticeable through formation of hinges from Figure 43.

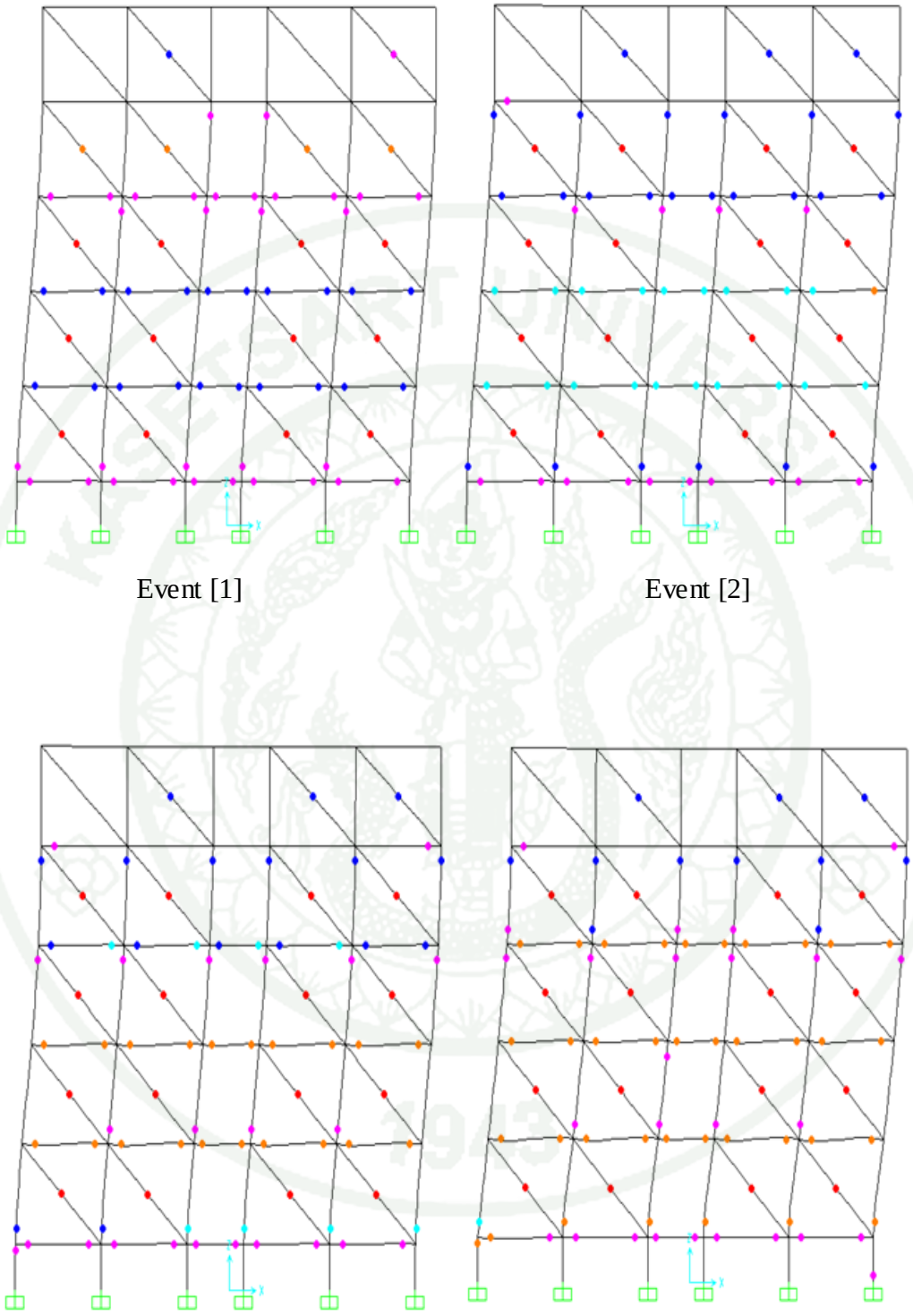

Figure 43 Damage distribution and failure mechanism of Infill Frame (X-Direction)

2.3 Hinges formation and failure mechanisms

In general, the plastic hinge formation for the bare frame begins with beam ends and then to column base of lower stories and then propagates to other members as the model is push sufficient until predetermine target displacement is achieved. In case of infill frame, hinge formation initiates from equivalent diagonal strut which reveals that infill is comparatively weak as compare to beams and column components when the structure is subjected to incrementally increasing lateral loads.

It should be noted that most of the beams starts falling from right end; this is because under combination of gravity and lateral loads the negative moment demand at right end is much higher than the positive moment demand at the left end. And also for this selected building the capacity of positive and negative moment is equal along the beam component. Mostly the column starts failing from opposite side of the applied lateral load at first storey level. This is because when the building is pushed sufficiently, the negative moment increases in this region and due to this high moment capacity flexural failure of column occurred. However, this selected building shows weak-beam strong-column mechanism from the analysis results.

2.4 Comparison of capacity curves

The comparison between the capacity curves with and without infill walls was made along weak and strong directions as shown in Figures 44 and 45 respectively. It was observed that infill walls contributes to increases the lateral initial stiffness of the building significantly and deformation capacity of the structure gets reduced within elastic region. The effect of masonry infill on the determination of ultimate lateral strength and its corresponding deformation capacity of the building was observed as less significant as compare to that of increased in initial stiffness when the structure is pushed till predetermine target displacement is achieved.

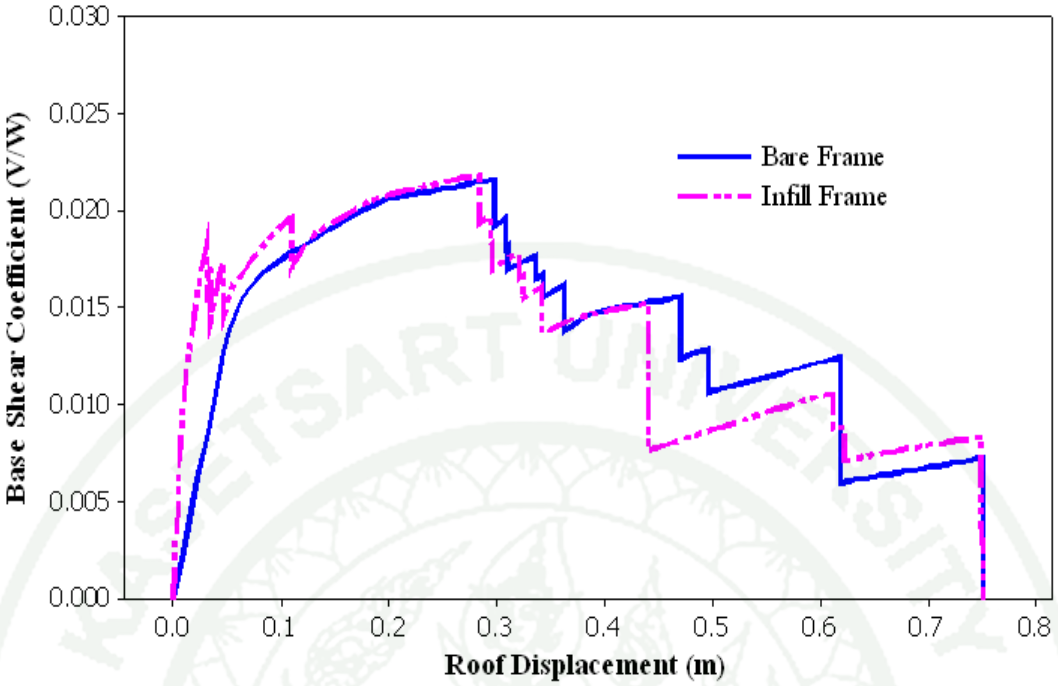

Figure 44 Comparison of capacity curves between Bare and Infill Frame (Y)

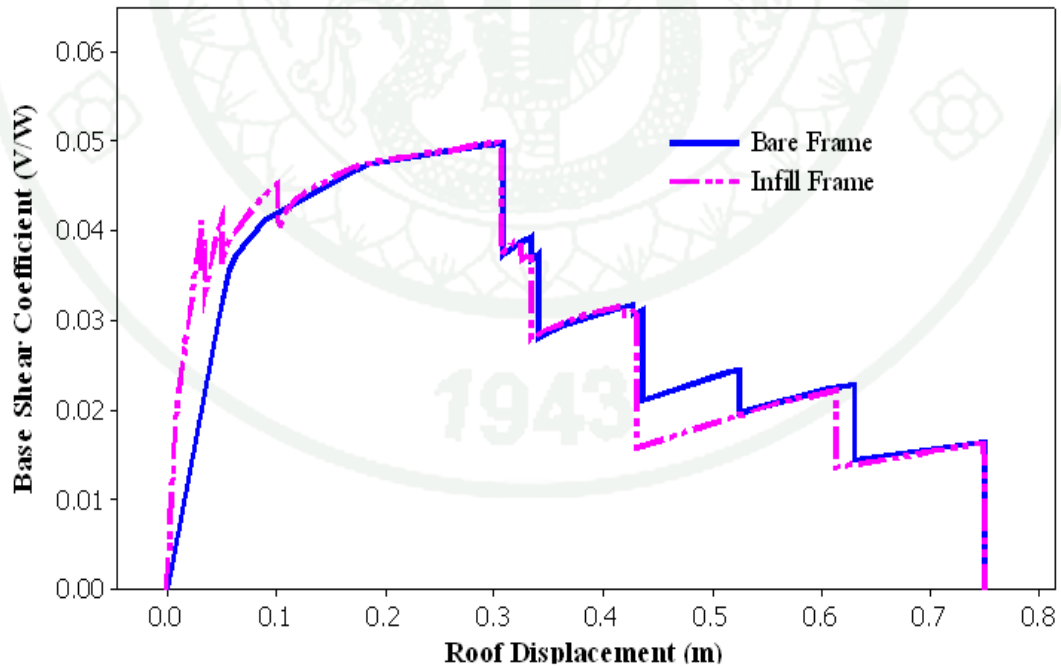

Figure 45 Comparison of capacity curves between Bare and Infill Frame (X)

It was observed that after failure of brick walls, the capacity curves (bare frame and with infill walls), shows very similar nature of sequence of yielding and failure of the structural components. The structural components start failing with beams at third floor levels B [3], beams at second floor levels B [2], columns at first floor levels C1, C2 [1] and beams at fourth floor levels B [4].

The comparison of the capacity curves along weak and strong direction was also made as shown in Figure 46. The initial stiffness and ultimate lateral strength of bare frame along X-direction increases approximately by 129 percent and 131percent respectively over bare frame along Y-direction. This is because as the number of bay increases it leads to increase the strength and stiffness of the frame.

In the case of infill frame, initial stiffness increases by 78 percent but the percent of increase in ultimate lateral strength remains almost unchanged as that of bare frame. Therefore, the ultimate lateral strength and initial stiffness obtained from the frame along strong direction gives overestimate results for seismic evaluation of building.

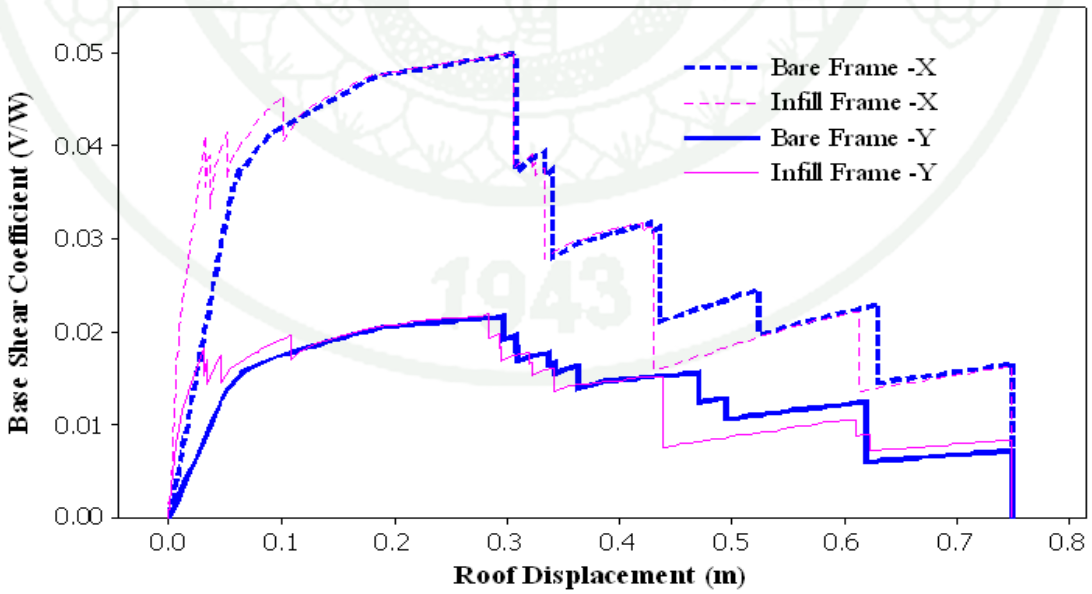

Figure 46 Comparison of capacity curves between X and Y Frames

2.5 Performance point of the building

Capacity spectrum method was adopted to evaluate the seismic performance of the selected residential building. The capacity curve of the building along weak and strong directions with and without infill walls were converted into acceleration displacement response spectra format. The earthquake demand was generated in accordance with IS-1893, 2002 for seismic zone factor 0.36 and converted to acceleration format. The capacity and demand spectra in acceleration displacement response spectra format were then superimposed to acquire performance point.

The performance point which represents the global behavior of the building is shown in Figure 47 for bare frame and Figure 48 for infill frame along Y direction. The demand curve intersects the capacity curve in between the point of immediate occupancy and collapse prevention for both cases. Similarly, for the bare frame and infill frame along strong direction, the demand curve intersects the capacity curve in between the event point of first yielding of components and immediate occupancy as shown in Figures 49 and 50 respectively. Therefore, inelastic response and security margin exist in both bare frame and infill frame along both the directions.

From the analysis results shows that marginal safety against collapsed is good enough and there exist sufficient strength and displacement reserved along both principal directions. This showed that the building has the capacity to withstand the considered earthquake ground motion. The collapse of building would not occur although failure of infill walls and yielding of beams are expected to occur when it is subjected to considered earthquake excitation.

The selected building doesn't require structural interventions as the inelastic deformation of structural components are not so significant to pose threat to the stability of the building and safety to its occupants from this analysis results.

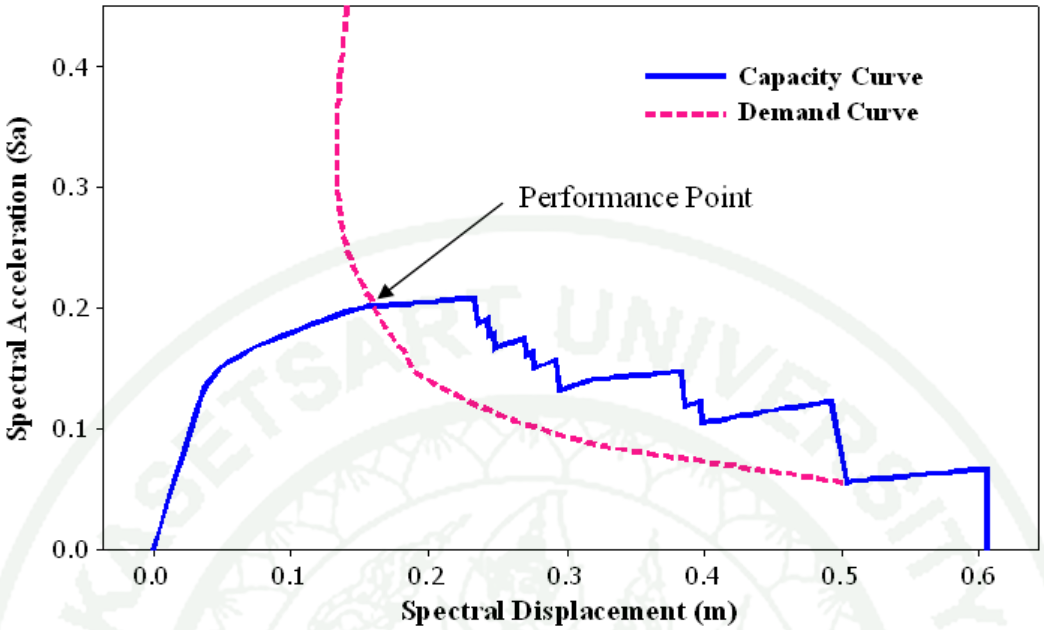

Figure 47 Performance point of building (Bare Frame Y-Direction)

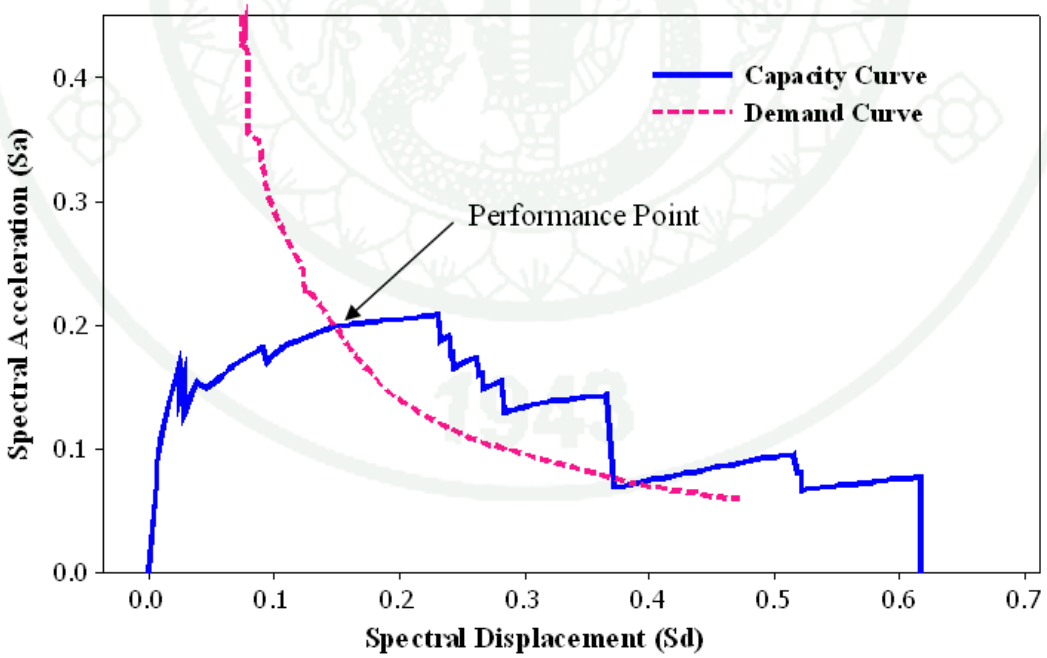

Figure 48 Performance point of building (Infill Frame Y-Direction)

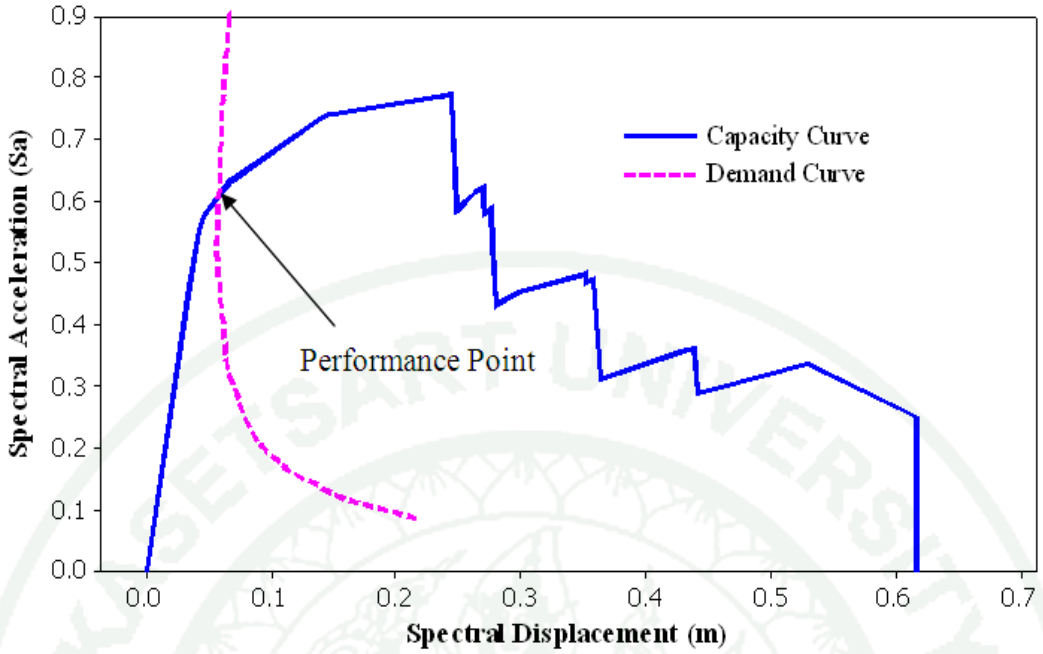

Figure 49 Performance point of building (Bare Frame X-Direction)

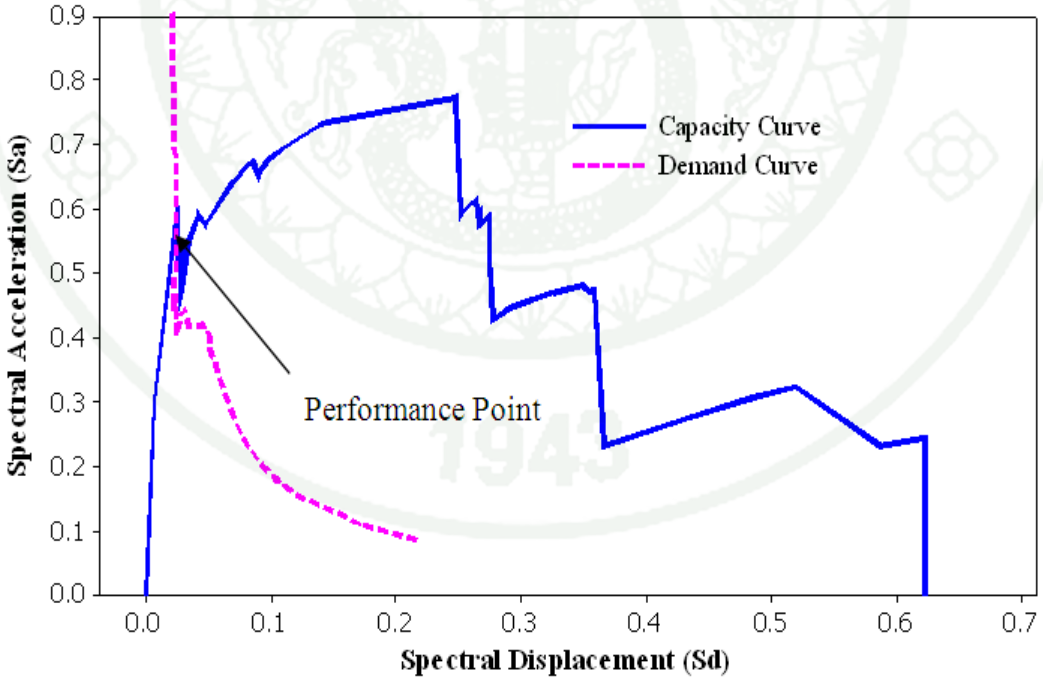

Figure 50 Performance point of building (Infill Frame X-Direction)

2.6 Capacity of the Building due to Variation of compressive strength of concrete (F_{ck})

The building along Y-direction was analyzed by varying compressive strength of concrete and keeping constant of all other parameters in order to examine its effect on capacity of the building. The result from the analysis shows that affects of compressive strength of concrete possesses marginally on both linear as well as in inelastic region as shown in Figure 51.

When compressive strength of the concrete was increased to *20 MPa* and *25 MPa*, it was observed that initial stiffness increased by 13.86 and 28.13 percent respectively over reference frame (F_{ck} = *15 MPa*). Similarly, the ultimate lateral capacity of the building increased by 4.20 and 7.60 percent approximately over the reference frame, when compressive strength of concrete increased to *20* and *25 MPa* respectively.

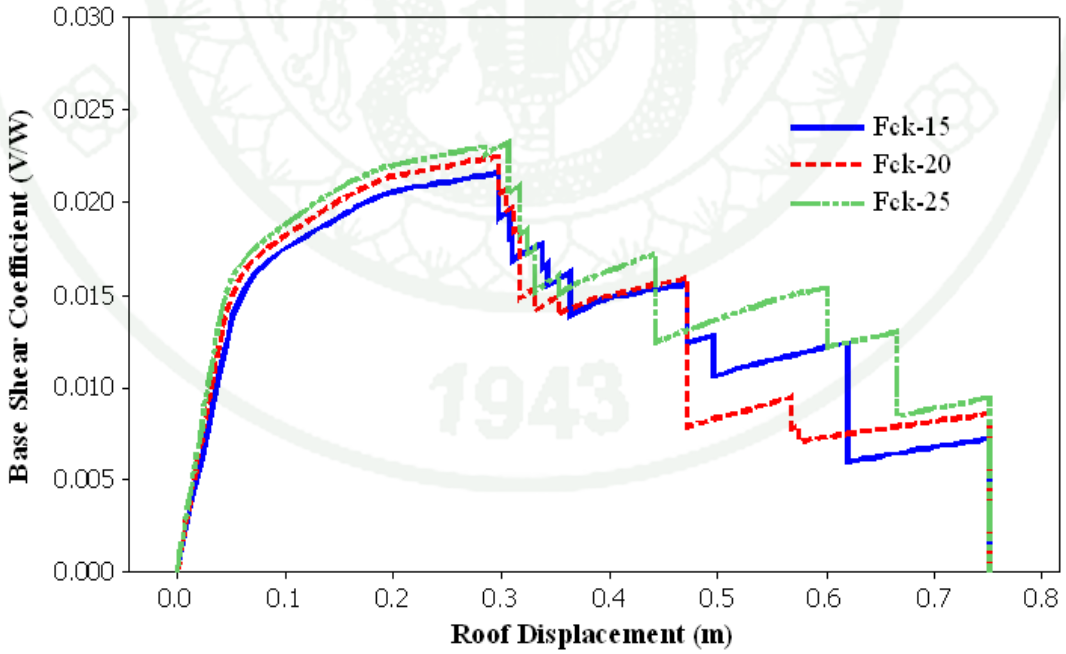

Figure 51 Comparison of capacity curves of the building for varying compressive strength of concrete

This is because, the yield moment capacity of the member increases when the compressive strength of the concrete increases due to increase in modulus of elasticity of concrete. The yield moment of the section can be estimated by using compatibility equations from equilibrium force of stress-strain diagram. The modulus of elasticity of concrete is related by 5000 times square root of compressive strength of concrete as per Indian standard code.

It was also observed that, roof displacements corresponding to ultimate lateral capacity of the building increases diminutively as the compressive strength of the concrete increases. The sequence of yielding and failure of components can be seen from appendix Figure B1-B4.

2.7 Capacity of the Building due to Variation of yield strength of reinforcement (F_y)

In order to investigate the effects of varying yield strength of reinforcement on the lateral strength of the building, the building was analyzed by maintaining all other parameters constant. The combined results are illustrated in Figure 52.

It was observed that variation of yield strength of reinforcement does not affect on initial stiffness of the building as all three curves (F_y *=250 MPa,* F_y *=350 MPa and* F_y *=415 MPa*) exactly coincide in a single line until linear region. On the other hand the initial yielding of the building increases drastically due to increase in yield strength of the reinforcement. When the yield strength of reinforcement increased to *350 MPa*, initial yield strength of the building increases by 54 percent as compare to the reference frame (F_y *=250 MPa*). Similarly, when yield strength of reinforcement increased to *415 MPa*, initial yield strength of the building increases by 17.52 percent and 80.96 percent over F_y *=350 MPa* and F_y *=250 MPa* respectively.

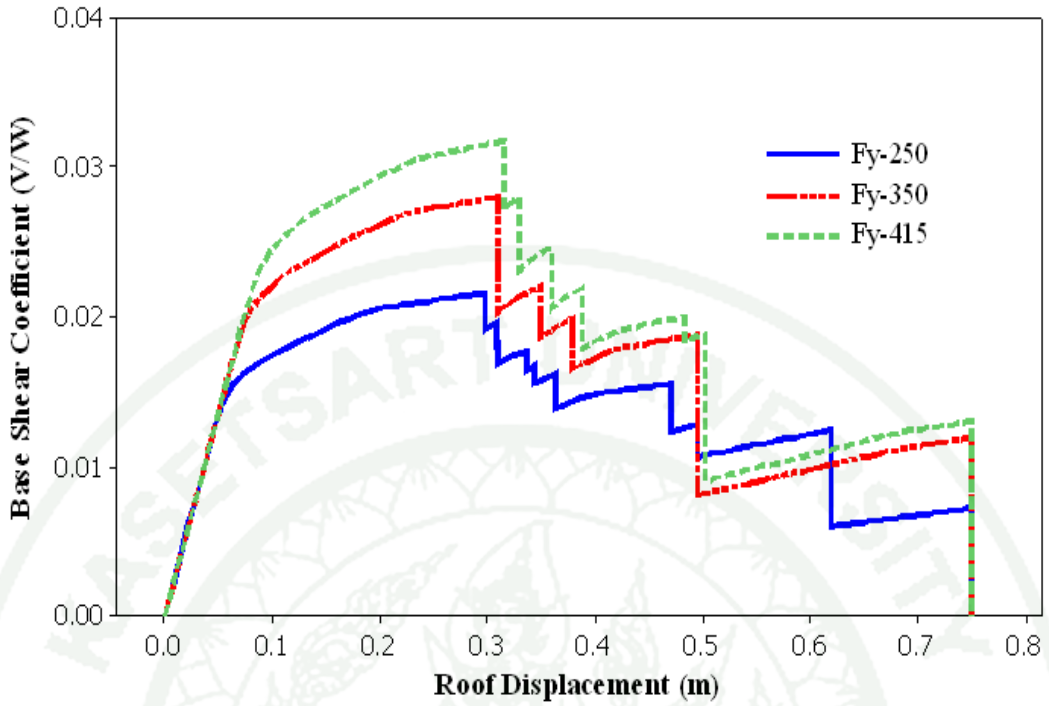

Figure 52 Comparison of capacity curves of the building for varying yield strength of reinforcement

The ultimate lateral capacity of the building increases with increase in yield strength of the reinforcement. When yield strength of reinforcement increased to F_y *=415 MPa* the ultimate lateral strength of the building is increased by 13.31 and 47.20 percent over the building having yield strength of reinforcement F_y *=350 MPa* and F_y *=250 MPa* respectively. In the same way for *350 MPa* of yield strength of reinforcement, the increased in lateral capacity of building was found to be 29.90 percent over F_y *=250 MPa*. This is because of the ductile behavior of the reinforcement steel.

The roof displacement corresponding to ultimate lateral capacity of the building increases slightly as the yield strength of the reinforcement increases. And further more the sequence of yielding and failure of components are shown in appendix Figures B5-B8 for F_y *=350 MPa* and F_y *=415 MPa*.

2.8 Capacity of the Building due to Variation of Infill Brick masonry thickness

The effect on lateral capacity of building due to variation of infill masonry thickness was considered by keeping all other parameters constant in the analyses. Figure 53 illustrates the results of the analysis due to variation of infill thickness on capacity curve of the building.

From this figure it was observed that initial stiffness of building with half brick thick wall was increased by 120.60 percent over the bare frame. When the thickness of infill wall increased to full brick (one brick) thick, stiffness increased by 235.90 percent as compare to bare frame.

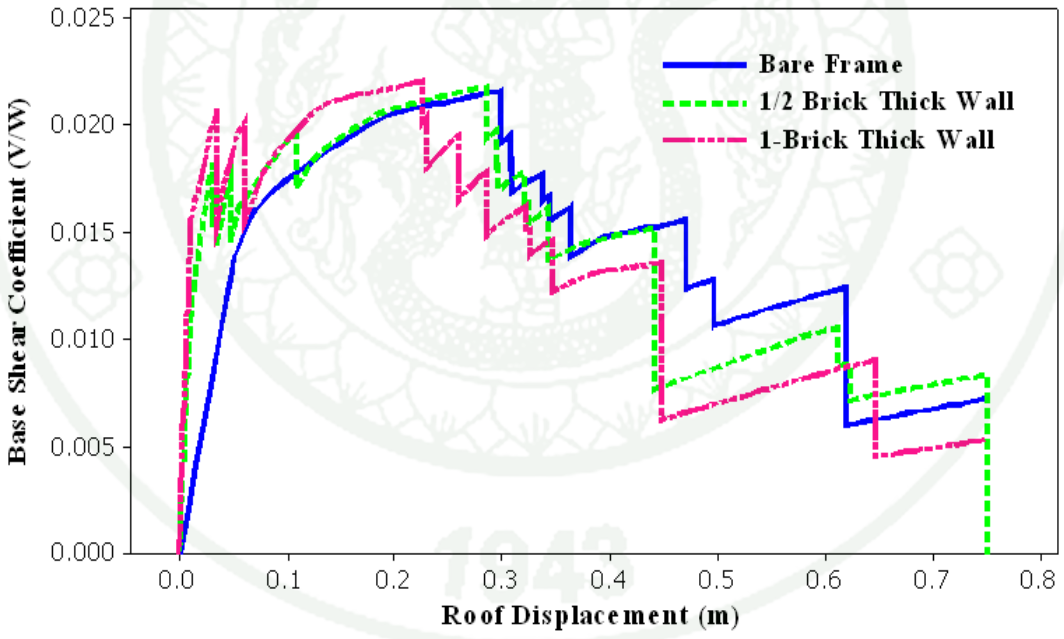

Figure 53 Comparison of capacity curves of the building for varying thickness of Brick masonry

It was obtained from the results that the ultimate lateral strength of frame due to presence of half brick thick wall increases marginally by 1.07 percent over bare

frame. When one brick thick wall was considered, the lateral strength of the frame was found to be increased approximately by 3.15 percent as compare to bare frame. Some infill panel especially at top floor level still resist lateral forces beyond elastic region due to increase in thickness of the infill wall, because cross sectional area increases of equivalent diagonal strut which replaced the infill panel increases simultaneously. Therefore stiffness of the equivalent diagonal strut increase which contributes to increased in overall stiffness and ultimate lateral capacity of the building as compare to half brick thick wall and bare frame.

The roof displacements corresponding to ultimate lateral capacity of the building for half brick and full brick thick wall was decreased by 4.50 percent and 31.77 percent over bare frame respectively. This is because when the infill fails large magnitude of force attack on structural components suddenly, resulting failure of structural component at lower roof displacement as compare to half brick wall and bare frame. The sequence of yielding and failure of components for half and full brick thick walls can be obtained from appendix Figures B9-B12.

2.9 Capacity of the Building due to Foundation effects

The foundation is one of the building components that may contribute significant effect on the lateral response of the building. The effects of foundation on lateral capacity of building were investigated by modeling the shallow foundation as uncoupled component model (Flexible base). These results were compared with fixed base and hinged base as shown in Figure 54.

The result from the analysis shows that capacity curve of the building obtained from fixed base, the yielding of the member starts first from beams and then to columns. The failure of components starts from beams at third floor and subsequently at fourth floor, second floor and then finally failure occur in the columns at first floor level.

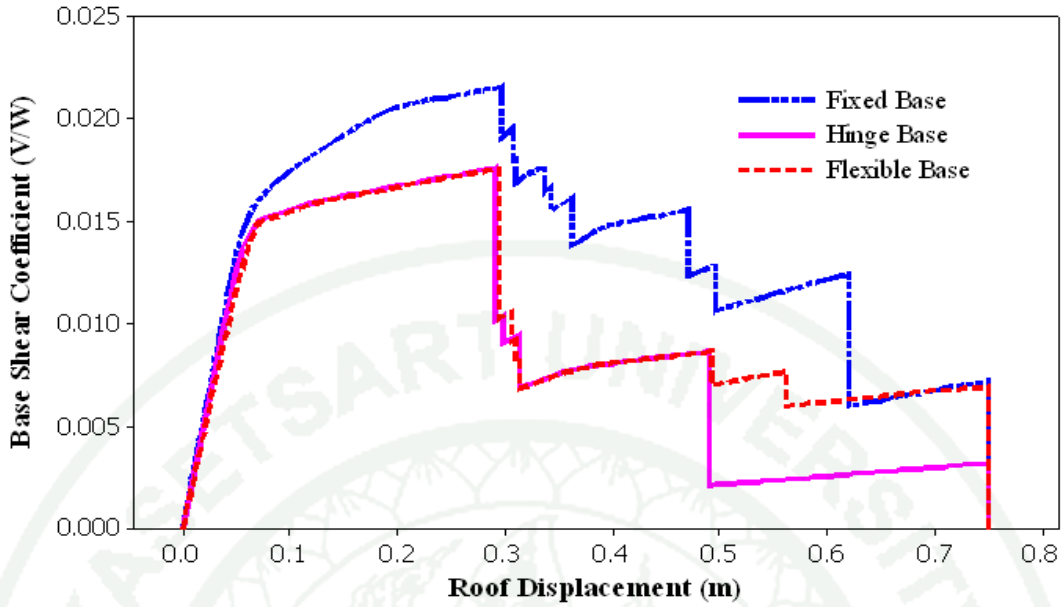

Figure 54 Comparison of capacity curves of the building for different supports.

In case of building with hinge base, the yielding and failure of components starts from beams at first, second and third floor levels. The collapse of column (C2) at second floor and third floor column (C3) occurs simultaneously along with failure of beams B [3] at third floor level. The detail of sequence of yielding and failure of individual components can be found from appendix Figures B13-B14.

When the flexible base is provided instead of fixed and hinge bases, the yielding starts from beams at first floor and columns at third floor level. Similar to that of hinge base, failure of components starts from beams at first floor level and then failure spread to the beams at second and third floor level. In this case, none of the column collapses completely but yields at second and third floor levels when the structure is pushed until predetermine target displacement is achieved. The sequence of yielding and failure of components for flexible base can be visible from appendix Figures B15-B16.

The initial slope until first yielding of components resembles for all three cases. The initial stiffness of the building due flexible base decreased by 26 percent

over fixed base and 1.73 percent over hinge base. The roof displacement corresponding to first yielding of member due to flexible base increases by 45 percent over fixed base.

The analysis results shows that ultimate lateral capacity of the building with foundation replaced by uncoupled component model and hinged base are found to be dropped down drastically as compare to fixed base foundation. The ultimate lateral capacity of the building decreased approximately by 22.75 percent for hinge base and uncoupled component model as compare to fixed base foundation. This is because the hinge base allows rotation and on the other hand uncoupled component model allows both rotation and translations of the structure there by building becomes less stiff to resist the lateral load in these cases.

When the structure is pushed sufficiently in to the nonlinear region, it was observed that there is no much affect on roof displacement corresponding to ultimate lateral capacity of the building. This is because; the component especially beams at first to third floor levels reaches its ultimate yielding capacity in their hinges in all three cases. Therefore the hinge base and uncoupled component model gives underestimate results for determining the lateral strength of the building as compare to fixed base.

2.10 Capacity curve for the newly designed and existing building

Having taken the same floor layout plan and material properties to that of existing building, the building was re-designed by using SAP2000 considering only vertical loads. The design sections obtained from SAP gives conservative sections especially beams and columns at upper floor level as compare to existing design sections. In order to compare the lateral capacity and its performance point under seismic loads with existing building, the pushover analysis of newly designed frame along weak direction with and without infill walls was performed. The capacity and its performance points are illustrated in the following sections.

The lateral capacity of the existing building along Y-direction was compared with newly designed building as shown in Figure 55. It was observed that initial stiffness and ultimate lateral capacity of the newly designed building is much lower to that of existing building. The deviation of ultimate lateral load carrying for newly designed building before initial failing of any structural components was obtained 30.76 percent lesser than existing building. This was happened because, the new designed sections gives conservative sections with respect to existing design sections or on the other hand the design sections used in the existing building might be overestimated. The roof displacement corresponding to ultimate lateral load carrying capacity does not differ much in both the cases.

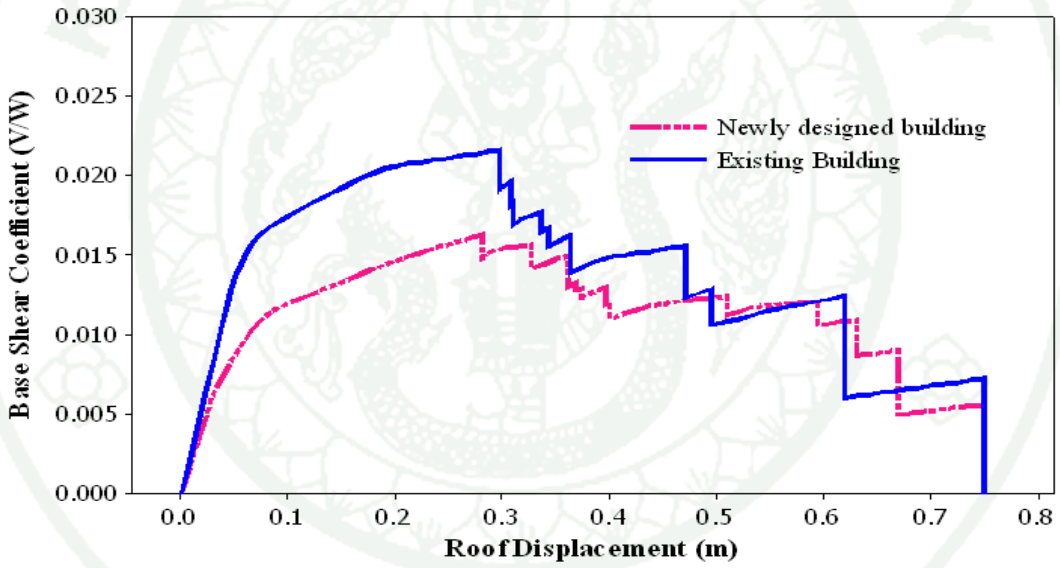

Figure 55 Comparison of capacity curves of existing and newly gravity load designed building

In the newly designed building, the lateral capacity of the building starts dropping down at first point when the beams at third floor B [3] under goes failure due to flexural yielding. The beams at forth floor B [4], second floor B [2], fifth floor B [5] and sixth floor B [6] fails sequentially when the building is pushed till predetermine target displacement is achieved. It was also noticed from the results that, the columns undergoes only yielding but do not collapse completely in the case of

new designed building. The sequence of yielding and failure of the components can be seen from appendix Figures B 17-B18.

2.11 Capacity of the Building due to Variation of Infill Brick masonry thickness

The performance point of newly designed building along Y direction was obtained and shown in Figures 56 and 57 for Bare Frame and Infill Frame respectively. These performance points were compared with the performance point for existing gravity load designed building used for seismic evaluation in this study.

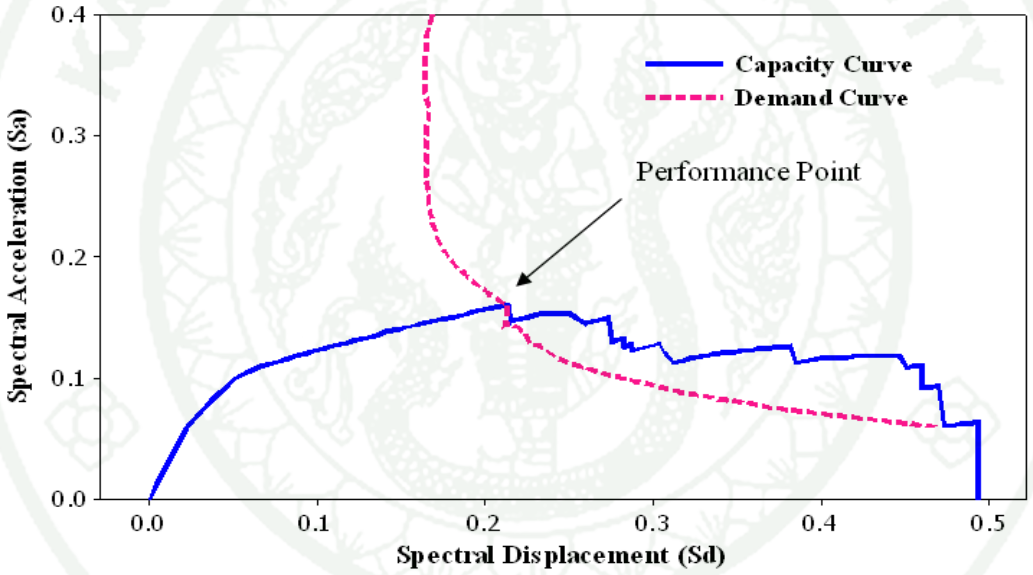

Figure 56 Performance point of newly designed building (Bare Frame)

The capacity and demand curve intersect near the point where structural components starts failing in the case of bare frame and for infill frame, there exists negligible distance between intersection point and initial dropping of lateral strength of the newly gravity load designed building. The performance points indicated from the newly designed building, there is no margin safety against collapse of structural components as compare to the existing gravity load designed building used for seismic evaluation in this study. Therefore it requires structural interventions to

enhance the lateral capacity of the structure to prevent the threat pose to the occupancy for the newly designed building.

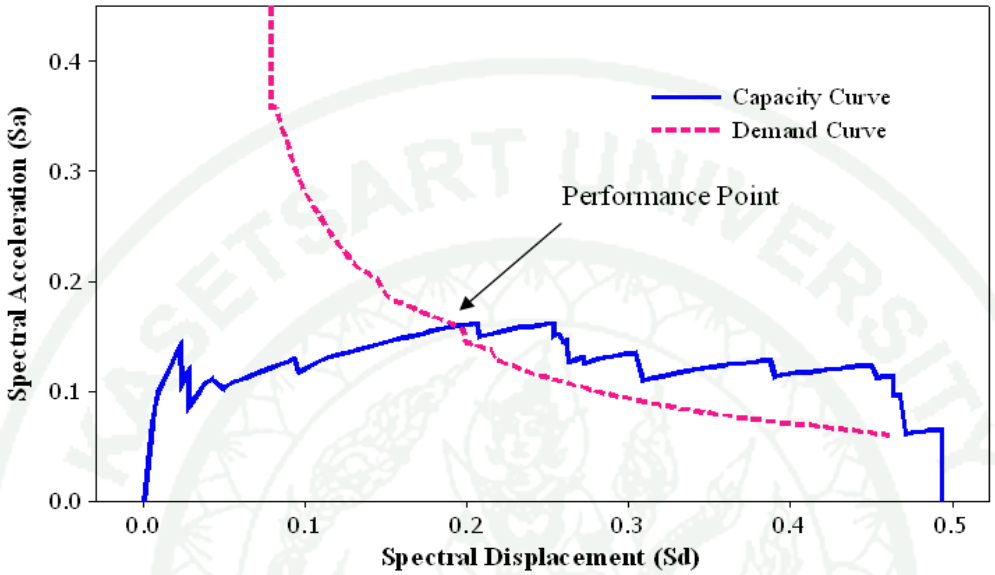

Figure 57 Performance point of newly designed building (Infill Frame)

From the above results, it can be concluded that gravity load designed building is more likely to collapse under considered seismic loads, all though the presence of infill walls increases the lateral resisting capacity and initial stiffness of the building significantly within elastic region. On the other hand, when the building is pushed beyond elastic region, the infill walls were found to be collapsed before the failure initiation of any structural components (beam or column). Therefore, the presence of infill tries to improve the performance point of the building but very negligible amount, since infill walls are too weak to resist lateral load until structural components exhibits structural instability. However, the lateral resisting capacity and its performance points of gravity load designed building is expected to enhance by providing higher compressive strength of concrete and higher yield strength of reinforcement.

CONCLUSIONS AND RECOMMENDATIONS

Conclusions

In this study, seismic evaluation of typical five-storey gravity load designed building has been carried out. This selected building was designed and constructed ahead of availability of seismic design code in our country. The structural members such as columns and beams are modeled as line element by introducing lumped plasticity at its ends base on FEMA-356 and ATC-40. Infill walls were modeled by replacing infill panel as equivalent single diagonal compression strut. Nonlinear static pushover analysis was performed by using SAP2000. The inverted triangular load was applied to the structure and this lateral load pattern remains unchanged throughout the pushover analysis. Seismic evaluation of the existing building was carried out in both major directions in accordance to IS: 1893-2000, ATC-40, 1996 and FEMA-356, 2000. Capacity spectrum method was adopted in this study to evaluate the seismic performance point of the building.

The parameters that affect the lateral capacity of the building were also examined in this study. To observe these effects, building along Y-direction was analyzed by varying compressive strength of concrete, varying yield strength of reinforcement bars, varying thickness of infill masonry wall and finally effect due to modeling of shallow foundation was carried out.

Following conclusions were drawn from the present study:

1. The effect of unreinforced infill masonry wall on seismic behavior of reinforced concrete frame building is significant within elastic region in which the initial stiffness and strength increases while the deformation capacity reduces.

2. There is no significant increase and decrease in terms of ultimate lateral strength and its corresponding roof displacement respectively for the building in presence of infill masonry walls.

3. The ultimate lateral strength and initial stiffness increases drastically along X-direction as compare to Y-direction. The frame along X-direction gives overestimate results for the determination of lateral strength and initial stiffness of the building.

4. The selected existing gravity load designed building in this case study shows good resistance to seismic loads. Therefore, it does not require structural interventions as the inelastic deformation of structural components are not so significant to pose threat to the stability of the building and safety to its occupants.

5. There is diminutively increased in initial stiffness and ultimate lateral strength of building due to increased in compressive strength of concrete. However, higher the compressive strength of concrete gives better resistance to seismic forces in both linear as well as nonlinear region.

6. The variation of yield strength of reinforcement does not affect much on initial stiffness of the building but there exist hefty increase on ultimate lateral strength of the building when the yield strength of reinforcement steel increases.

7. The effect of increase in infill masonry wall thickness on the capacity curve of the building was observed to be appreciably increased in initial stiffness of the building but on the other hand the ultimate lateral capacity of the building was found to be less considerable.

8. The uncouple component modeling (Flexible base) for shallow foundation and hinge base for the building gives underestimate results in determining ultimate lateral strength of the building for seismic evaluation as compare to assumed fixed base foundation.

9. The analysis result from the newly gravity load designed building shows that the structure is vulnerable to collapse when subjected to earthquake load. The performance point of such building is expected to be enhanced by increasing compressive strength of concrete and yield strength of reinforcement. Of course, in presence of infill increases its performance point of the building with marginal amount.

10. The results obtained from the pushover analysis gives the physical behavior of the structures in terms of capacity, demand and plastic hinge formation. The pushover analysis is comparatively easier to explore the inelastic action of the building structures through tracing the sequence of yielding and failure of each element of the structure.

Recommendations

In this study, two dimensional analytical model of symmetrical plan with five storey building was investigated by using non-linear static pushover analysis. Base on the present study, some recommendations are made for future investigations as follows:

1. The present study was carried out on symmetrical building lay out plan. This could be extended in incorporating torsion effects for unsymmetrical building plans.

2. This study was based on selected low-rise reinforced concrete building in Bhutan. Further study can be done on other buildings or structural systems for the evaluation of seismic performance, so that more rational and vivid conclusions can be achieved in this field of research.

3. The present study assumed that panels are fully infilled. Further study on seismic evaluation of existing building can be done by taking accounts of openings within the infill panel such as windows and doors which are unexceptional features left for the buildings.

4. Two-dimensional model have been deployed in this study and further study can be done with three-dimensional model of the building structures.

5. Non-linear static pushover analysis was carried out in the present study and this can be extended to nonlinear dynamics and Time history analysis in order to obtained more rational and realistic conclusions.

LITERATURE CITED

Al-Chaar, G., M. Issa and S. Sweeney. 2002. Behavior of Masonry Infilled Non-ductile Reinforced Concrete Frame. **Journal of Structural Engineering** ASCE, 128 (8): 1055-1063.

Angelo Masi, 2003. Seismic Vulnerability Assessment of Gravity Load Designed R/C Frames. **Bulletin of Earthquake Engineering** 1: 371–395, 2003.

Ashraf and Stephen, 1998. Practical Three Dimensional Nonlinear Static Pushover Analysis. **Published in Structure Magazine**, Winter, 1998.

Applied Technology Council, ATC 40. **Seismic Evaluation and Retrofit of Concrete Buildings**, California, 1996.

Buonopane. S.G. and R.N. White. 1999. Pseudo dynamic testing of masonry in filled reinforced concrete frame. **Journal of Structural Engineering** ASCE, 125 (6): 578-589.

Cagatey, I. H. 2005. Failure of Industrial Building during a recent Earthquake in Turkey. **Engineering Failure Analysis** 12 (2005) 497-507.

FEMA-273. 1997. **NEHRP Guidelines for the Seismic Rehabilitation of Buildings**. Building Seismic Safety Council, Federal Emergency Management Agency, Washington (DC).

FEMA-306. 1998. **Evaluation of Earthquake Damaged Concrete and Masonry Wall Buildings, Basic Procedures Manual**. Federal Emergency Management Agency, Washington (DC).

FEMA-450. 2003. **NEHRP Recommended Provisions for Seismic Regulations for New Buildings and other Structures**. Building Seismic Safety Council, Federal Emergency Management Agency, Washington (DC).

Fajfar, P. 2000. A Non-linear Analysis Method for Performance Based Seismic Design. **Earthquake Spectra**, Vol. 16, No. 3, PP. 573-592.

Freeman, S.A. 2004. Review of the development of the capacity spectrum method. **ISET Journal of Earthquake Technology**, Paper No. 438, Vol. 41, No. 1, March 2004, pp. 1-13.

Holmes, M. 1961. Steel Frames with Brickwork and Concrete Infilling. **Proceedings of Institution of Civil Engineers** London, Vol. 19: 473-478.

Hossein, M and Toshimi, K. 2004. Effect of Infill Masonry Walls on the Seismic Response of Reinforced Concrete Buildings Subjected to the, 2003 Bam Earthquake Strong Motion: A Case Study of Bam Telephone Center. **Bull. Earthq. Res. Inst. Univ. Tokyo** Vol. (79) 2004, PP. 133-156.

IS 1893 (Part 1): 2002. **Criteria for Earthquake Resistant Design of Structure**, Bureau of Indian Standards. New Delhi.

IS 456-2000. **Plain and reinforced concrete code of practice**. 4th Revision, Bureau of Indian Standards. New Delhi.

Kadid, A and Boumrkik, A. 2008. Pushover Analysis of Reinforced Concrete Frame Structures. **Asian Journal of Civil Engineering** (Building and Housing) Vol. 9, No. 1 (2008) pages 75-83.

Kiattivisanchai, 2001. **Evaluation of seismic performance of an existing medium rise Reinforced Concrete frame building in Bangkok**. Master Thesis, AIT, Bangkok.

Korkmaz, A.K., Demir, F. and Sivri, M. 2007. Earthquake Assessment of R/C Structures with Masonry Infill Walls. **International Journal of Science & Technology**, Volume 2, No 2, 155-164, 2007.

Kunnath, S.K., R.E.Valles-Mattox and A.M. Reinhorn. 1996. Evaluation of Seismic Damageability of a Typical R/C in Midwest United States. **Eleventh World Conference in Earthquake Engineering** (11WCEE), Acapulco, Mexico, June 1996.

Phuvoravan. K and Shrestha, B.C. 2008. Effect of Unreinforced Full and Partial Infilled Brick Masonry Wall in RC Frame Under Seismic Loading. **The 13th National Convention in Civil Engineering.**

Liauw, T.C. 1978. Test on Multistorey Infilled Frrames Subjected to Dynamic Lateral Loading. **ACI Structural journal** April, 1979.

Lee, Choi, Cheong and Kim. 2006. Evaluation of Seismic Performance of Multistorey Building Structures based on Equivalent Responses. **Engineering Structures** 28 (2006) 837–856.

Lakshmanan, N. 2006. Seismic Evaluation and Retrofitting of Buildings and Structures. **ISET Journal of Earthquake Technology**, Paper No. 469, Vol. 43, No. 1-2, March-June 2006, pp. 31-48.

Magents, G and Pampanin, S. 2004. Seismic Response of Gravity Load Designed Frames with Masonry Infills. **13th World Conference on Earthquake Engineering Vancouver**, B.C. Canada August-2004.

Mehmet and Altin. 2006. Behavior of Reinforced Concrete Frames with Reinforced Concrete Partial Infills. **ACI Structural Journal**, 2006.

Maria Polese, Gerado Mario, Cristiano, Iunio and Gaetano. 2008. Vulnerability Analysis for Gravity Load Designed RC Buildings in Naples – Italy. **Journal of Earthquake Engineering**, 12(S2):234–245, 2008

Mohamed Nour. 2007. **Application of Recent Techniques of Pushover for Evaluating Seismic Performance of Multistory Buildings**. Master Thesis, Cairo University, Egypt.

Mallick, D.V and Garg, R.P. 1971. Effect of Openings on the Lateral Stiffness of Infilled Frames. **Proceedings of Institute of Civil Engineers**, 49(6): 193-209.

Murty and Das. 2004. Brick masonry infill in seismic design of RC frame buildings. **The Indian Concrete Journal**, August 2004.

Phati Wet. 2002. **Seismic Evaluation of Beam-column Frame building with non ductile reinforced Concrete details**, Master Thesis, AIT, Bangkok.

Pauley, T. and M.J.N. Priestley. 1991. **Seismic Design of Reinforced Concrete and Masonry Buildings**. John Wiley & Sons, Inc.

Shrestha, B.C. 2008. **Effect of Unreinforced Full and Partial Infilled Brick Masonry Wall in RC Frame Under Seismic Loading**. Master Thesis, Kasetsart University, Bangkok.

Smith, B.S. 1967. Method for Predicting the Lateral Stiffness and Strength of Multi-Storey Infilled Frames. **Building Science** Vol. 2: 247-257.

Smith, B.S. and A. Coull. 1991. **Tall Building Structures: Analysis and Design**. John Wiley & Sons, Inc. USA.

SAP2000 Integrated Finite Elements Analysis and Design of Structures. SAP2000 Web Tutorials. **Computers and Structures, Inc.** Berkeley, California, USA.

Tangsaereemankong, P. 1998. **Seismic over-strength of multistory reinforced concrete frame buildings in low seismic zone**. Master Thesis, AIT, Bangkok.

Zarnic. 1995. Modeling of Response of Masonry Infill Frames. **10th European Conference of Earthquake Engineering**, Balkema, 1995.

Zine. A and Kadid, A. 2007. Pushover Analysis of Reinforced Concrete Structure Designed According to the Algerian Code. **Journal of engineering and applied sciences** 2(4):733-738, 2007.

Zou, X.K and Chan, C.M, 2005. Optimal Seismic Performance-based Design of Reinforced Concrete Buildings using Nonlinear Pushover Analysis. **Engineering Structures** 27 (2005) 1289–1302.

APPENDICES

Appendix A

Effective width calculations of diagonal strut and spring constants of shallow foundation modeling.

A.1 Equivalent diagonal strut width

A method base on equivalent diagonal strut approach for analysis and design of infill frames subjected to in-plane forces are proposed in the past studies. It provides rational bases for estimating the lateral strength and stiffness of the infill frames. The contribution of masonry infill panels to the response of infill frame is modeled by replacing the infill panels with equivalent single diagonal strut. The width of the equivalent diagonal strut Z was obtained from FEMA-273 which was proposed by Mainstone (1971) by following equations:

$$Z = 0.175(\lambda h)^{-0.4} d_m \tag{A1}$$

$$\lambda = \left[\frac{E_m t \sin 2\theta}{4E_c I_g h_m}\right]^{1/4} \tag{A2}$$

Where, h = 3.2 m, and h_m = 2.7 m are the height of the column and infill wall respectively. E_c = 19364916.73 kN/m^2, and E_m = 1650000 kN/m^2 are the modulus of elasticity of frame and infill panel. I_g = 0.00125052 m^3 is the moment of inertia of column. d_m = 4.54 m is the diagonal length of infill panel. l_m = 3.65 m, and t = 0.125 m are length and thickness of infill wall from appendix Figure A1.

$$\text{Where } \theta = \tan^{-1}\left(\frac{h_m}{l_m}\right) = \tan^{-1}\left(\frac{2700}{3650}\right) = 36.49^{\circ}$$

$$\lambda = \left[\frac{E_m t \sin 2\theta}{4E_c I_g h_m}\right]^{1/4} = \left[\frac{1650000x125x0.96}{4x19364917x0.001250521x2.7}\right]^{1/4} = 0.932789647$$

$$Z = 0.175(\lambda h)^{-0.4} d_m = 0.175\left(0.932789647 \ \ x3.2\right)^{-0.4} x4.54 = 0.513 \text{ m}$$

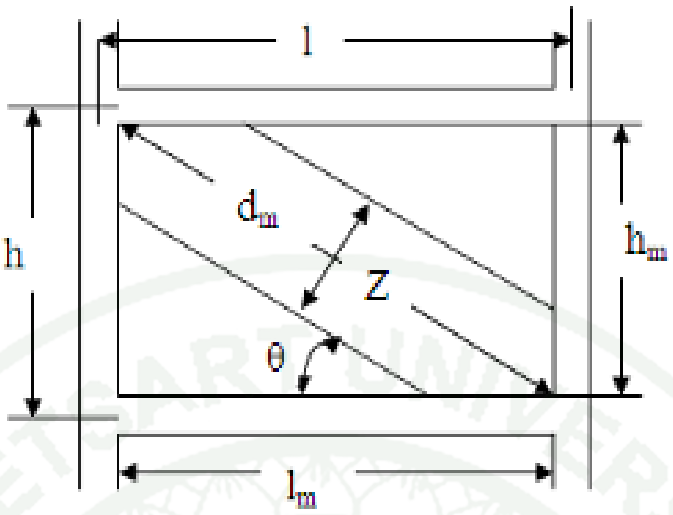

Appendix Figure A1 Idealization of infill panel as equivalent diagonal strut

A.2 Initial stiffness (k_0), yield force and yield displacement for equivalent diagonal strut

The sliding shear failure is the governing failure mode and the Mohr Coulomb failure criterion was applied to assess the maximum horizontal shear force given by equation A3.

$$V_f = \tau_0 t l_m + \mu N \quad \text{(A3)}$$

From Figure A1, maximum horizontal shear force V_f can be estimated by equation A4.

$$V_f = R_c \cos\theta \quad \text{(A4)}$$

From equations (A3) and (A4) V_f was calculated from equation A5

$$V_f = \frac{\tau_0 t l_m}{(1 - \mu \tan\theta)} = V_m \quad \text{(A5)}$$

Where

$$\tau_0 = 3\% f_m^{'}$$

$f_m^{'}$ =3000 kN/m^2 =3 *MPa* (masonry compressive strength)

$$V_f = \frac{90x0.125x3.65}{(1-0.2x0.74)} = V_m = 48.2 \quad \text{kN}$$

The maximum displacement at maximum lateral force is estimated by equation A6

$$U_m = \frac{\varepsilon_m^{'} d_m}{\cos\theta} \tag{A6}$$

$\varepsilon_m^{'}$ = Masonry compressive strain

$$U_m = \frac{0.002\,x4.54}{\cos(36.49)} = 0.01135$$

The initial stiffness K_0 can be obtained from equation A7.

$$K_0 = 2(V_m / U_m) \tag{A7}$$

$$K_0 = 2(48.2 / 0.01135) = 8492.48 \ \text{KN/m}^2$$

The lateral yield force V_y and displacement U_y was determined by equations A8 and A9 respectively.

$$V_y = \frac{V_m - \alpha K_0 U_m}{1-\alpha} \tag{A8}$$

$$V_y = \frac{48.2 - 0.2x8492.48x0.01135}{1-0.2} = 36.15KN$$

$$U_y = \frac{V_y}{K_0} \tag{A9}$$

$$U_y = \frac{36.1}{8492.48} = 0.0043m$$

A.3 Calculation of radius R for equivalent circular footing

The size (L, B) of the footing =2.42x2.42 m
Depth (D) of the footing is 2 m

$$\text{For translation, } R = \left(\frac{BL}{\pi}\right)^{1/2}$$

$$R = \left(\frac{2.42x2.42}{\pi}\right)^{1/2} = 1.365\,\text{m}$$

$$\text{For rotation, } \quad R = \left(\frac{B^3 L}{3\pi}\right)^{1/4}$$

$$R = \left(\frac{2.42^3 x2.42}{3\pi}\right)^{1/4} = 1.38\,\text{m}$$

A.4 Calculation of spring constants

Poisson's ratio may be assumed as ν =0.25 for rock, stiff clay and nearly dry sand Young's modulus of elasticity for medium normally consolidated sand ranges in between 20000-40000 *kPa*.

The stiffness parameters for shallow bearing foundation such as shear modulus G for a soil is related to Young's modulus of elasticity E and Poisson's ratio ν as shown below.

$$G = \frac{E}{2(1+\nu)}$$

$$G = \frac{40000}{2(1+0.25)} = 16000 \quad \text{KN/m}^2$$

$$K_0 = \left(\frac{8GR}{2-\nu}\right) \quad \text{For horizontal stiffness coefficient}$$

$$K_0 = \left(\frac{8x16000\ x1.365}{2-0.25}\right) = 99840$$

$$K_0 = \left(\frac{4GR}{1-\nu}\right) \quad \text{For vertical stiffness coefficient}$$

$$K_0 = \left(\frac{4x16000\ x1.365}{1-0.25}\right) = 116480$$

$$K_0 = \frac{8GR^3}{3(1-\nu)} \quad \text{For rotational stiffness coefficient}$$

$$K_0 = \frac{8x16000\ x1.38^3}{3(1-0.25)} = 149508\ .096$$

Appendix Table A1 Spring constants for shallow foundation modeling

Spring constants	K_0	α	β	$K = \alpha\beta K_0$ (KN/m)
Horizontal ($K_s h$)	99840	1.025	1.65	168854.4
Vertical ($K_s v$)	116480	1.035	1.25	150696
Rotation ($K_s r$)	149508.096	1.05	1.85	290419.4765

Appendix B

Sequence of Yielding and failure of the members under parametric studies

B. The parameters that affects the lateral capacity of the building

The effects on lateral capacity of the building by varying material properties such as compressive strength of concrete and yield strength of reinforcement, infill wall thickness, shallow foundation modeling and redesigned of building by using SAP2000 were carried out as parametric studies. The pushover analysis was carried out for all of these cases individually.

The sequence of failure and yielding of components are explained vividly in the following capacity curves. Furthermore, the damage distribution and failure mechanisms are shown in the following figures where the hinges formation can be traced out along the member as a result of pushover analysis.

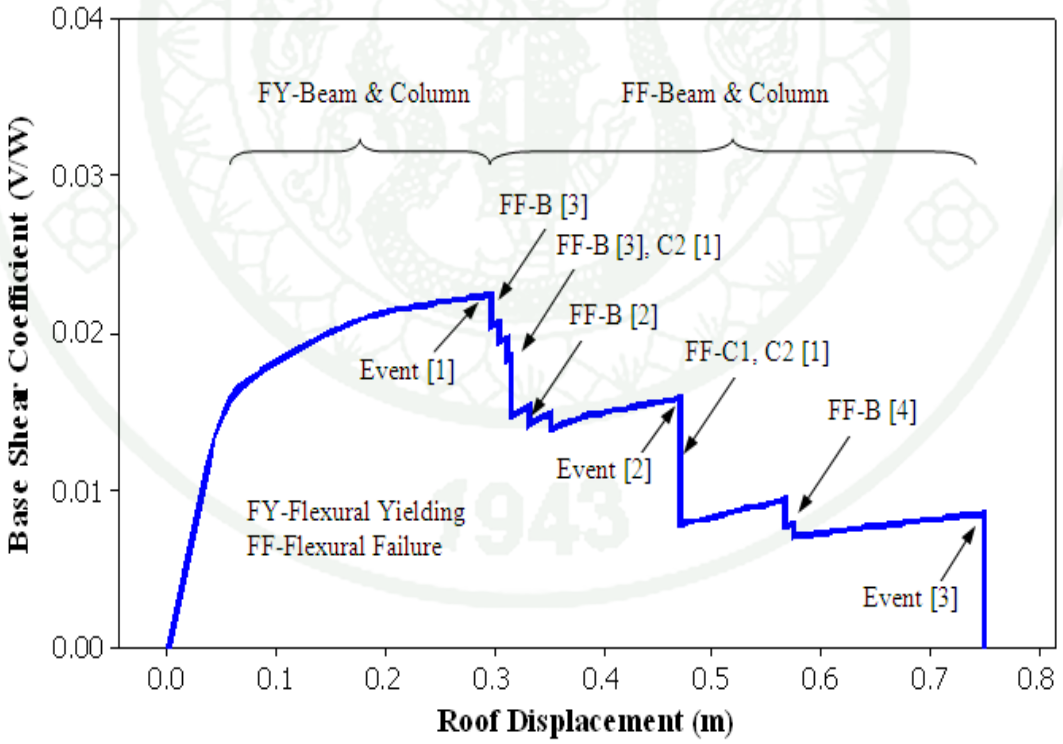

Appendix Figure B1 Capacity curve of the building for F_{ck} *-20 MPa*

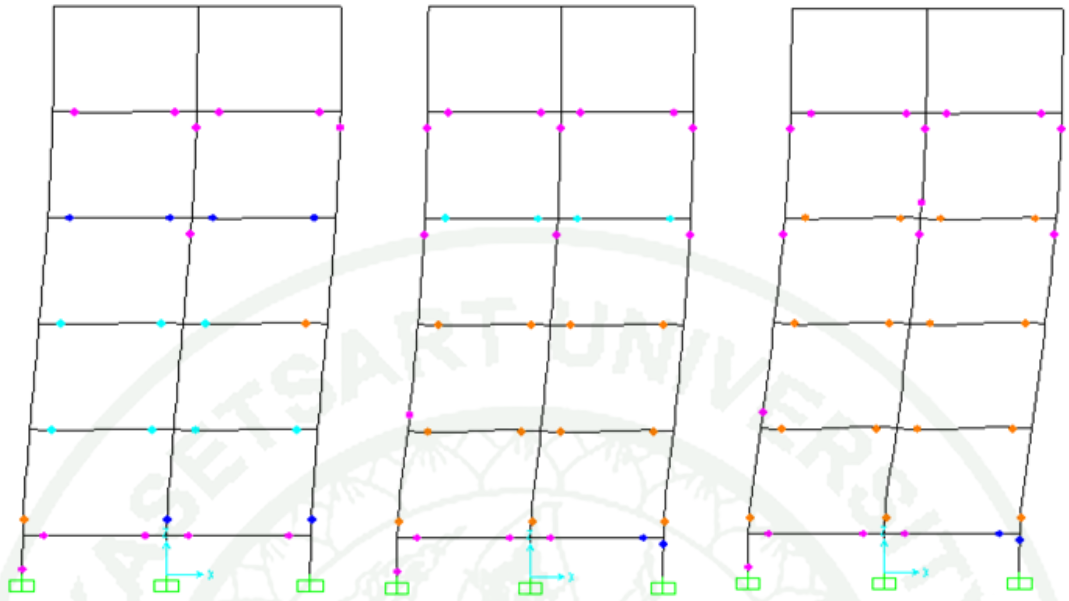

Appendix Figure B2 Damage distribution and failure mechanism for F_{ck} *-20 MPa*

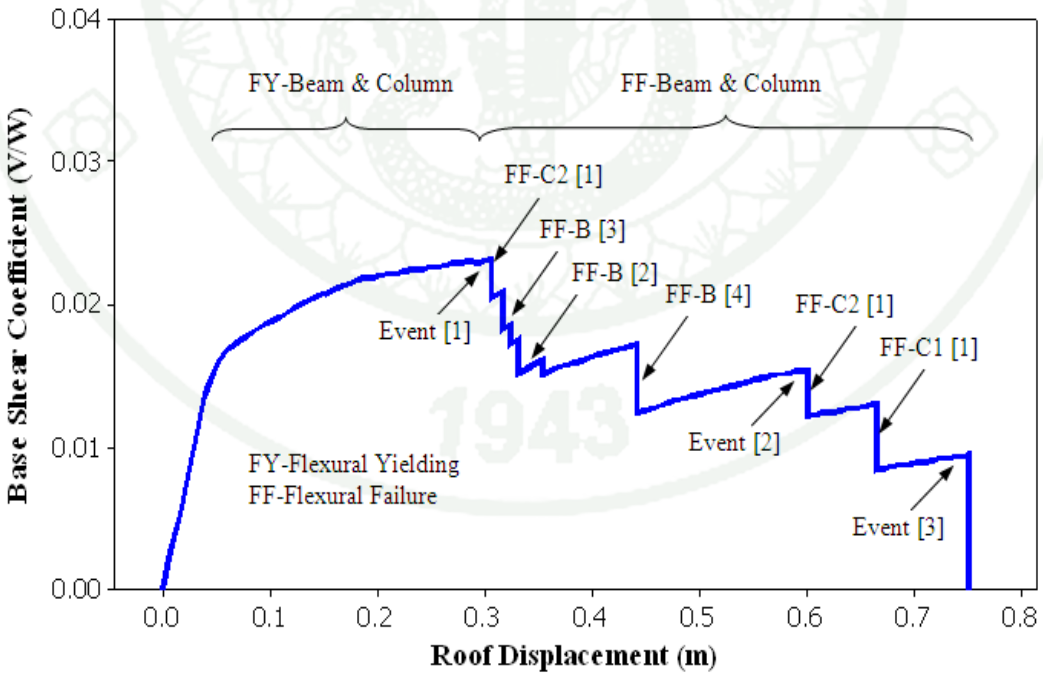

Appendix Figure B3 Capacity curve of the building for F_{ck} *-25 MPa*

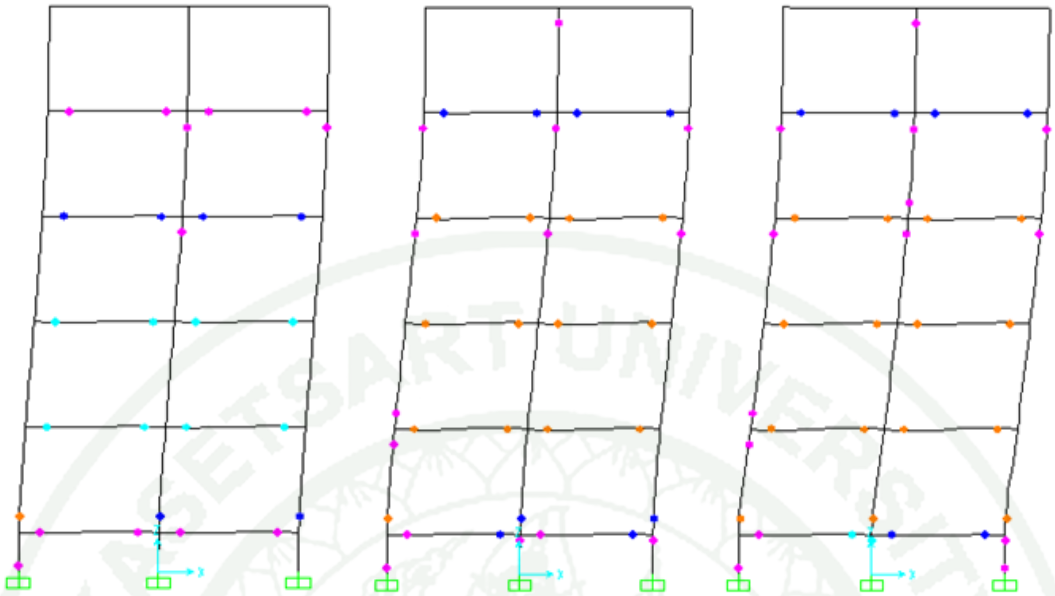

Appendix Figure B4 Damage distribution and failure mechanism for F_{ck} *-25 MPa*

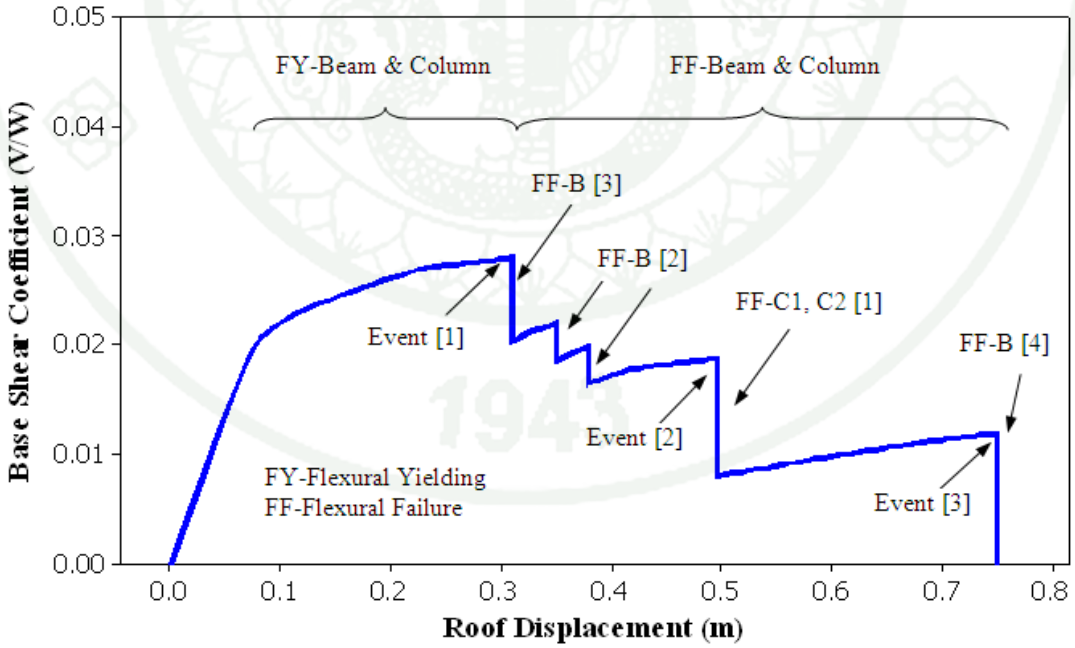

Appendix Figure B5 Capacity curve of the building for F_y *-350 MPa*

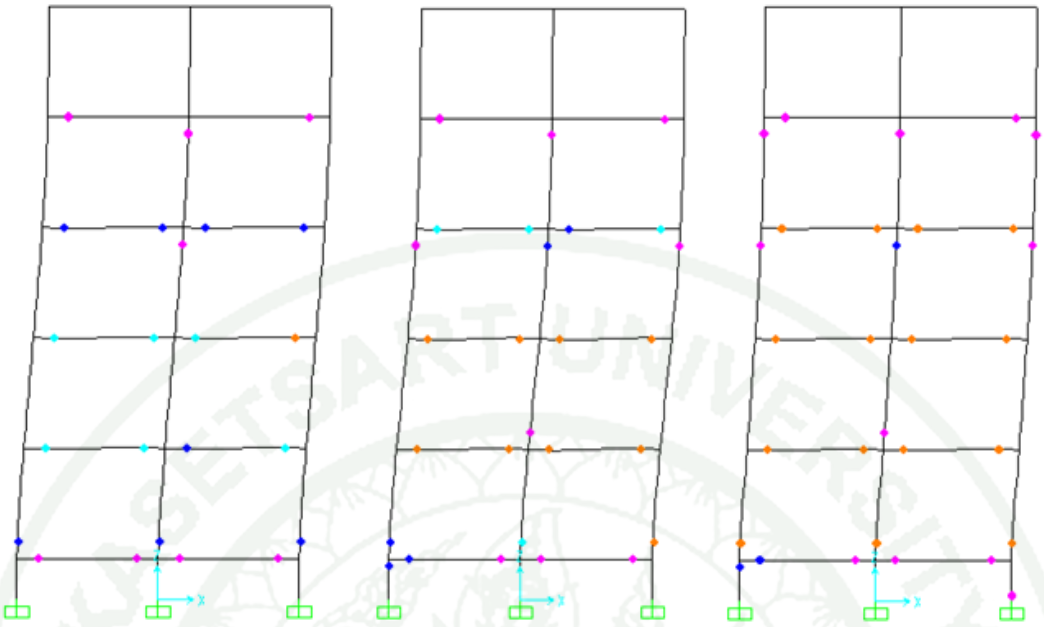

Appendix Figure B6 Damage distribution and failure mechanism for F_y *-350 MPa*

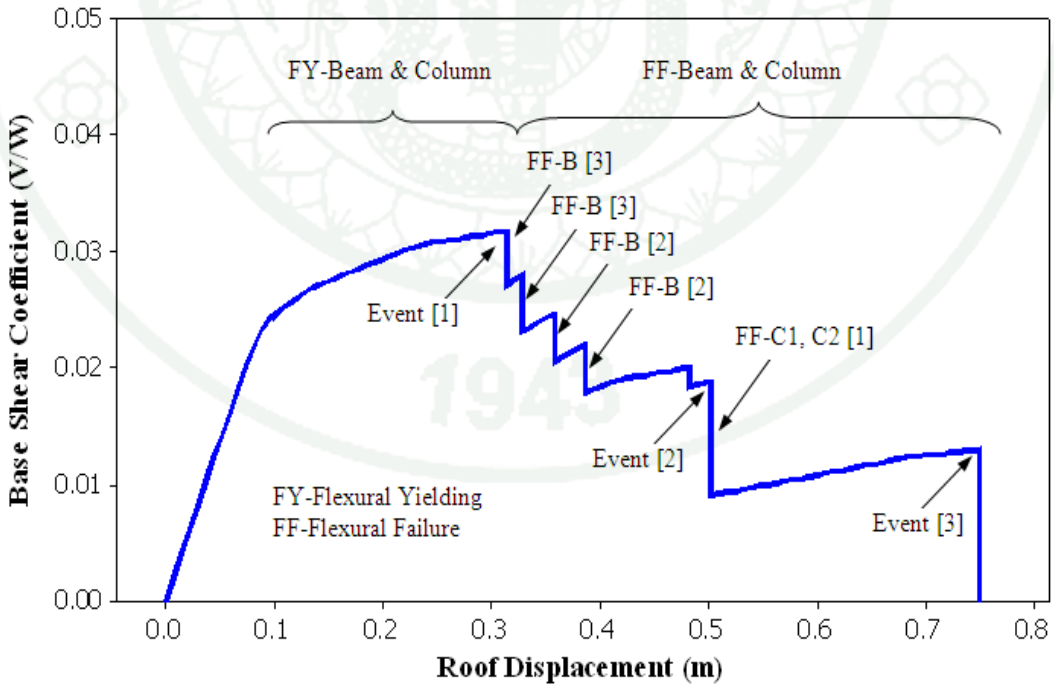

Appendix Figure B7 Capacity curve of the building for F_y *-415 MPa*

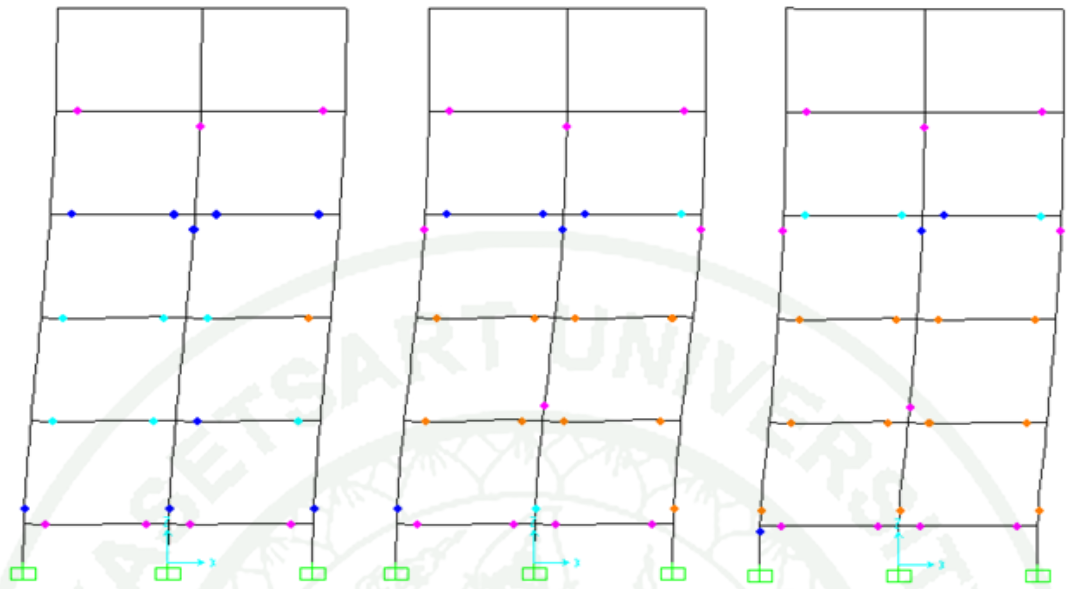

Appendix Figure B8 Damage distribution and failure mechanism for F_y *-415 MPa*

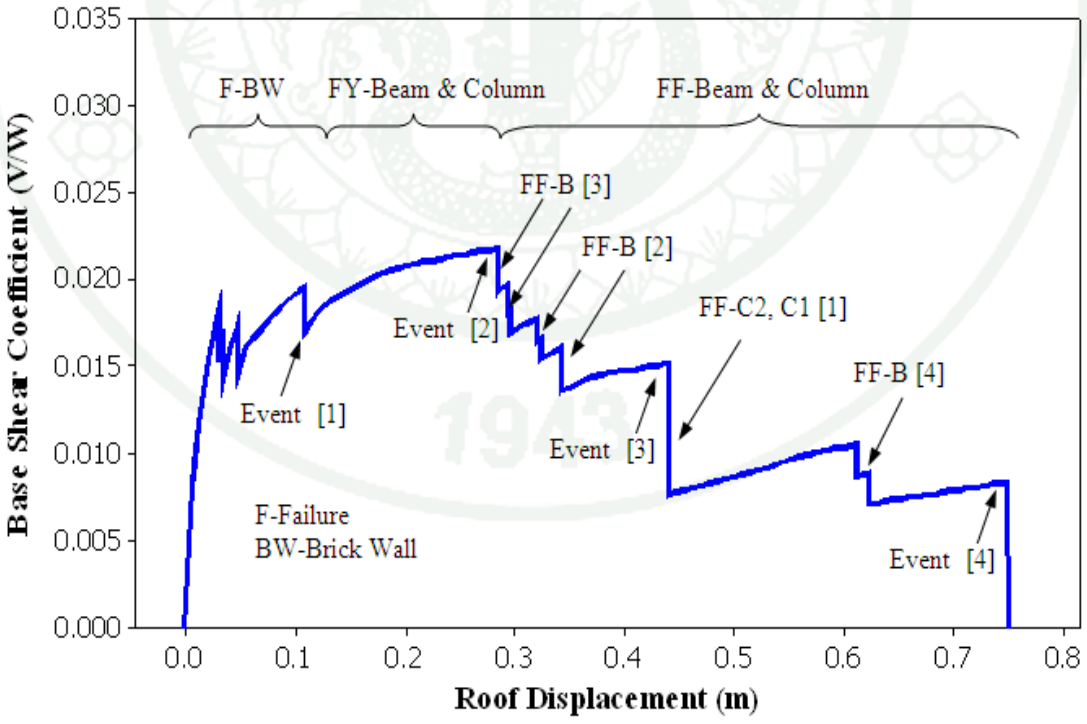

Appendix Figure B9 Capacity curve of the building with half brick thick wall

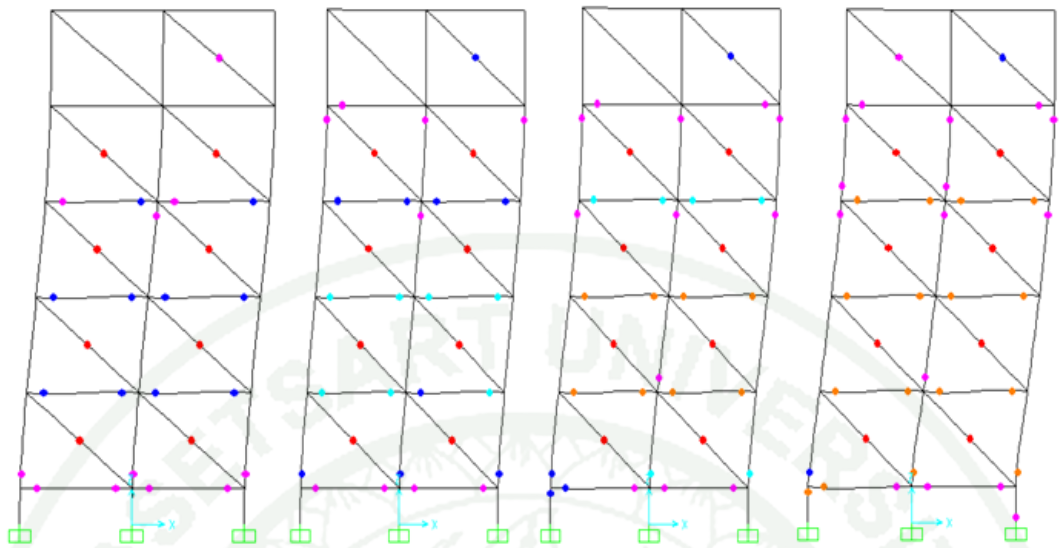

Appendix Figure B10 Damage distribution and failure mechanism for half brick thick wall

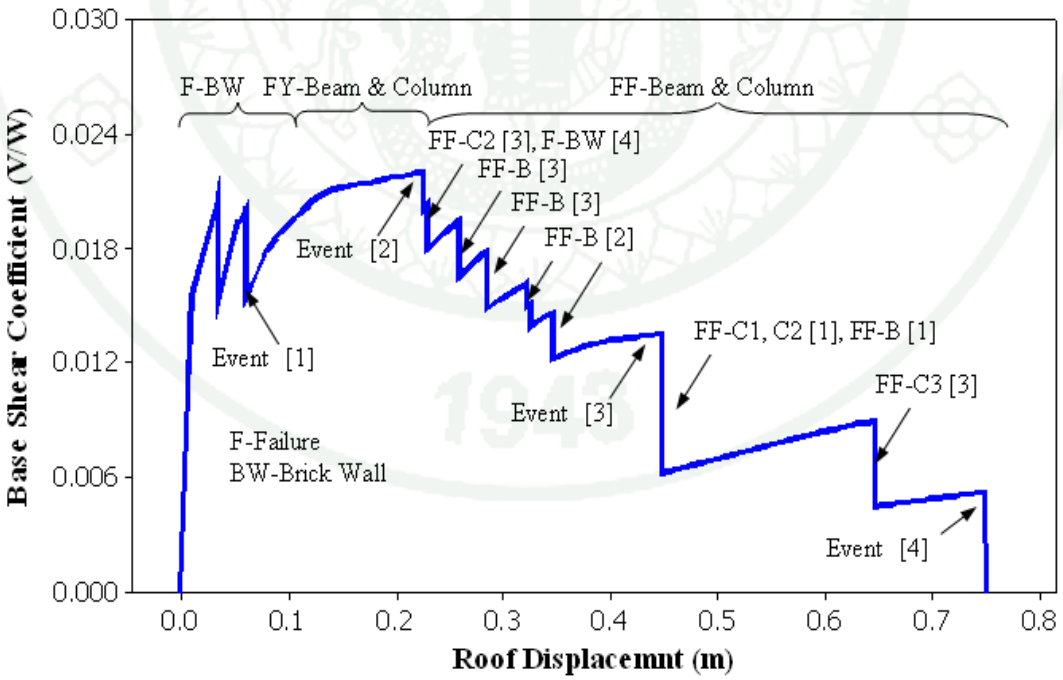

Appendix Figure B11 Capacity curve of the building with one brick thick wall

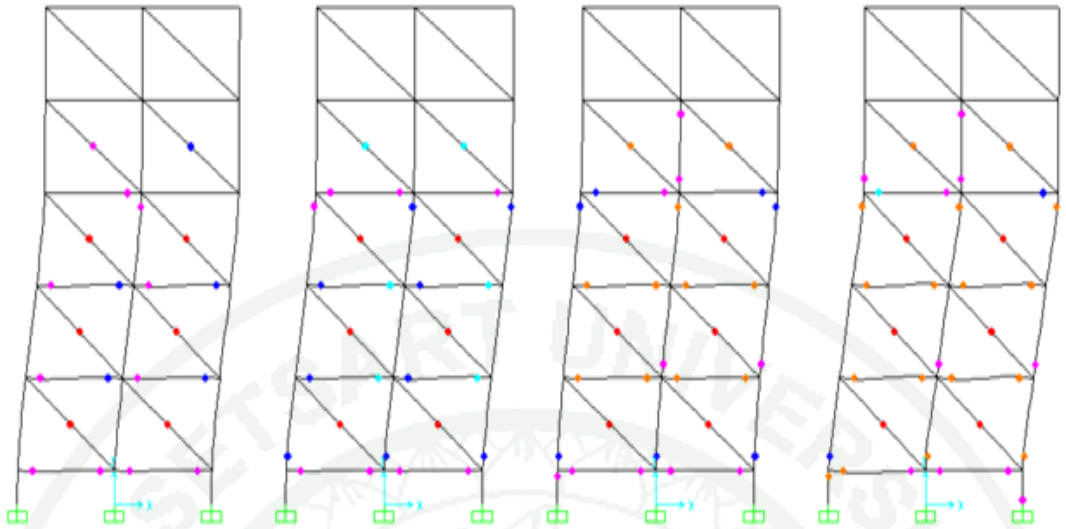

Appendix Figure B12 Damage distribution and failure mechanism for one brick thick wall

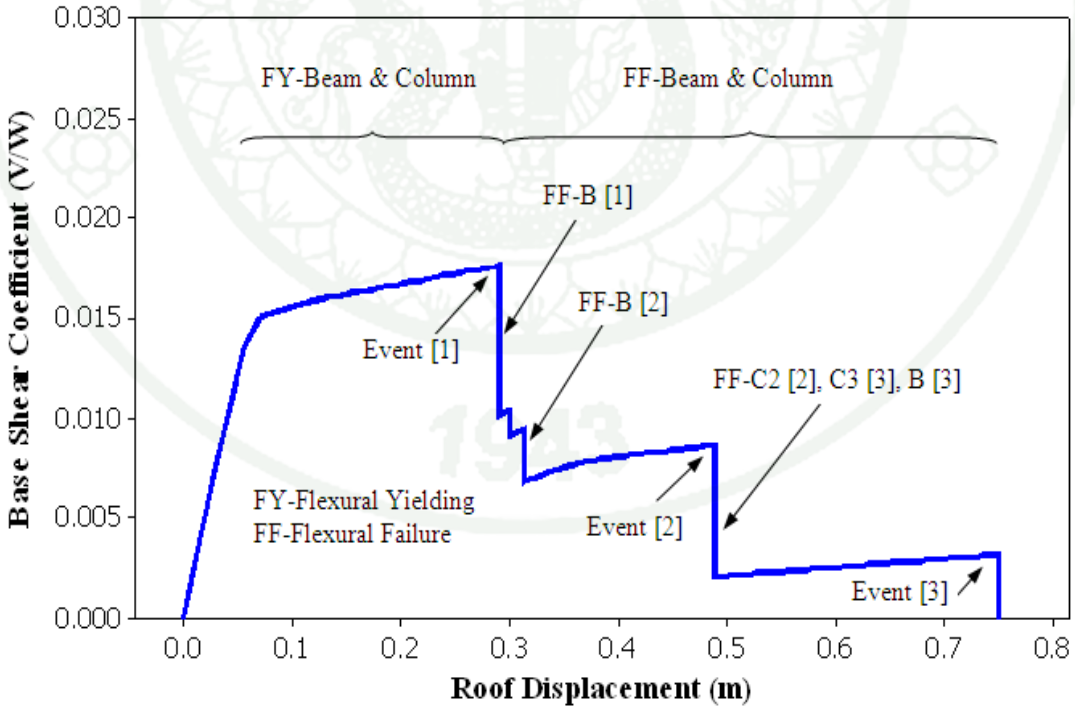

Appendix Figure B13 Capacity curve of the building with Hinge Base

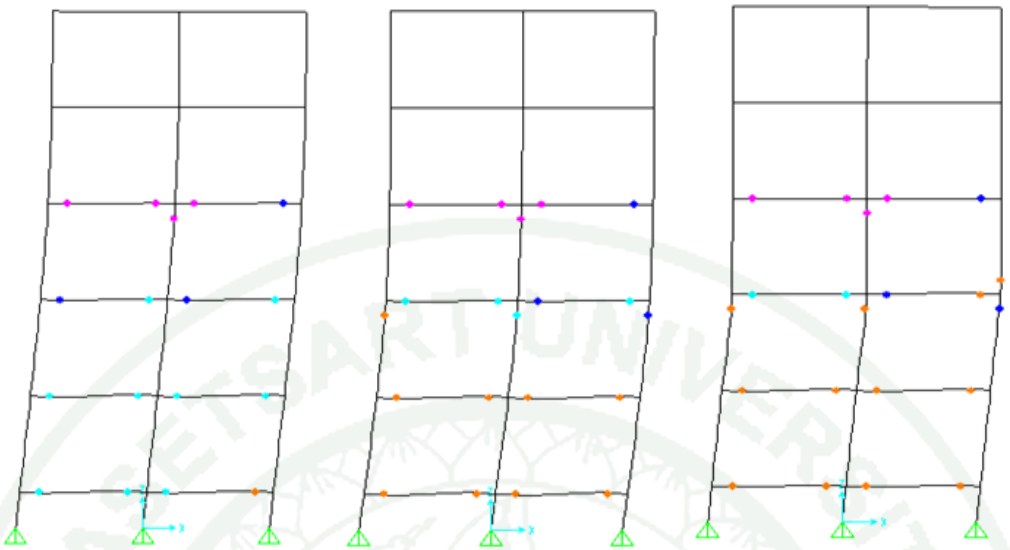

Appendix Figure B14 Damage distribution and failure mechanism of Hinge Base

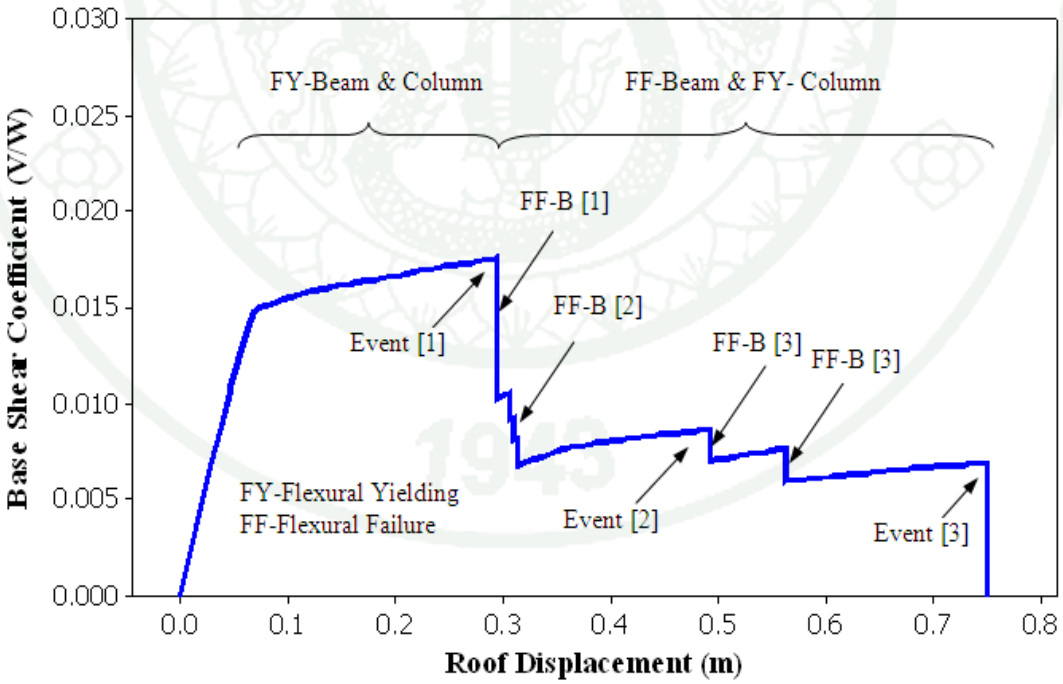

Appendix Figure B15 Capacity curve of the building with flexible base

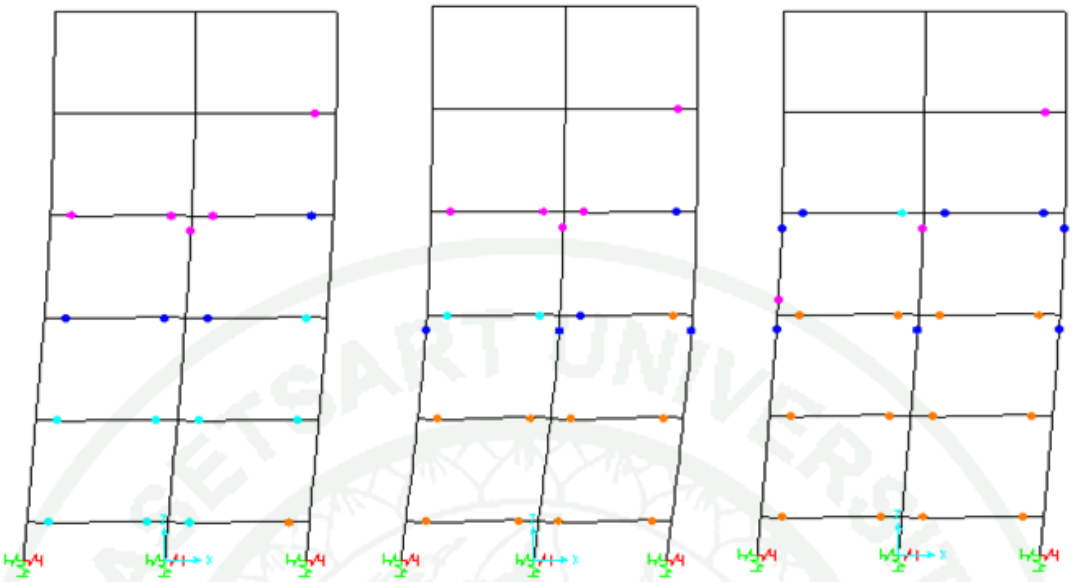

Appendix Figure B16 Damage distribution and failure mechanism of Flexible Base

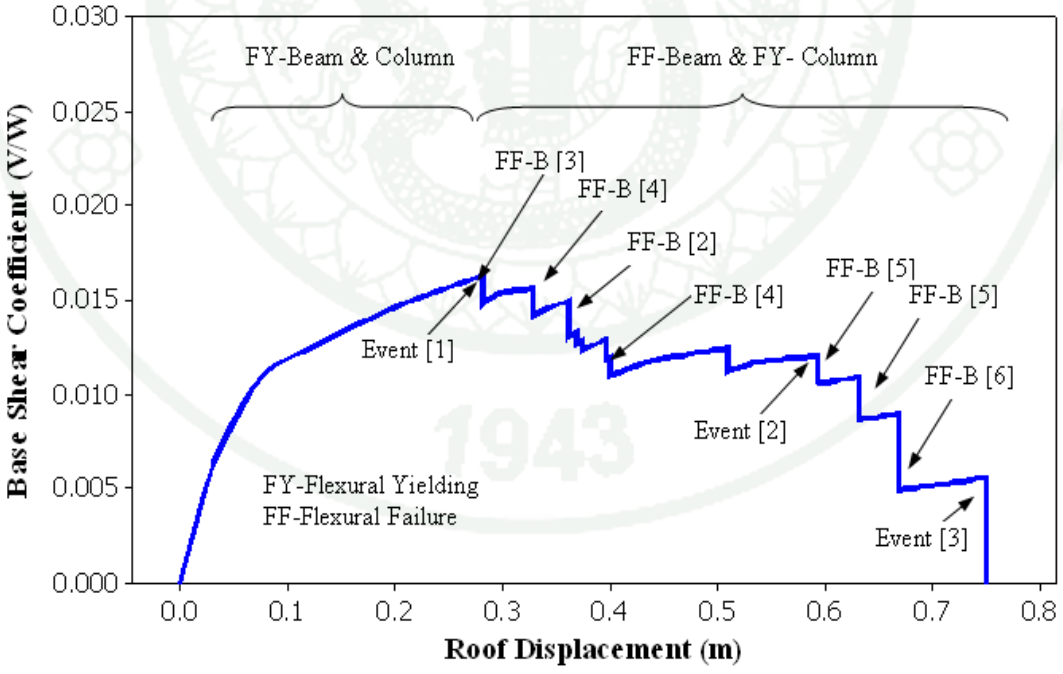

Appendix Figure B17 Capacity curve of newly gravity load designed building

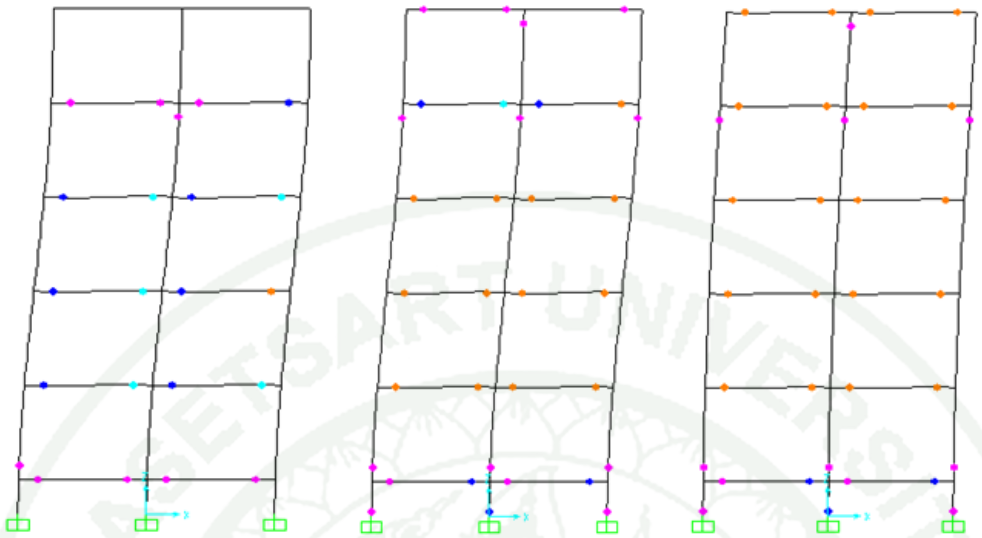

Event [1] Event [2] Event [3]

Appendix Figure B18 Damage distribution and failure mechanism of newly designed building

Appendix C

Pushover Analysis Steps

Pushover Analysis Steps

The recent advent of performance based design has brought the nonlinear static pushover analysis procedure to the forefront. Pushover analysis is a static nonlinear procedure in which the magnitude of the structural loading is incrementally increased in accordance with a certain predefined pattern. With the increased in the magnitude of the loading, weak links and failure modes of the structure are found.

The steps of pushover analysis of reinforced concrete building are summarized herein. The following steps are included in the pushover analysis. Steps 1 through 9 discuss creating the computer model, step 10 runs the analysis, and review the pushover analysis results.

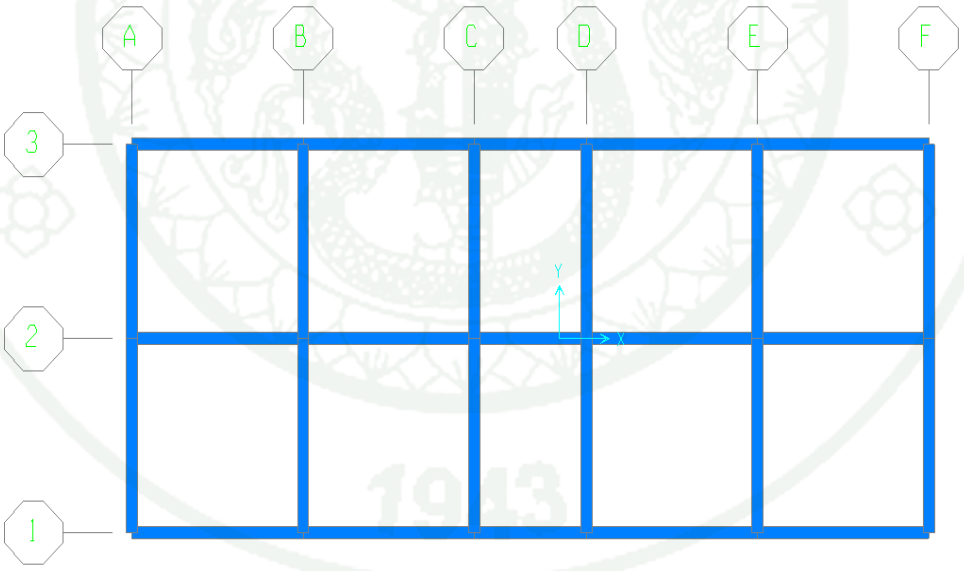

Plan

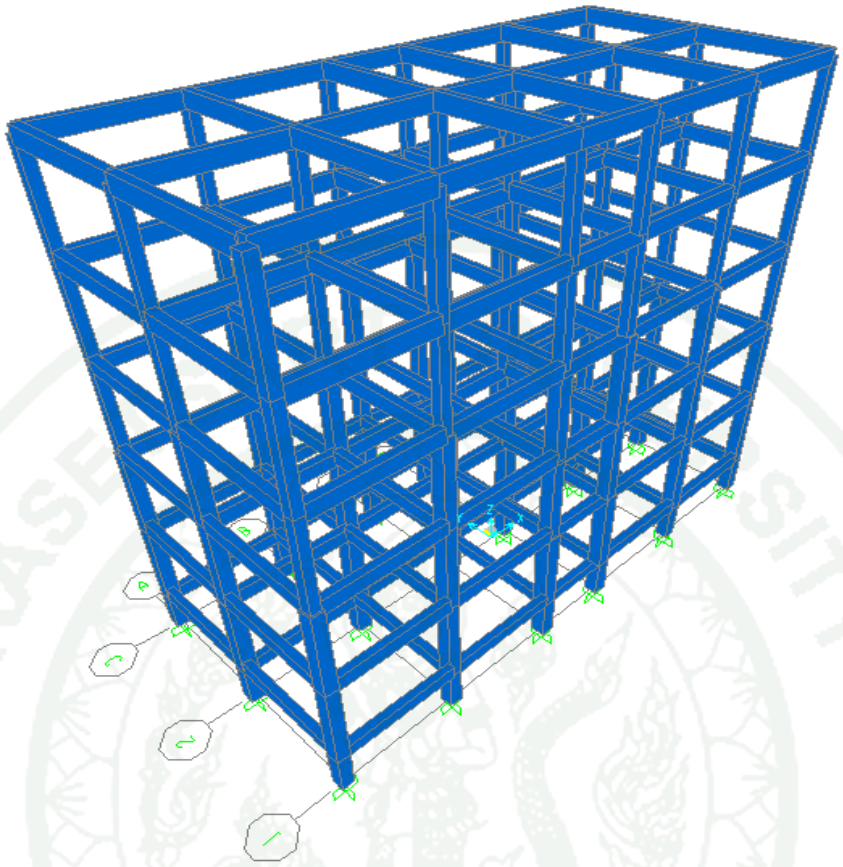

3D-View

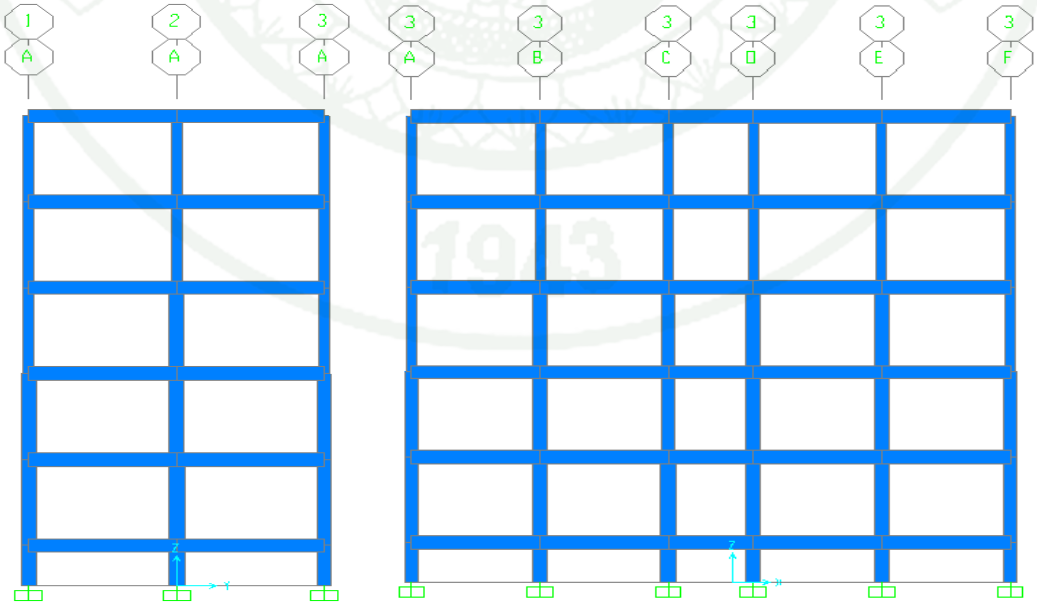

Elevation View

1. **Start Model with Template**

Start up screen of SAP2000, Select working unit to be *KN-m* at drop down menu on the bottom-right of screen and click on *New Model* button to start new model using template. Choose **portal** and enter the dimensions as shown in the Figure below.

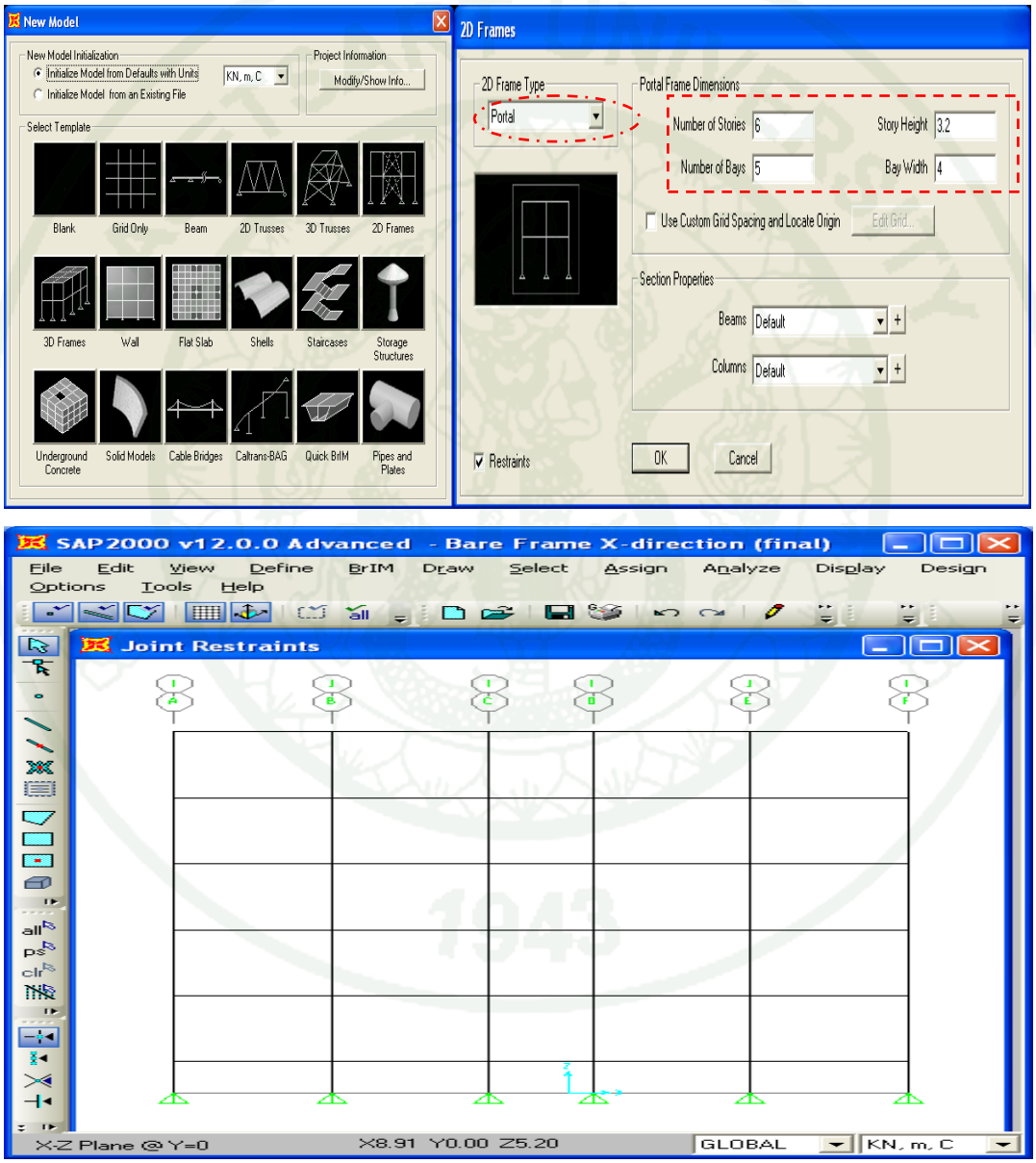

2. **Define Material Properties of Concrete and Rebar**

Go to **Define >> Materials**, and display define materials as shown in Figure below

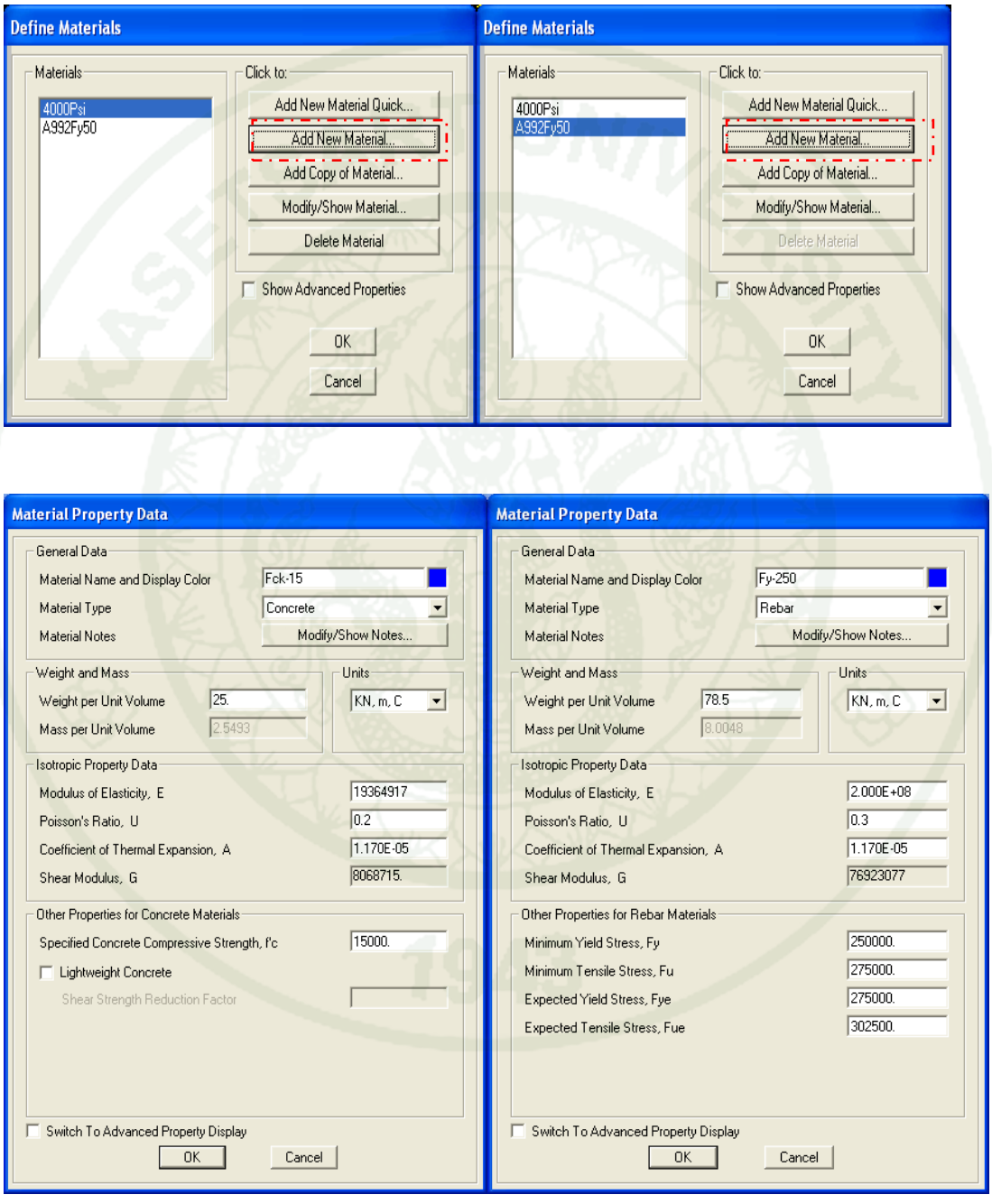

3. **Define Frame Section Properties for Column and Beam**

Go to **Define >> Section Properties >> Frame Sections**, and display following Figures

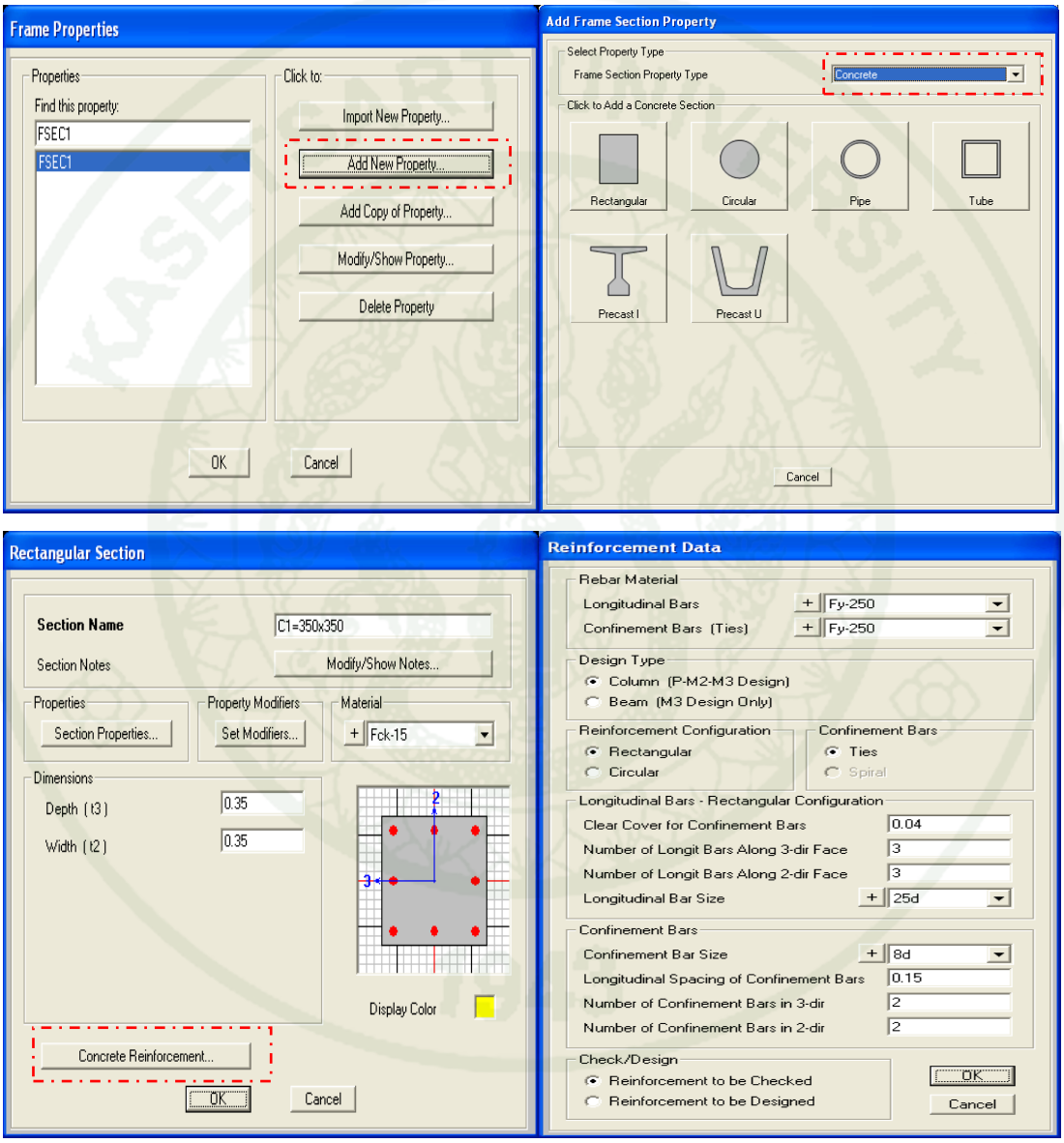

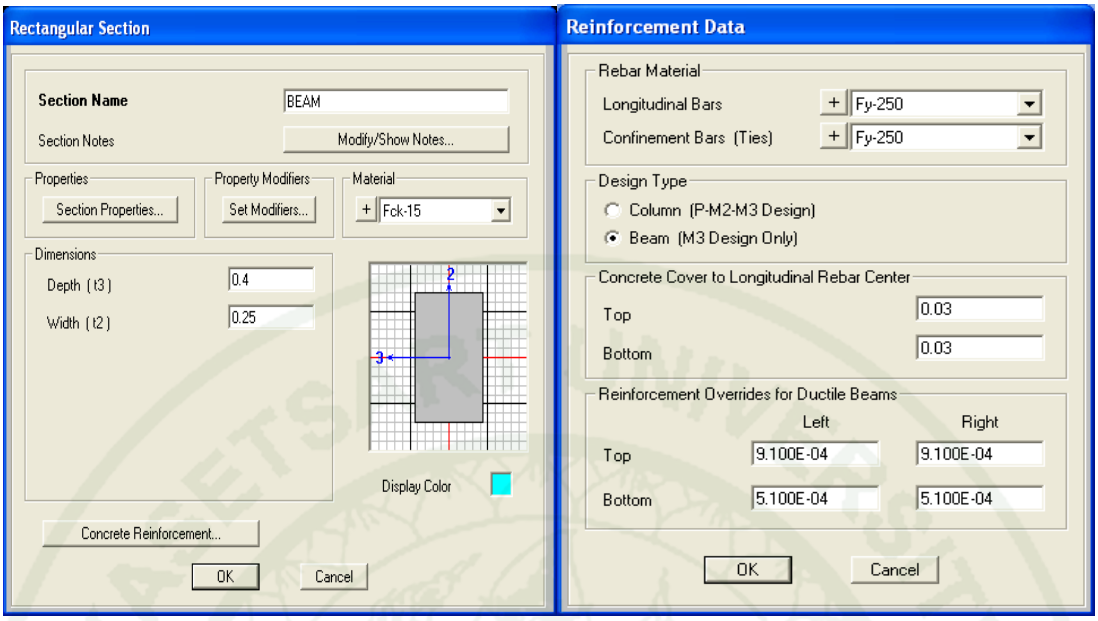

4. **Assign the Supports**

Go to **Assign** >> **Joint** >> **Restraints**, and display following Figure

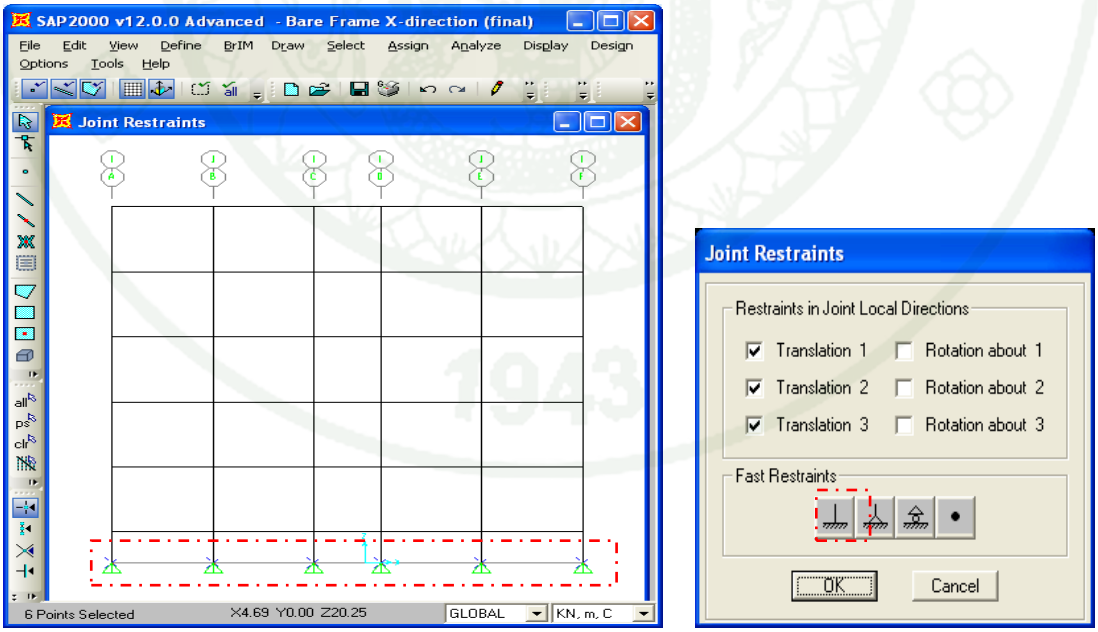

5. **Defining Load Cases**

Go to **Define>> Load Patterns**, and define the load cases as shown in the following Figure

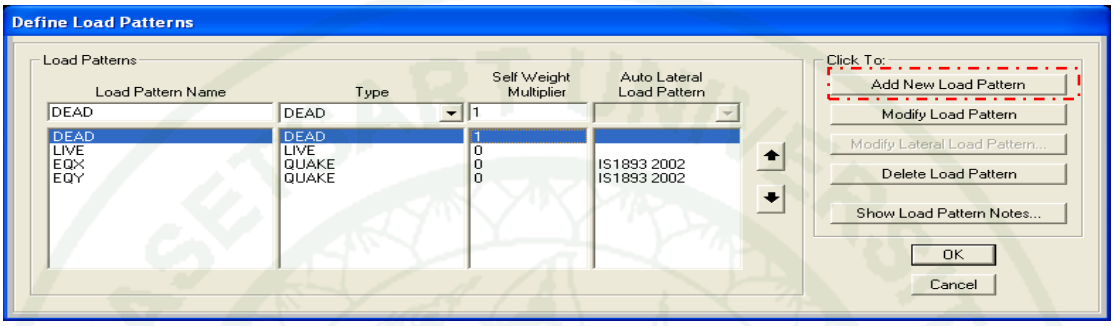

6. **Assign Loading**

Go to **Assign >> Frame Loads >> Distributed,** and assign the dead load as shown in the following Figure.

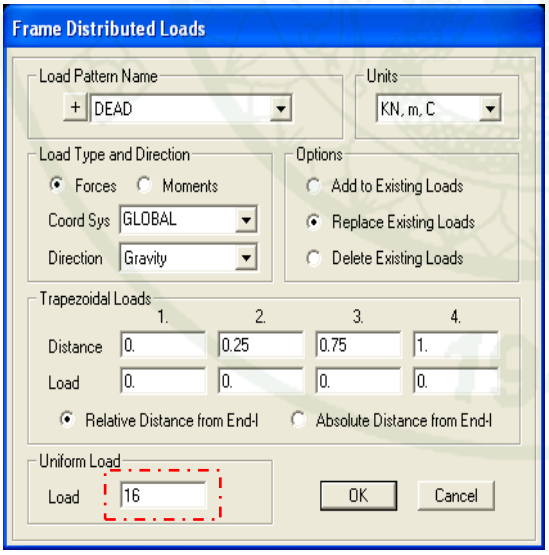

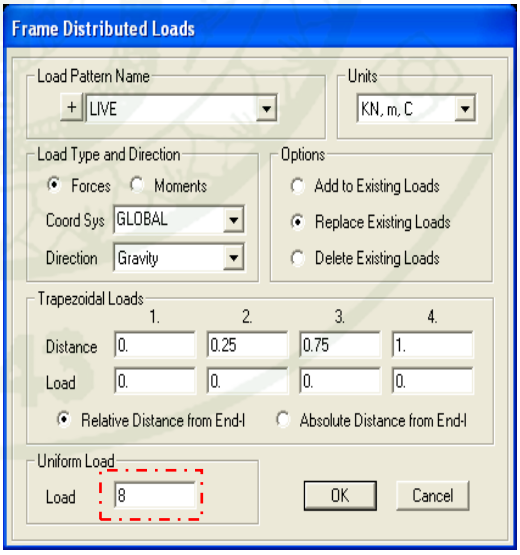

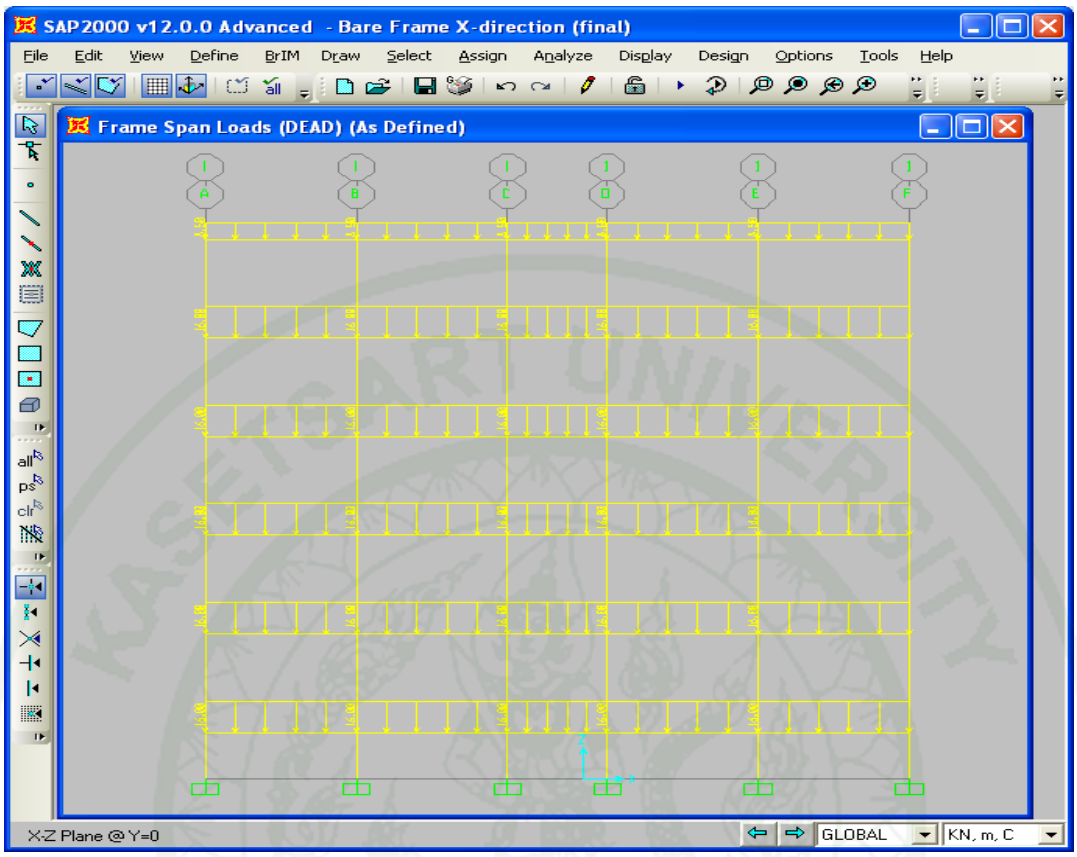

7. **Determine the Lateral Loading Pattern**

Go to **View >> Set 3D View**, Select the XZ plane view

1. Select the columns and go to **View >> Show Section only** to show the columns only. Select the columns and points at the base of the columns in the second floor as shown in the following figure. Then selected items are assigned to the group and give the level L2. Repeat this step up to assign the columns in to group (L3, L4, L5 and L6) for each floor up to Roof level.

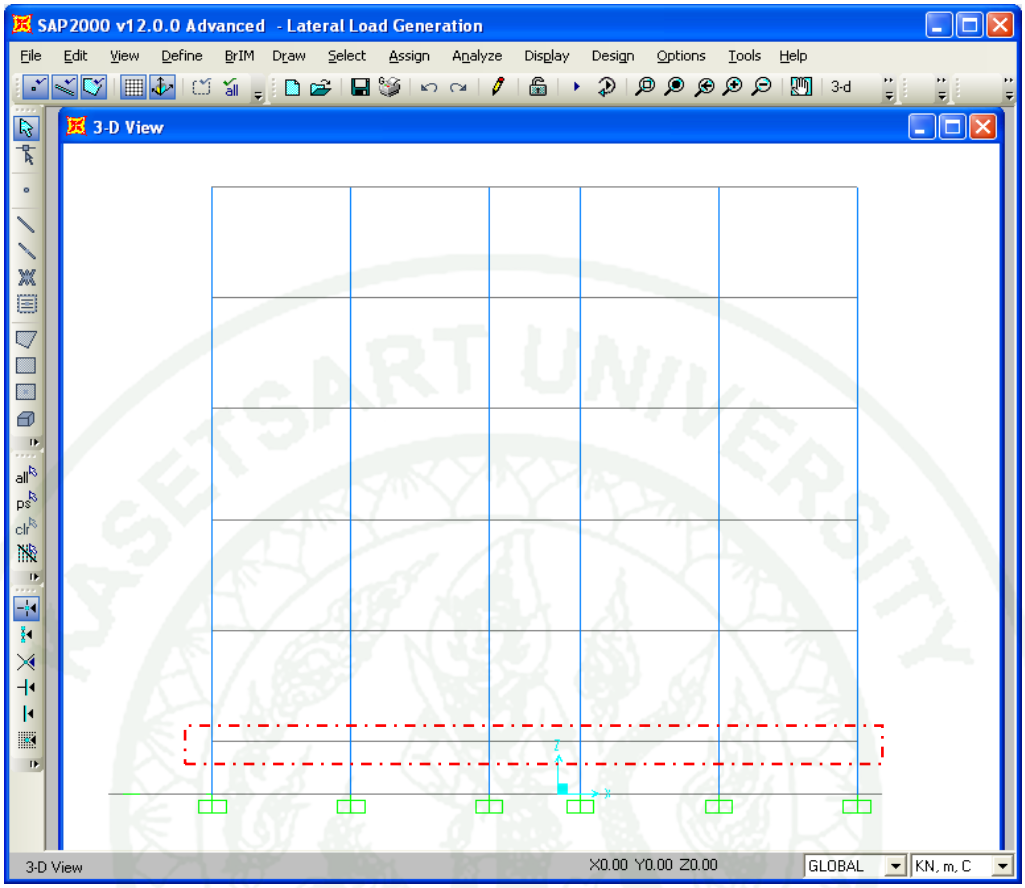

2. Go to **Define** >> **Groups**, and define the groups with respect to the columns in each floor

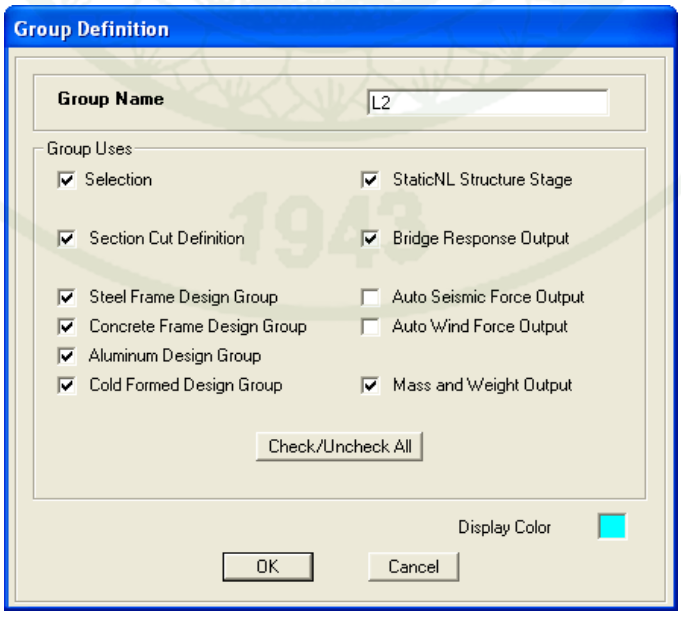

3. Go to **Define >> section cuts**, and define the section cuts with respect to the groups of columns in each floor and run analysis.

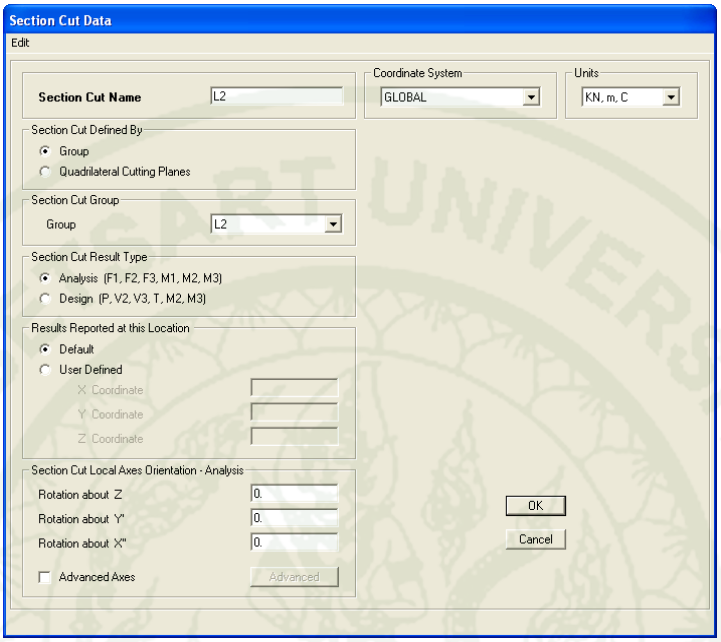

4. Go to **Display >> Show Tables**, and display the section cut forces EQX and EQY load cases.

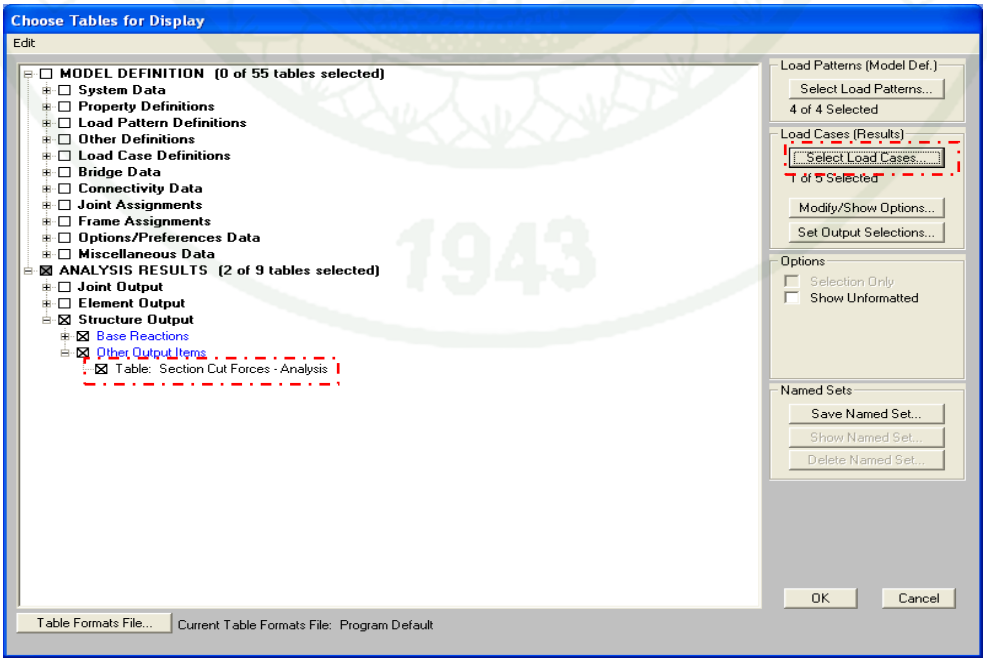

Section Cut Forces - Analysis

File View Format-Filter-Sort Select Options

Units: As Noted

Section Cut Forces - Analysis

	SectionCut Text	OutputCase Text	CaseType Text	F1 KN	F2 KN	F3 KN	M1 KN-m	M2 KN-m	M3 KN-m
▶	L2	EQY	LinStatic	2.403E-14	-699.795	6.821E-13	8436.9728	-4.547E-13	000000002281
	L3	EQY	LinStatic	3.741E-14	-673.043	6.963E-13	6197.6272	7.958E-13	000000002256
	L4	EQY	LinStatic	7.973E-14	-597.782	1.918E-13	4043.8894	7.958E-13	000000001993
	L5	EQY	LinStatic	1.552E-14	-452.055	1.634E-13	2130.9881	-4.832E-13	000000001294
	L6	EQY	LinStatic	2.481E-14	-213.879	-1.483E-13	684.4123	000000003482	000000001791

Record: 1 of 5 Add Tables... Done

Section Cut Forces - Analysis

File View Format-Filter-Sort Select Options

Units: As Noted

Section Cut Forces - Analysis

	SectionCut Text	OutputCase Text	CaseType Text	F1 KN	F2 KN	F3 KN	M1 KN-m	M2 KN-m	M3 KN-m
▶	L2	EQX	LinStatic	-767.824	2.778E-14	-2.842E-13	-4.547E-13	-9257.1502	000000000866
	L3	EQX	LinStatic	-738.471	3.555E-14	-3.695E-13	-2.275E-13	-6800.1127	000000007419
	L4	EQX	LinStatic	-655.893	4.895E-14	-3.126E-13	9.379E-13	-4437.0052	000000007901
	L5	EQX	LinStatic	-496	5.101E-14	-1.421E-13	4.057E-17	-2338.1463	000000001038
	L6	EQX	LinStatic	-234.671	5.517E-14	2.132E-13	-6.609E-13	-750.9456	000000006651

Record: 1 of 5 Add Tables... Done

8. **Apply Lateral Load Pattern**

1. Go to **Define** >> **Load Case**, and define lateral load case.

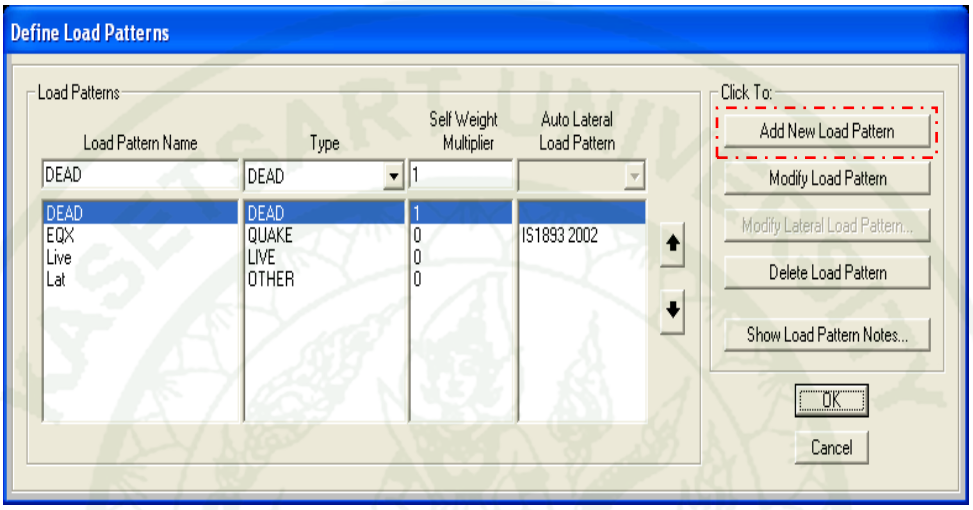

2. Go to **Assign** >> **Joint Loads** >> **Forces**, and display in the following Figures

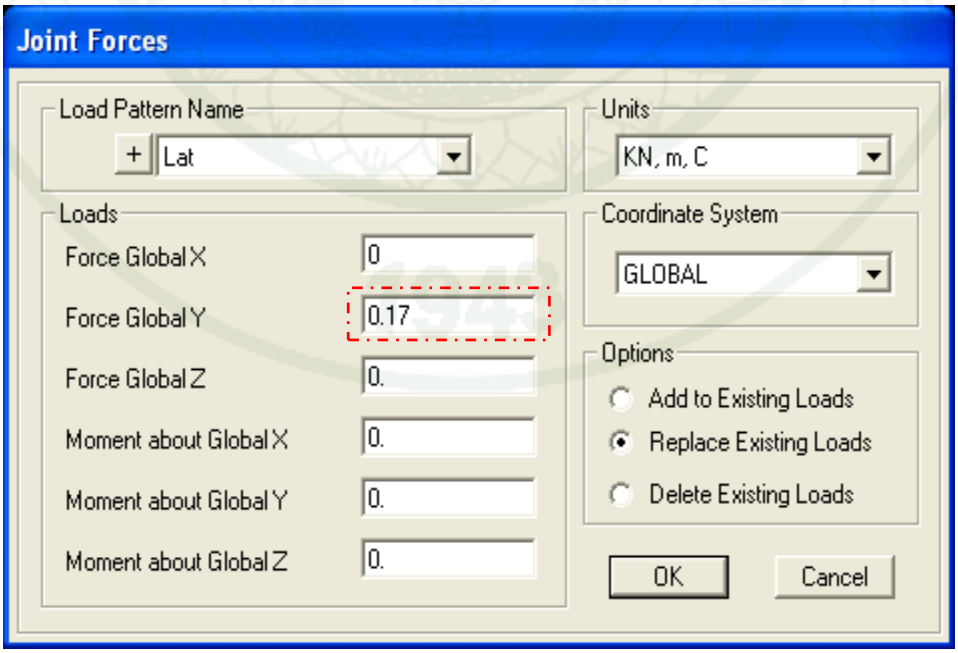

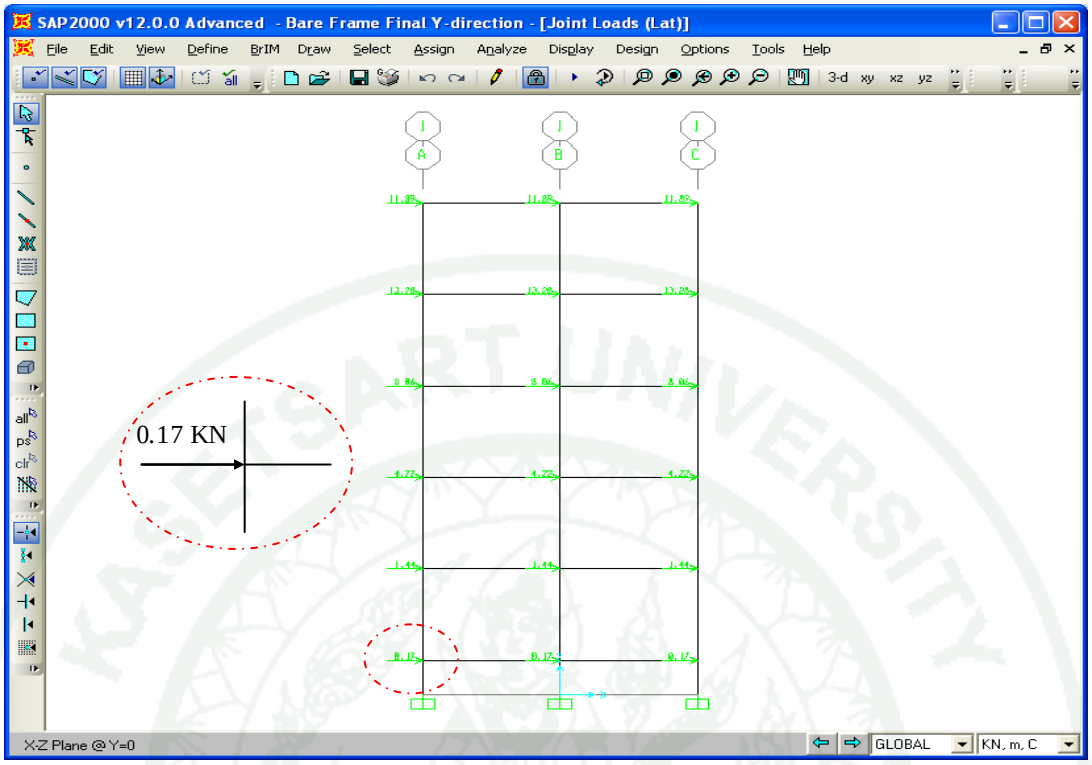

3. Go to **Define >> Combinations**, and define load combination of **DL+0.25LL** for pushover analysis

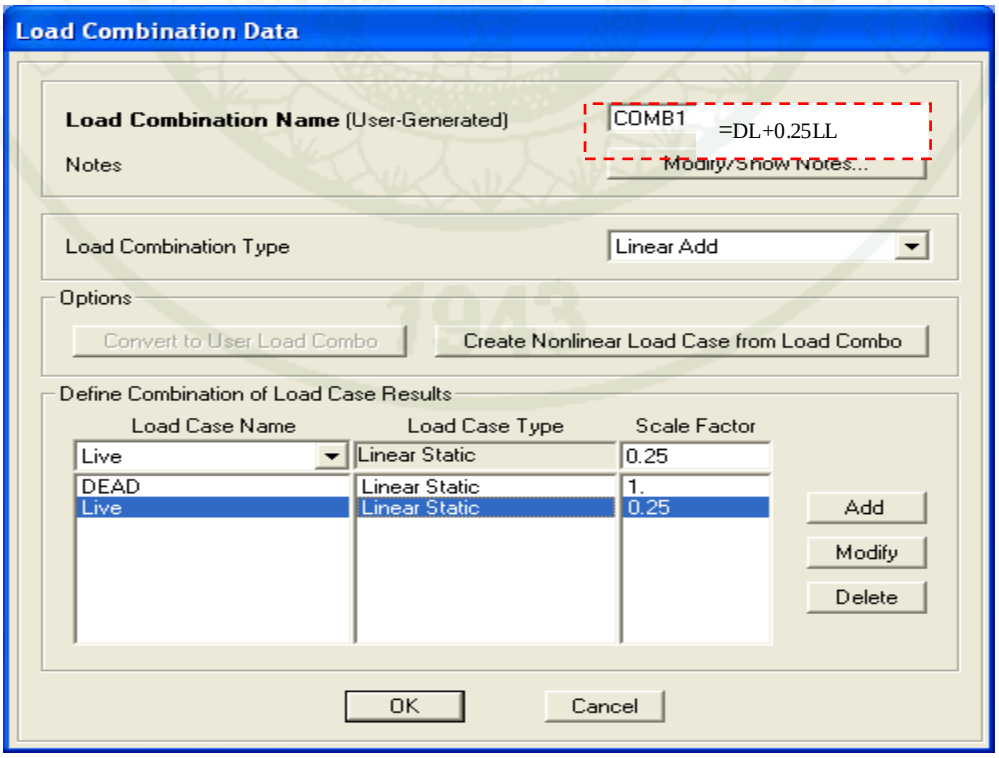

9. **Assign Hinge**

1. Select all the beams. Go to **Assign** >> **Frame** >> **Hinges**, and assign the hinge in both ends as shown in the following Figures.

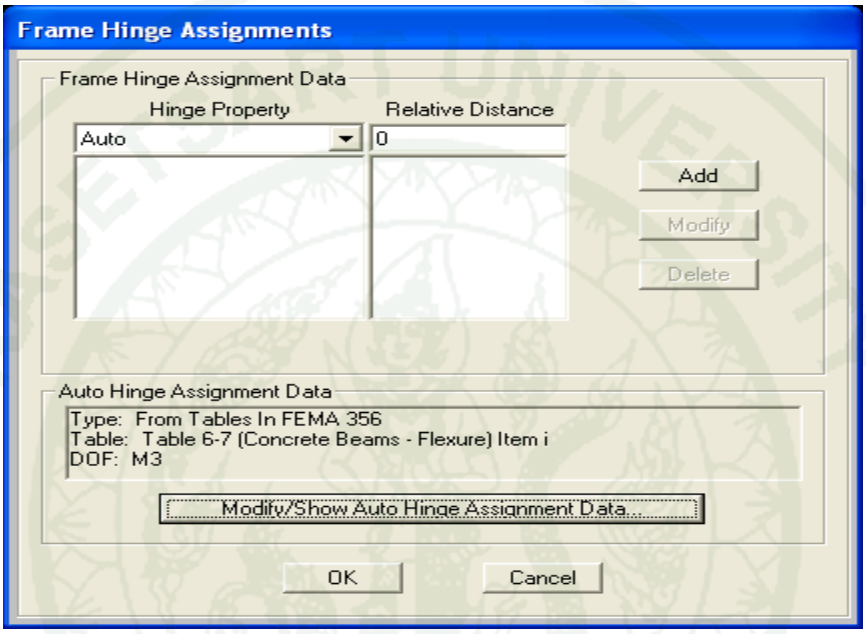

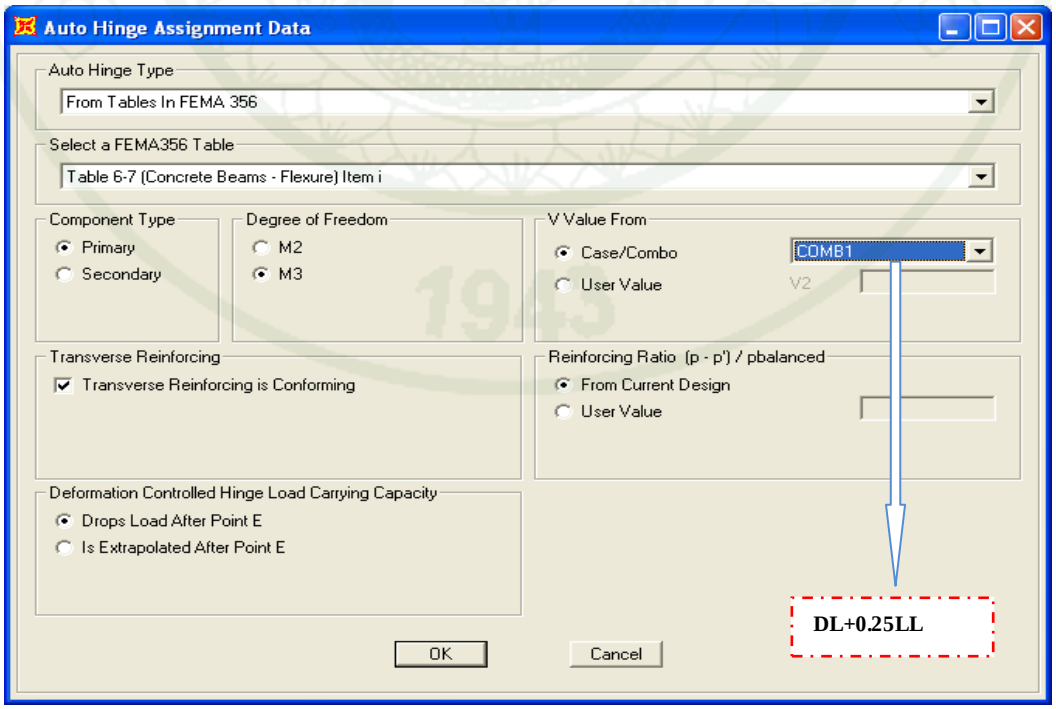

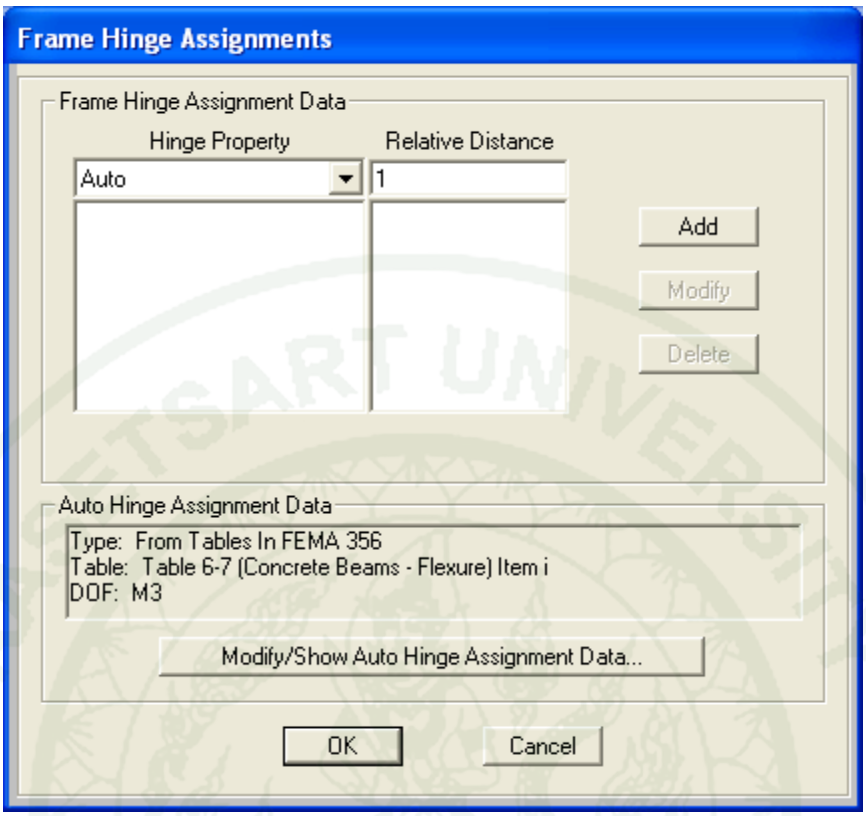

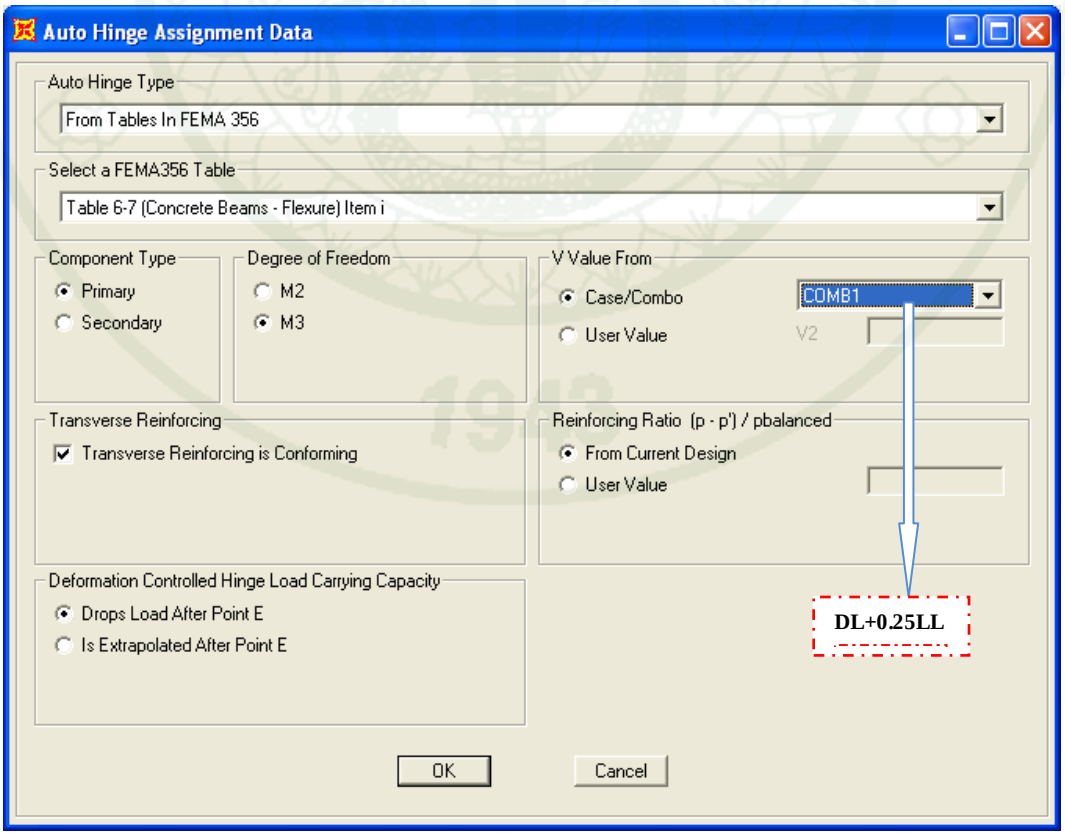

2. Select all the columns. Go to **Assign** >> **Frame** >> **Hinges**, and assign the hinge in both ends as shown in the following Figures.

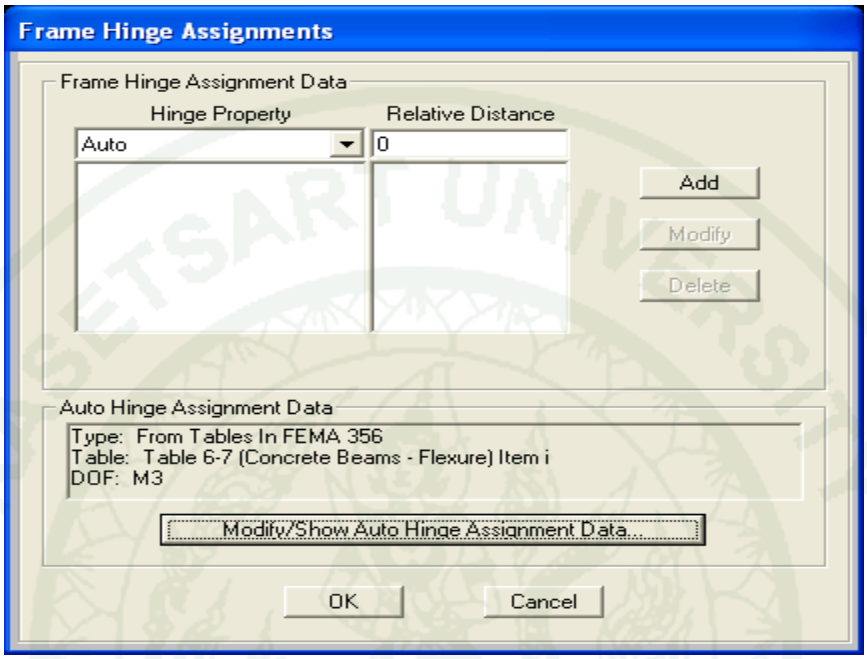

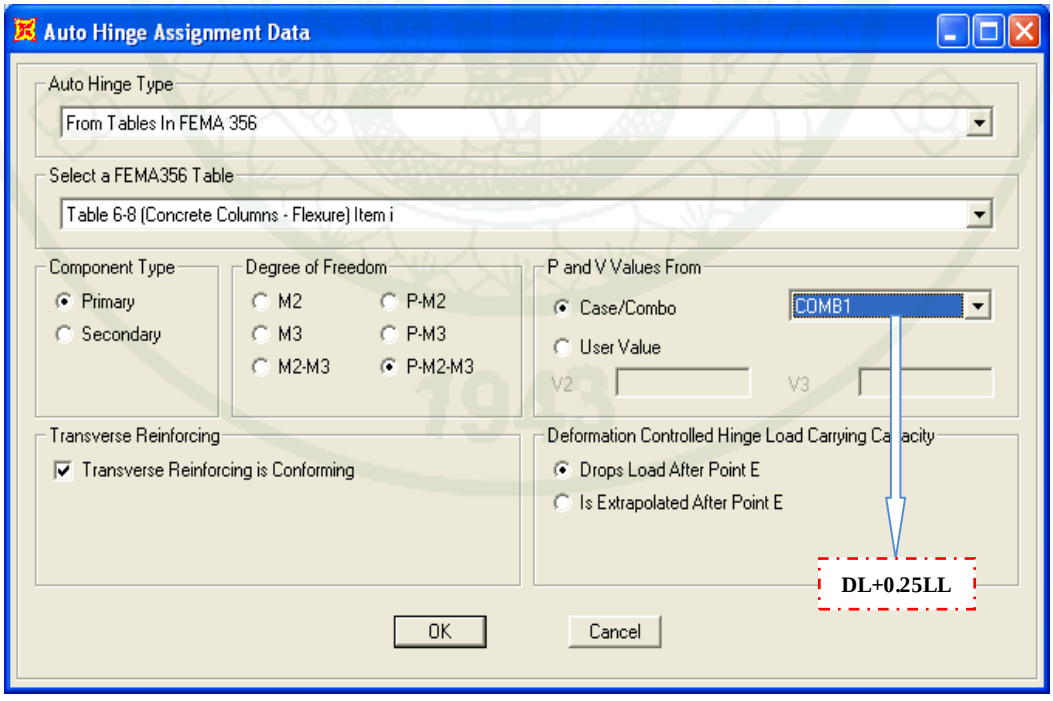

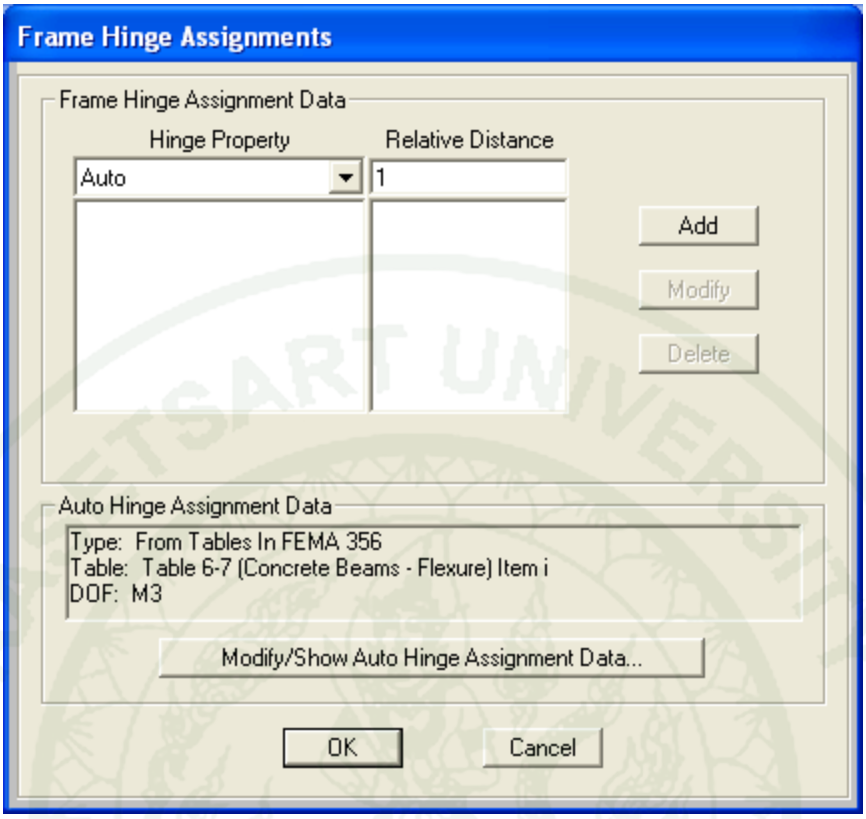

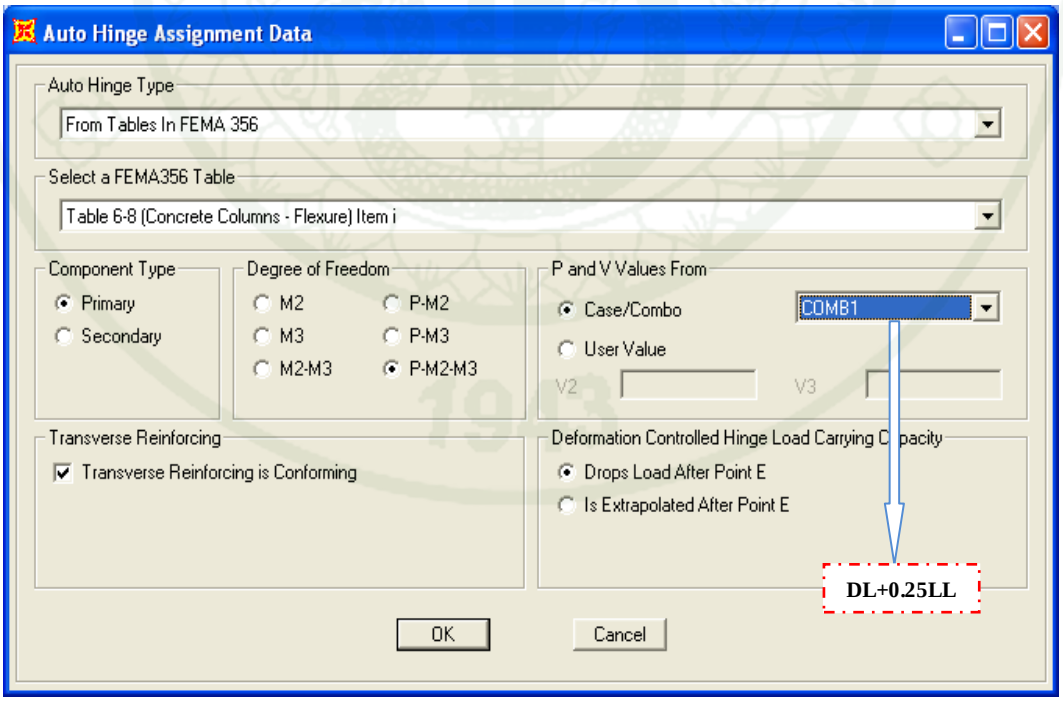

10. **Define Pushover Analysis Cases**

1. Go to **Define >> Load Cases**, and define the static nonlinear analysis case for gravity load as shown in the following Figures.

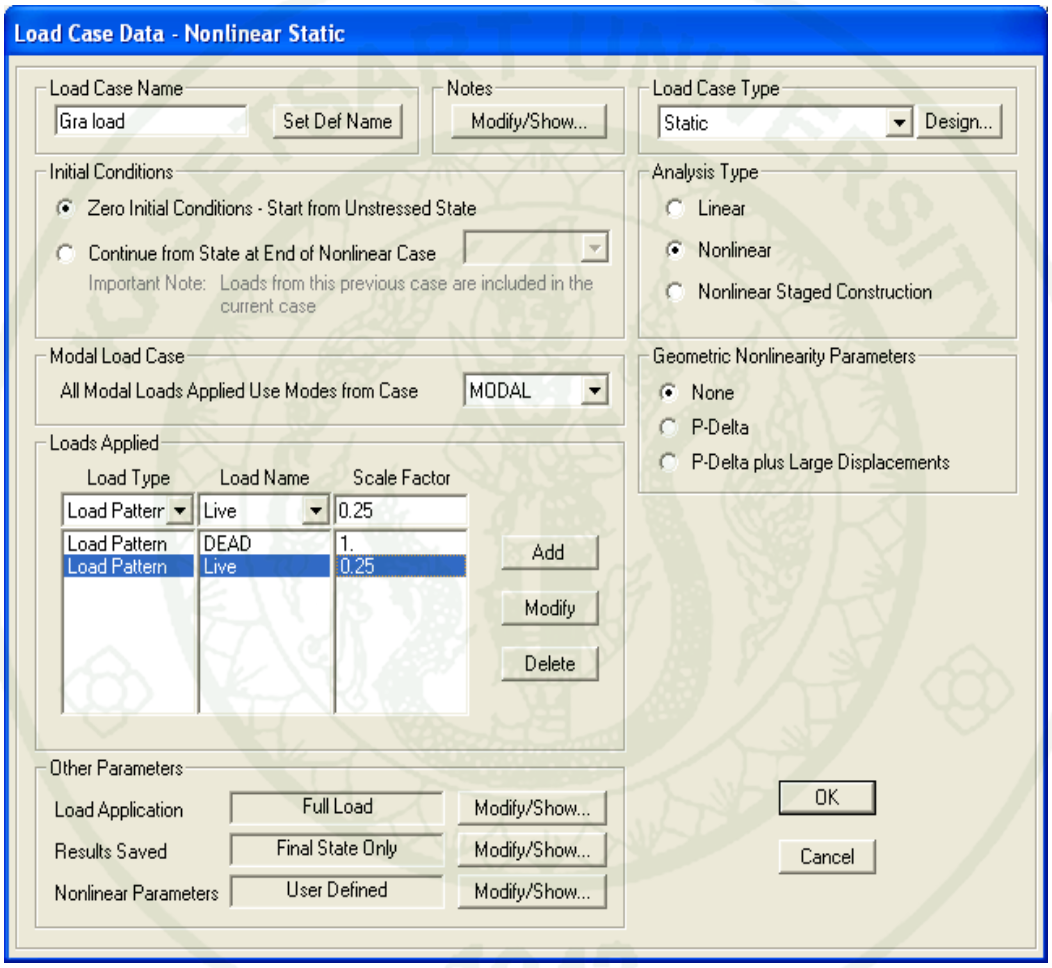

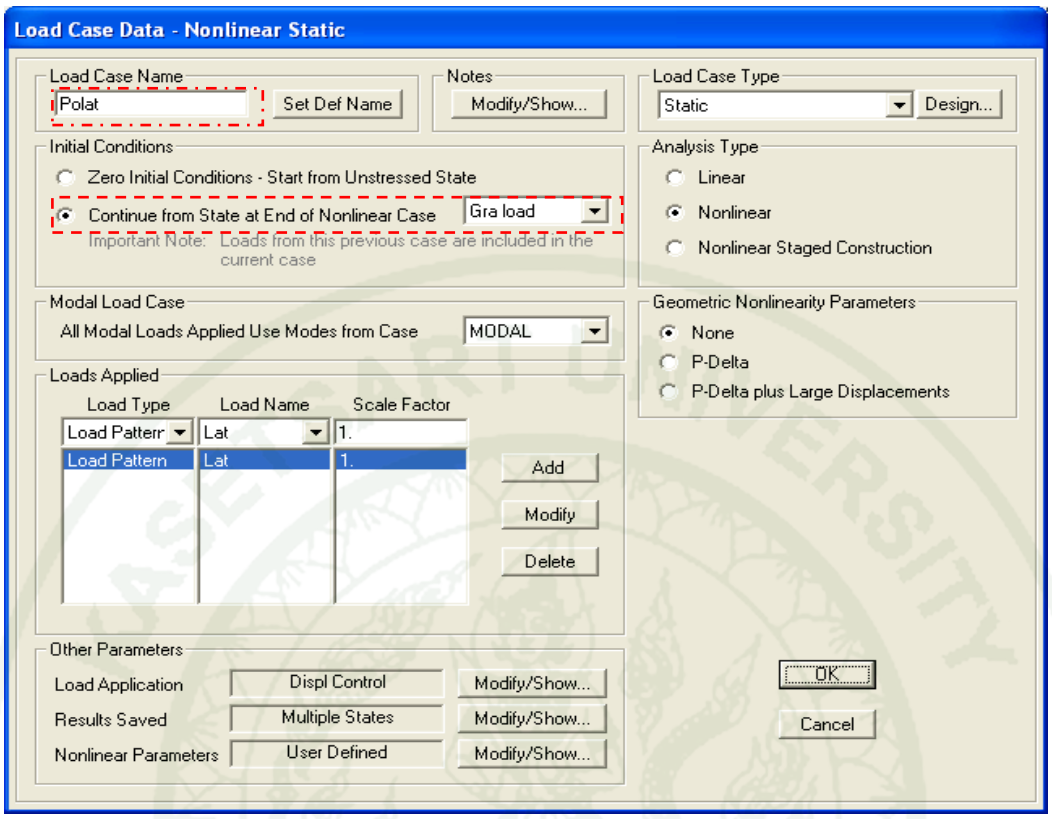

2. Go to **Analyze >> Run the Analysis**, and display **Set Load Cases to Run** as shown in Figure below.

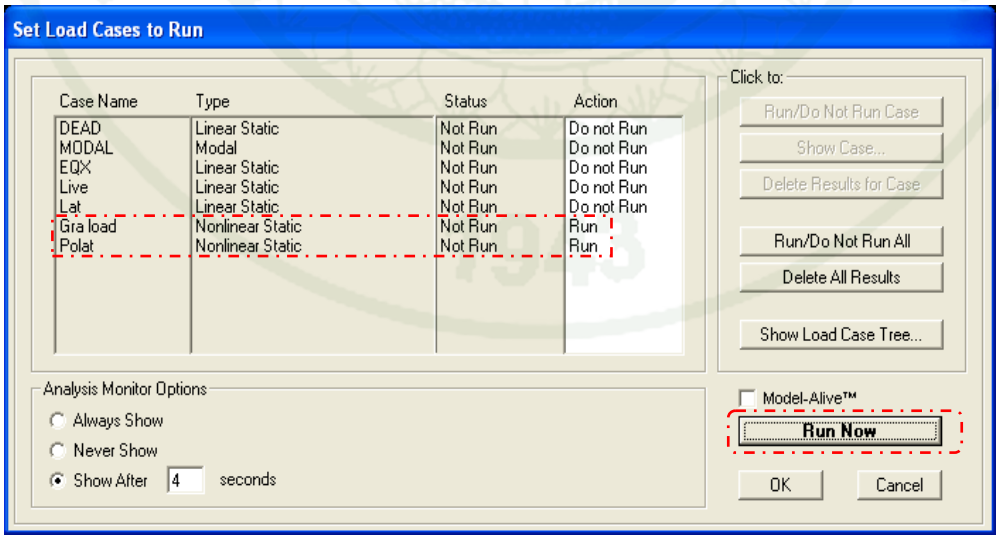

3. Go to **Display >> Show Static Pushover Curve**, and display Pushover Curve as shown below.

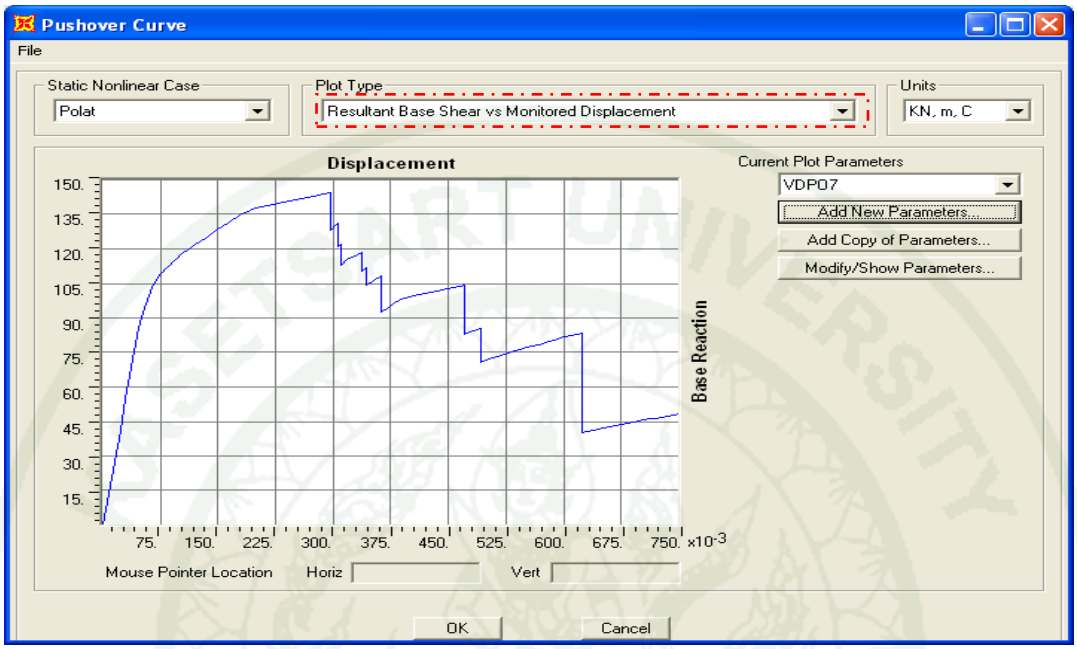

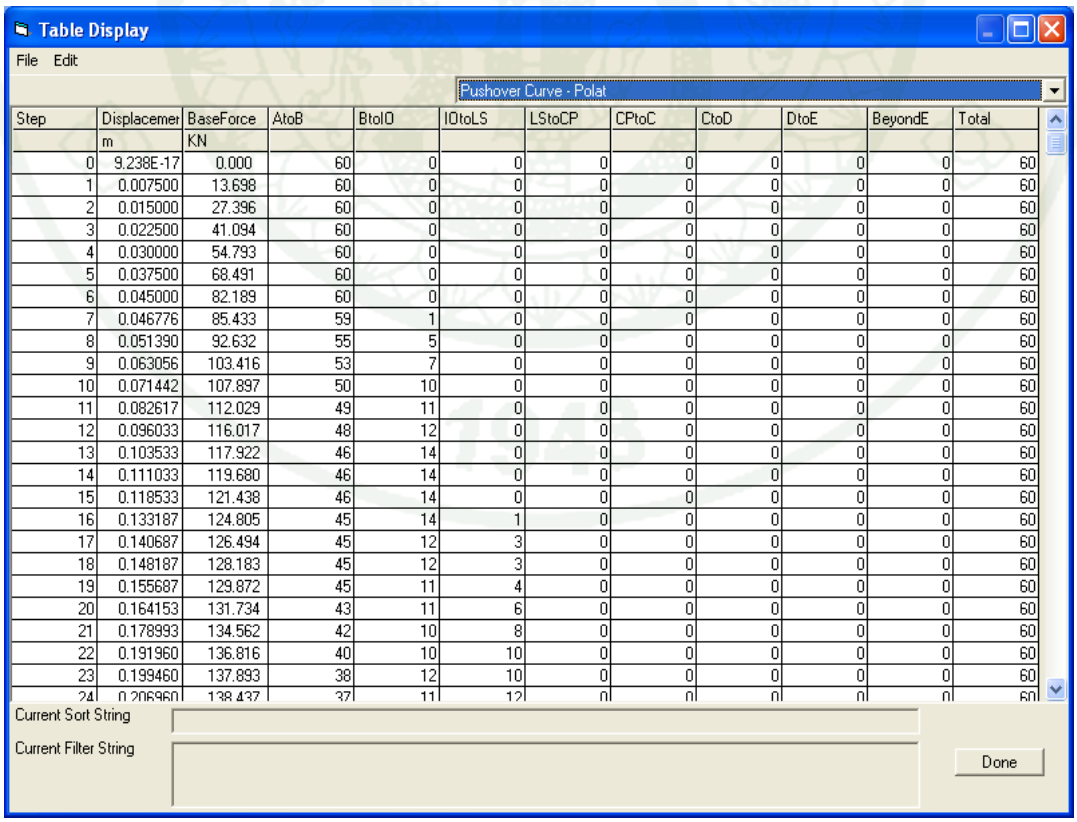

Step	Displacemer	BaseForce	AtoB	BtoIO	IOtoLS	LStoCP	CPtoC	CtoD	DtoE	BeyondE	Total
	m	KN									
0	9.238E-17	0.000	60	0	0	0	0	0	0	0	60
1	0.007500	13.698	60	0	0	0	0	0	0	0	60
2	0.015000	27.396	60	0	0	0	0	0	0	0	60
3	0.022500	41.094	60	0	0	0	0	0	0	0	60
4	0.030000	54.793	60	0	0	0	0	0	0	0	60
5	0.037500	68.491	60	0	0	0	0	0	0	0	60
6	0.045000	82.189	60	0	0	0	0	0	0	0	60
7	0.046776	85.433	59	1	0	0	0	0	0	0	60
8	0.051390	92.632	55	5	0	0	0	0	0	0	60
9	0.063056	103.416	53	7	0	0	0	0	0	0	60
10	0.071442	107.897	50	10	0	0	0	0	0	0	60
11	0.082617	112.029	49	11	0	0	0	0	0	0	60
12	0.096033	116.017	48	12	0	0	0	0	0	0	60
13	0.103533	117.922	46	14	0	0	0	0	0	0	60
14	0.111033	119.680	46	14	0	0	0	0	0	0	60
15	0.118533	121.438	46	14	0	0	0	0	0	0	60
16	0.133187	124.805	45	14	1	0	0	0	0	0	60
17	0.140687	126.494	45	12	3	0	0	0	0	0	60
18	0.148187	128.183	45	12	3	0	0	0	0	0	60
19	0.155687	129.872	45	11	4	0	0	0	0	0	60
20	0.164153	131.734	43	11	6	0	0	0	0	0	60
21	0.178993	134.562	42	10	8	0	0	0	0	0	60
22	0.191960	136.816	40	10	10	0	0	0	0	0	60
23	0.199460	137.893	38	12	10	0	0	0	0	0	60
24	0.206960	138.437	37	11	12	0	0	0	0	0	60

4. Go to **Display >> Show Static Pushover Curve**, and display ATC-40 Capacity Spectrum as shown below.

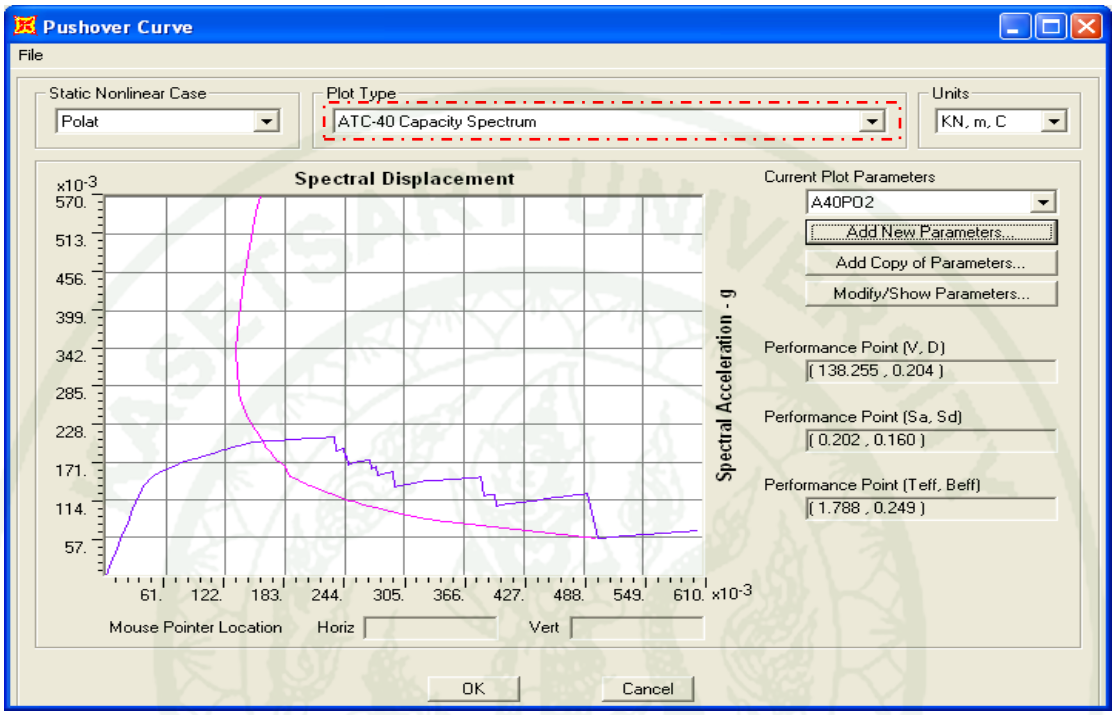

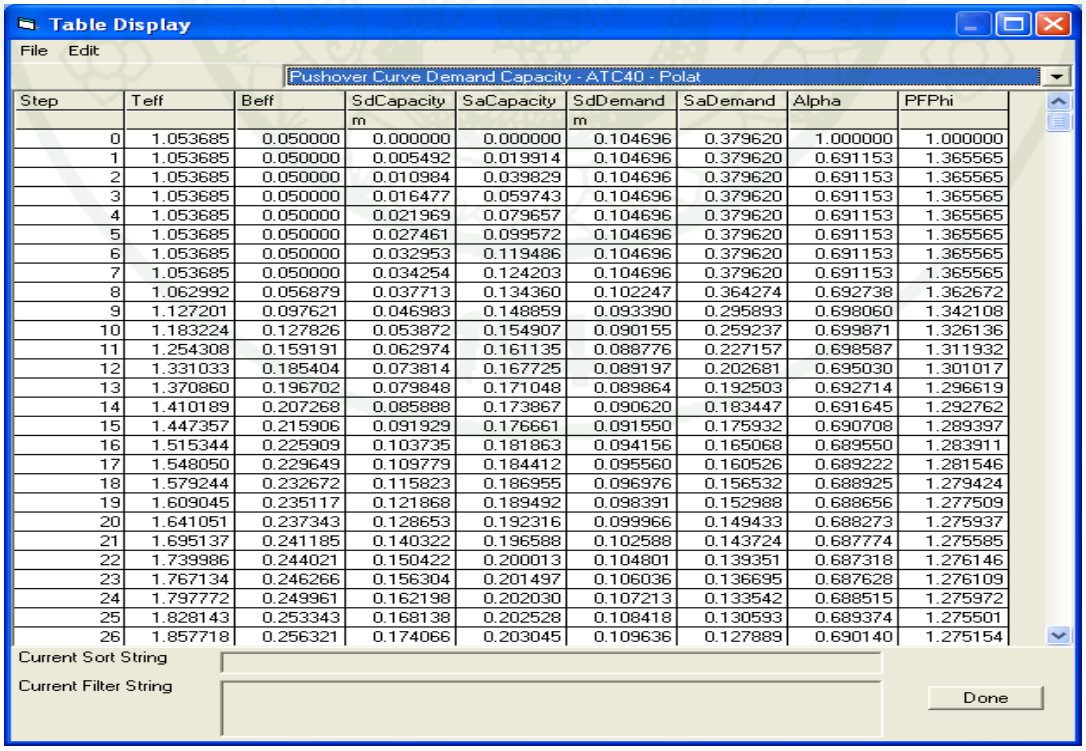

Step	Teff	Beff	SdCapacity	SaCapacity	SdDemand	SaDemand	Alpha	PFPhi
			m		m			
0	1.053685	0.050000	0.000000	0.000000	0.104696	0.379620	1.000000	1.000000
1	1.053685	0.050000	0.005492	0.019914	0.104696	0.379620	0.691153	1.365565
2	1.053685	0.050000	0.010984	0.039829	0.104696	0.379620	0.691153	1.365565
3	1.053685	0.050000	0.016477	0.059743	0.104696	0.379620	0.691153	1.365565
4	1.053685	0.050000	0.021969	0.079657	0.104696	0.379620	0.691153	1.365565
5	1.053685	0.050000	0.027461	0.099572	0.104696	0.379620	0.691153	1.365565
6	1.053685	0.050000	0.032953	0.119486	0.104696	0.379620	0.691153	1.365565
7	1.053685	0.050000	0.034254	0.124203	0.104696	0.379620	0.691153	1.365565
8	1.062992	0.056879	0.037713	0.134360	0.102247	0.364274	0.692738	1.362672
9	1.127201	0.097621	0.046983	0.148859	0.093390	0.295893	0.698060	1.342108
10	1.183224	0.127826	0.053872	0.154907	0.090155	0.259237	0.699871	1.326136
11	1.254308	0.159191	0.062974	0.161135	0.088776	0.227157	0.698587	1.311932
12	1.331033	0.185404	0.073814	0.167725	0.089197	0.202681	0.695030	1.301017
13	1.370860	0.196702	0.079848	0.171048	0.089864	0.192503	0.692714	1.296619
14	1.410189	0.207268	0.085888	0.173867	0.090620	0.183447	0.691645	1.292762
15	1.447357	0.215906	0.091929	0.176661	0.091550	0.175932	0.690708	1.289397
16	1.515344	0.225909	0.103735	0.181863	0.094156	0.165068	0.689550	1.283911
17	1.548050	0.229649	0.109779	0.184412	0.095560	0.160526	0.689222	1.281546
18	1.579244	0.232672	0.115823	0.186955	0.096976	0.156532	0.688925	1.279424
19	1.609045	0.235117	0.121868	0.189492	0.098391	0.152988	0.688656	1.277509
20	1.641051	0.237343	0.128653	0.192316	0.099966	0.149433	0.688273	1.275937
21	1.695137	0.241185	0.140322	0.196588	0.102588	0.143724	0.687774	1.275585
22	1.739986	0.244021	0.150422	0.200013	0.104801	0.139351	0.687318	1.276146
23	1.767134	0.246266	0.156304	0.201497	0.106036	0.136695	0.687628	1.276109
24	1.797772	0.249961	0.162198	0.202030	0.107213	0.133542	0.688515	1.275972
25	1.828143	0.253343	0.168138	0.202528	0.108418	0.130593	0.689374	1.275501
26	1.857718	0.256321	0.174066	0.203045	0.109636	0.127889	0.690140	1.275154

5. Go to **Display >> Show Deformed Shape**, and display Deformed Shape as shown in the following figures.

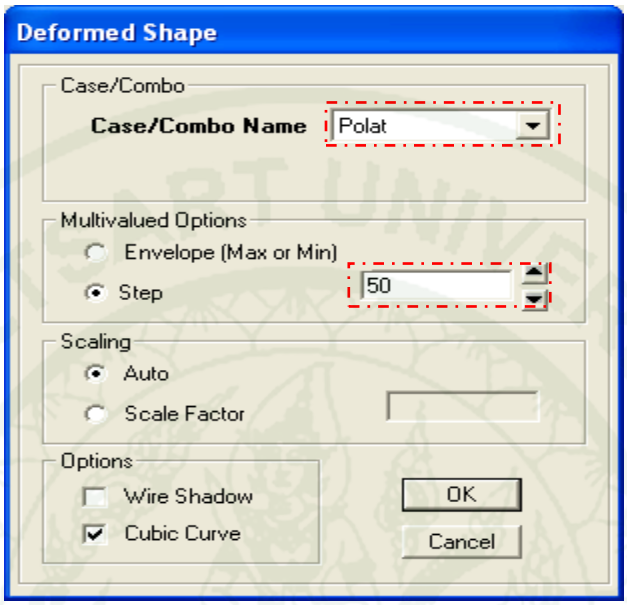

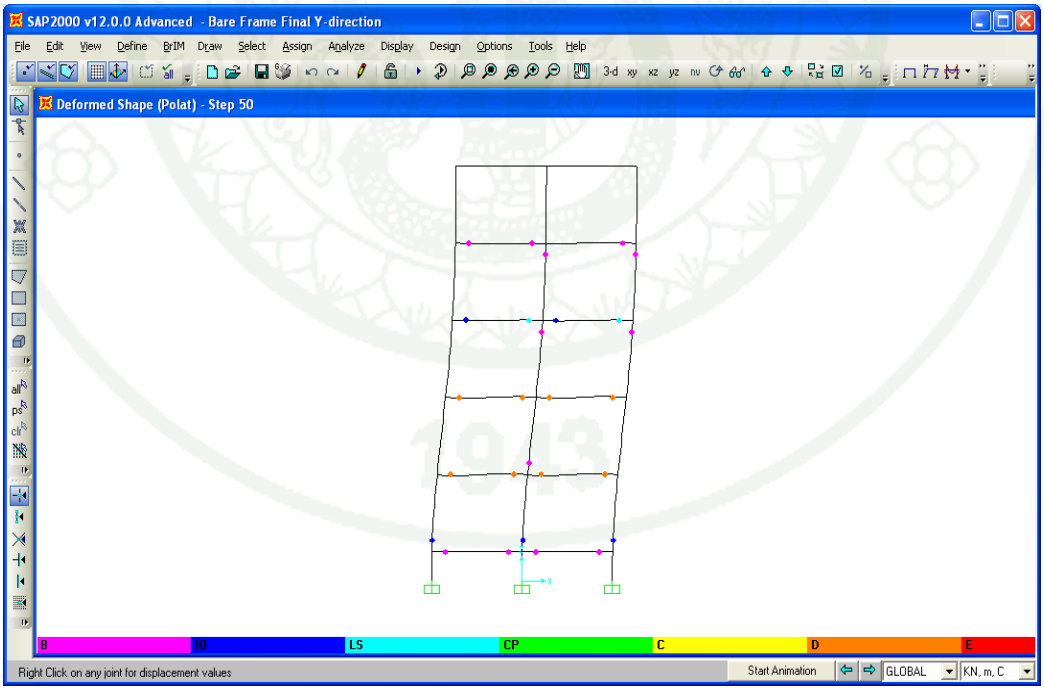

Appendix D

Building Drawings

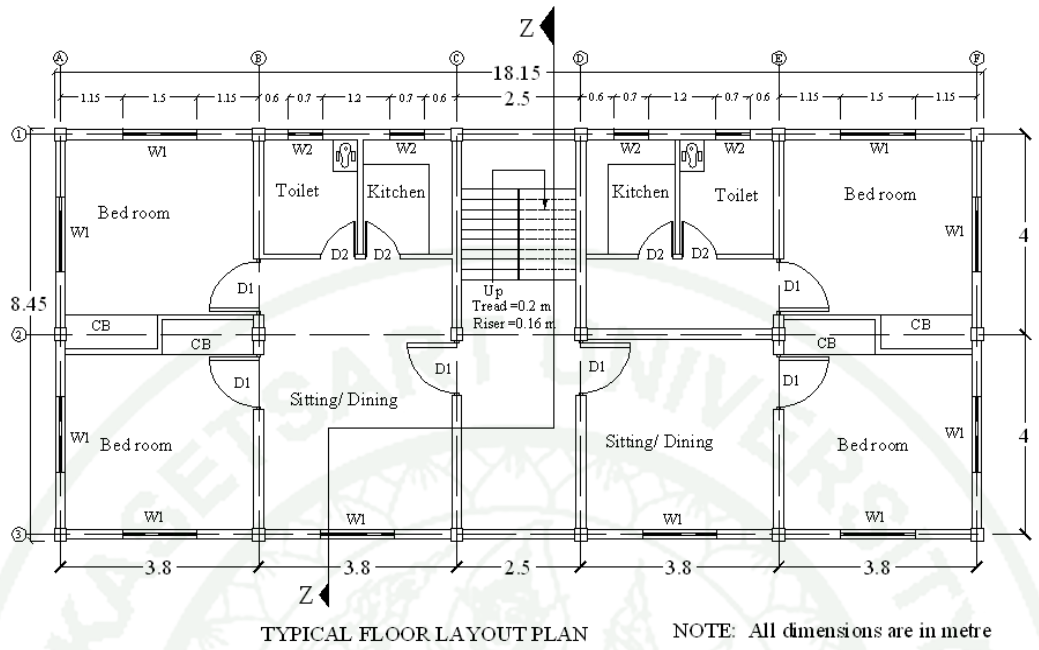

Appendix Figure D1 Floor layout plan for existing building

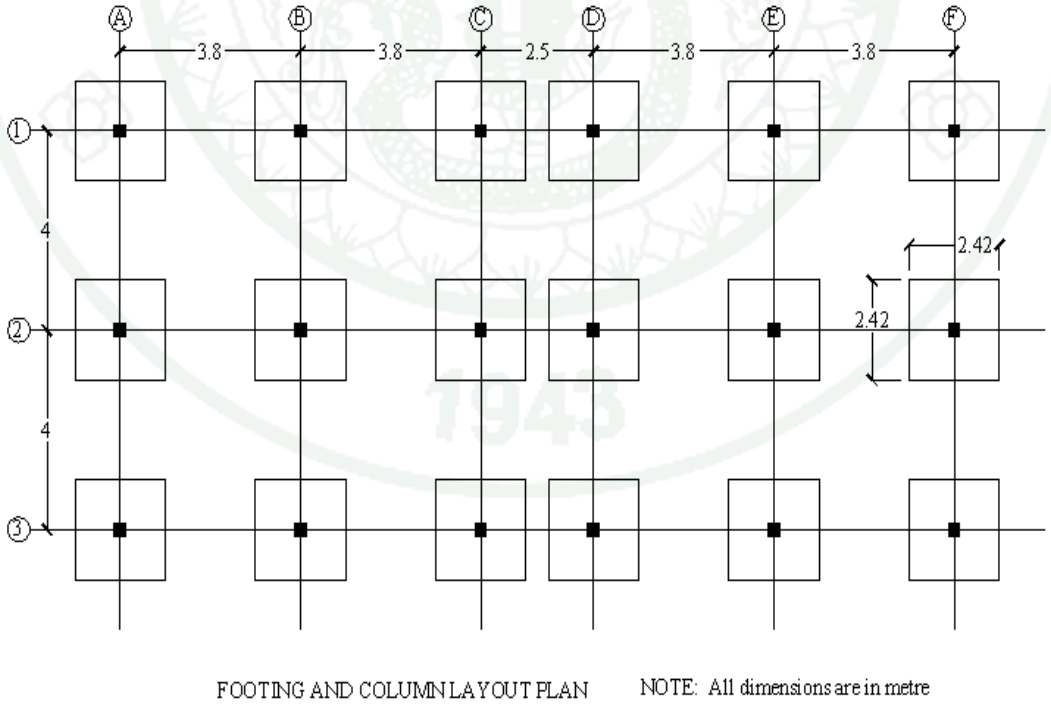

Appendix Figure D2 Foundation layout plan for existing building

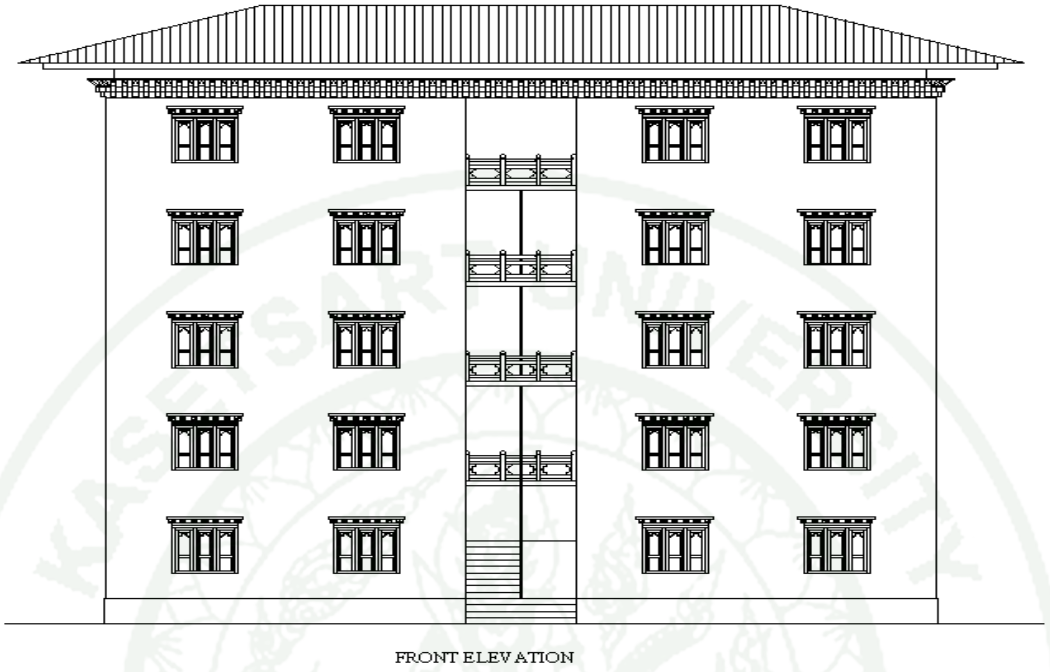

Appendix Figure D3 Front Elevation of existing building

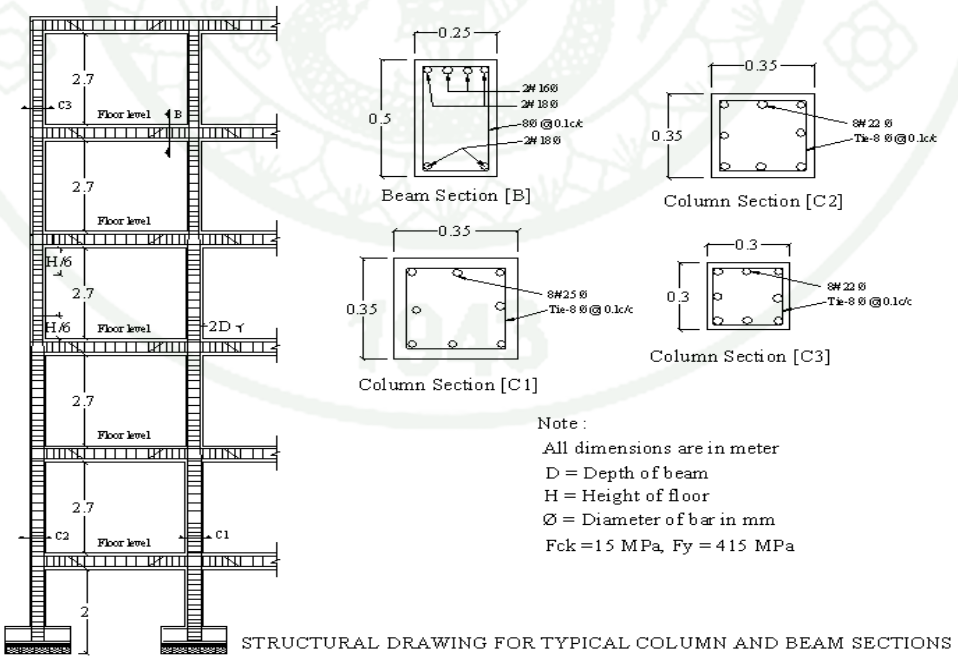

Appendix Figure D4 Structural Drawing details

CIRRICULUM VITAE

NAME : Mr. Lobzang Dorji

BIRTH DATE : October 20, 1978

BIRTH PLACE : Ramchongma, Trashigang, Bhutan

EDUCATION :

YEAR	INSTITUTE	DEGREE/DIPLOMA
2006	Royal Bhutan Institute of Technology. Royal University of Bhutan.	B.Eng. (Civil Engineering)
2010	Kasetsart University Bangkhen Campus. Bangkok, Thailand.	M.Eng. (Civil Engineering)

POSITION/TITLE : Lecturer

WORK PLACE : Jigme Namgyel Polytechnic, Dewathang.
Department of Civil Engineering.
Royal University of Bhutan, Thimphu Bhutan.